ANNUAL TEMPERATURE AND PRECIPITATION TRENDS IN THE UNITED STATES

BY

MATTHEW STOKLOSA

THESIS

Submitted in partial fulfillment of the requirements
for the degree of Master of Science in Agricultural and Biological Engineering
in the Graduate College of the
University of Illinois at Urbana-Champaign, 2017

Urbana, Illinois

Master's Committee:

Professor Prasanta Kalita
Professor Rabin Bhattarai
Dr. Wade Wall

Abstract

With rising global temperatures and clear trends in changing weather patterns, it is important to develop a framework for regional changes in climate since not all regions experience the same changes. As these regions begin to experience shifts in their climate, it is important to analyze not only general rising trends in temperature and precipitation, but more precise patterns that help flesh out how drastic these changes are. By utilizing indices created by the Expert Team on Climate Change Detection and Indices (ETCCDI), this project aims to better understand regional climate shifts in terms of annual temperature and precipitation trends in the United States. By first applying these indices to climate data from Agricultural Research Service the and then to the future projection based on Global Climate Model simulations available, we can determine what direction climate change has been headed in various parts of the United States and see if those trends will continue.

ACKNOWLEDGMENTS

I would like to deeply thank the following people for their continued support and for helping make the project possible.

Dr. Prasanta Kalita, for support, instruction, and the profound impact he has had on me throughout my time at the University of Illinois.

Dr. Rabin Bhattarai, for assisting me over many hurdles and his dedication to ensuring this project would find success.

Dr. Wade Wall, for entrusting this project to me and for always motivating me to take on new challenges for the sake of growing as a researcher.

The Academic Staff, for their continued hard work and encouragement.

The Soil and Water team, for the feedback, motivation, and many fond memories over the years.

TABLE OF CONTENTS

Chapter 1

Introduction

As humans entered the industrial age, new technologies, transportation, and manufacture ring processes improved quality of life and increased the efficiency in which we complete a wide array of tasks. All of this was possible due to new energy sources which powered machinery to complete these tasks. However, these energy sources were not without cost as burning high quantities of fossil fuels led to rapid elevation in greenhouse gas emissions at an unprecedented rate. The Earth's atmosphere maintains a level of greenhouse gases to regulate the Earth's temperature by trapping infrared light remitted from the Earth after sun light hits the surface. Normally, a certain amount of infrared light escapes back into space, keeping the Earth's surface temperature at a level conducive to sustaining life. With the rapid increase in greenhouse gas concentrations, the warming effect has increased greatly.

Over the last decades, human caused emissions of greenhouse gases are at their peak, greatly influencing several aspects of the Earth's Climate system (Pachauri et al., 2014). Across the globe, regions are experiencing shifts in average temperatures, changes in annual precipitation amounts, extreme storms, and increases in the number of extreme weather patterns. As regional climate's shift, decisions will need to be made to preserve basic societal norms such as a sustainable water supply, continued food availability, and a basic human comfort level. At present, is not clear how climate will change in different regions and to what extent. Predictions are constantly being made to try and understand what will happen based of observed climate shifts over the past decades as well as projected greenhouse gas emissions. Policy decisions hinge on the various projected scenarios making it vital they are well understood and cover the possibility spectrum of climate shifts (Jones & Patwardhan, 2014).

Much of climate change research focuses on analyzing and predicting average shifts in temperature and precipitations. These average changes are often the best understood, most apparent, and most noticeable impacts that affect society. Extreme weather events and extreme weather patterns tend to

go underreported and analyzed. These extreme events often have large impacts on regions. Several groups have looked to research extreme weather patterns and create frameworks for doing so with climate indices. One group, the Expert Team on Climate Change Detection, Monitoring, and Indices (ETCCMDI) developed a set of 27 climate indices that could be used to monitor extreme weather trends over time. By looking at the highs and lows in climate shifts, these indices help flesh out specific ways in which local climate systems will shift and impact people.

This study aims to apply these indices to several sets of climate data to understand how extreme patterns have been shifting in the United States, and in what ways they can be expected to change. Eight indices were selected to summarize extreme temperature and precipitation trends. These indices first were applied to daily weather data sets from the United States Department of Agriculture's Agricultural Research Service. The indices were calculated for each year in the data set and the trend was analyzed at each weather station in the data set to examine both temporal and spatial trends in the country. Next, the Community Climate System Model's CCSM4 climate model and the Geophysical Fluid Dynamics Laboratory's GFDL-CM3 climate model were analyzed used these indices. Each climate model contains simulated historical daily data which could be used to calculate climate indices over time. A trend could again be calculated at each weather station's location to compare the climate model's prediction for extreme weather trends against the observed data. Finally, the CCSM4 and GFDL-CM3 historical simulations were used to calculate and analyze trends in the climate indices. This was done for the two of Representative Concentration Pathways (RCPs) that climate models use to predict future climate trends based on different possible greenhouse gas concentrations.

Extreme weather pattern analysis is vital to understanding the ways in which climate will shift beyond global averages. This study will provide a framework for analyzing both observed extreme trends as well as possible future trends from different predicted scenarios.

Chapter 2

Objectives

The primary objective of this study was to analyze extreme climate trends across the United States using daily temperature and precipitation data to establish a framework for determining changes in extreme temperature trends at varying levels. The study's specific goals were:

1. Analyze the ETCCDMI indices for historical data pulled from weather stations across the United States to determine historical shifts in extreme weather trends.
4. Analyze the ETCCDMI indices for historical climate model simulation data at each of the weather stations and compare the simulated trends to the observed historical data to determine how accurately they measure shifts in historical extreme weather trends.
3. Analyze the ETCCDMI indices for future projected simulations from the CCSM4 and GFDL-CM2 climate models over two RCPs to determine potential future changes in extreme weather trends.

Chapter 3

Historical Climate Trends

3.1 Introduction

Global Climate Change remains an ever-pressing issue threatening the globe and society in many ways. In the span of 1880 to 2012, land and ocean surface temperatures have risen by 0.85°C on average (Pachauri et al., 2014). Throughout the United States, an increase of 1 to 2°C can be expected over the coming decades (Walsh, Wuebbles et al., 2014). In addition to rising temperatures across the United States, land precipitation across North America has steadily risen throughout the 20th Century (Trenberth, 2011). While global trends indicate a very clear path for temperature and precipitation, regional trends tend to be far more variable in their outcomes. Furthermore, these analyses focus on changes to the mean values as opposed to extremes (Petersen, 2005).

The Workshop on Indices and Indicators for Climate Extremes sought to compile a group of climactic indices to be used in analyzing climate extreme trends (Karl et al., 1999). Over time, the Expert Team on Climate Change Detection, Monitoring, and Indices (ETCCDMI) was formed in a joint effort between the WMO Commission for Climatology (CCI), World Climate Research Programme (WCRP) Climate Variability and Predictability (CLIVAR) project. The Expert Team (ET) eventually settled on 27 core indices that could best represent extreme climate trends (Peterson, 2005). Rather than simply indicating temperatures are rising or precipitation is increasing, these indices focus on breaking down how this occurs in terms of extremes. Examining if things like minimum daily temperatures are on the rise, or number of dry spells in each year better indicates what exactly is occurring with a shifting climate.

This study used historical daily weather data to calculate ETCCMDI indices across the United States from 1950-2010. These indices were used to analyze changes in extreme weather patterns over this time. By forcing a linear fit onto the indices over time, shifts in extreme events at each weather station

could be determined. This allowed for a close look at spatial as well as temporal trends of extreme weather change across the country.

3.2 Literature Review

3.2.1 Climate Change

Over a long enough period, noticeable shifts in the climate patterns of the globe can be found and analyzed. The Earth's climate naturally shifts to highs to lows, spanning the spectrum of ice ages to extreme heat. The Earth's climate system responds to factors such as orbital shifts and tilt changes, solar irradiance levels, and volcanic activity which can all impact global temperatures over time (Masson-Delmotte et al., 2013). Climate change refers to the process by which a significant deviation from the mean climactic state is observed for a significantly long period whether from natural fulgurations or anthropomorphic influences (Solomon, 2017). Over the past century, a noticeable shift has occurred as global temperatures have begun to rise. Starting around the 1950s, rapid warming of the Earth's climate system has taken place with changes unlike any that have occurred over several time frames (Pachauri et al., 2014). Natural climactic changes tend to slowly take place and results in small shifts. This unprecedented warming can largely be attributed to greenhouse gases such as CO_2 which trap energy from the sun in the atmosphere, leading to higher temperatures. Human activities have drastically increased the amount of greenhouse gases found in the atmosphere over the past decades (National Research Council, 2001). These drastic climate shifts will have a wide array of impacts including increased temperatures, shifting precipitation amounts, rising sea levels, and higher variability in storm events.

3.2.2 Historic Temperature Trends

Global temperatures rose significantly throughout the 20th century. The impacts of increased temperatures due to greenhouse gases can be felt almost uniformly over the Earth. As energy from the sun hits the surface of the Earth, it gets absorbed and then emitted back out into the atmosphere as infrared light. This infrared light is what keeps the surface of the Earth warm as it naturally gets kept in the

atmosphere by various greenhouse gases. Much of it eventually escapes the atmosphere, keeping the Earth's temperature at a level suitable for sustaining life. In 2011, CO_2 concentrations were up 40% since 1750 while CH_4 concentrations were up 150% in the same time frame (Ciais et al., 2013). With the current increases in greenhouse gas concentrations in the atmosphere, too much heat is being trapped causing temperatures to rise steadily.

The warming of the global climate is an irrefutably observed trend over the last century. Global temperatures have risen 0.13°C per decade over the past fifty years which is double the decadal rise over the last 100 years (Solomon, 2007). In addition to rising global temperatures, observations have revealed significant variability in temperature trends within decades and even within individual years, leading to extreme swings in regional temperatures (Stocker, 2014). This increase of global temperatures has led to several adverse effects such as melting of polar ice caps, increased droughts, rising ocean temperatures, and degradation of ecological systems as vegetation and animal life struggles to adapt at the rate temperatures rise.

As temperatures rise, several positive feedback loops can emerge which create conditions that result in further temperature increases. Rising temperatures impact the exchange of greenhouse gases, such as CO_2 and CH_4, between land and ocean ecosystems (Raynaud et al., 1993). These gas cycles are heavily influenced by temperature. Rising temperatures tend to cause these cycles to output more gas into the atmosphere than the surface takes back, resulting in higher greenhouse gas concentrations which in turn continue to raise temperature.

3.2.3 **Historical Precipitation Trends**

The steady warming of the Earth's surface can have varying impacts on the precipitation an area receives over time. Increased temperatures lead to an increase in evaporation of water from the Earth's surface. Higher evaporations rates will lead to higher atmospheric moisture in several parts of the world. Rainfall rates rely heavily on moisture convergence rates so as the rate moisture increases, the rate of rainfall will increase with it (Trenberth et al., 2003). Not only will precipitation likely increase, the

number of extreme precipitation events will rise as well. From 1939 to 1996, a 3% per decade increase of 7-day, 1-year rainfall events occurred in the United States (Kunkel et al., 1999).

A general pattern emerges of wet areas receiving more rainfall and dry areas receiving less rain fall. Overall, rainfall rates will decrease in the drier subtropics and rise in the wetter subpolar regions (GFDL, 2007). Several large areas across the globe has observed increased precipitation trends such as the eastern Americas, and northern Europe and Asia, while the Mediterranean, southern Africa, and Southern Asia has experienced declining rainfall amounts (Solomon, 2007). Decreased precipitation in areas that will likely only get warmer can lead to damaging effects such as increased droughts and wildfires.

3.2.4 **Climate Indices**

Various indices have been created to try to explain and categorize the climate change trends being observed around the world. These indices hope to create clear criteria for different kinds of patterns to form a consistent framework when discussing and analyzing climate change. Climate indices cover a wide range of climate topics and aim to explain large scale general trends to small scale specific event trends.

In the late 1990s, several meetings across the world took place on the topic of climate change in preparation for the IPCC Third Assessment Report. At these meetings, it was determined there was not enough time to collaborate on a global daily data set for the report, so instead only derived indicator time series would be shared (Frich et al., 2002). From this, the WMO/CLIVAR Joint Working Group on Climate Change Detection held a meeting in 1999 and agreed to establish 10 simple climate indices for use in climate change analysis (Frich et al., 2002). These climate indices were intended to be simple and independent enough to effectively describe temperature and precipitation patterns on a regional basis. The WMO/CLIVAR ETCCDMI then held several workshops to better develop and test indices.

The indices not only create a framework for understanding climate patterns, but also a means to better share climate data when complete data is hard to procure (Easterling et al., 2003). Much in the

spirit of the original talks before the IPCC Third Assessment Report, these workshops aimed to derive a data set capable of analyzing climate change without having to share a global daily dataset. While a much more accurate and rigorous analysis could be made with a complete raw data set, these data sets are not always easy to compile and share, making some alternative significant (Easterling et al., 2003).

Climate change analysis generally focuses on the change of mean values and deviations for normal variability. This can easily be accomplished utilizing monthly global data sets that provide strong coverage across the world (Alexander et al., 2006). When trying to analyze extreme changes and more detailed patterns, a complete daily data set is required. The ETCCDMI workshops worked to address this problem by bringing together climate scientists in regions of the world with limited data to form strategies to fix this issue (Alexander et al., 2006).

The ETCCDMI formed 27 indices to be used in pursuit of their mission to better detect climate change and create methods for explaining trends in extreme events. These final indices focus on both extreme temperature and precipitation trends.

3.3 Methods

Many agencies across the United States have worked over the past decades compiling, organizing, and correcting climate data, leading to excellent coverage of climate data over the country. The United States Department of Agriculture (USDA) Agricultural Research Service (ARS) compiled NOAA weather data spanning 1950 to 2010. This dataset is comprised of the Cooperative Observer network and Weather-Bureau-Army-Navy weather stations. To complete the daily data sets when data is missing, the ARS used an inverse distance weighted interpolation algorithm pulling values from the nearest 5 stations to calculate missing values. This results in a data set that is virtually 100% complete. The daily data sets contain minimum temperature, maximum temperature, and precipitation amounts. The data was extracted from their database resulting in 7542 weather stations across the continental United States (Figure 3.1).

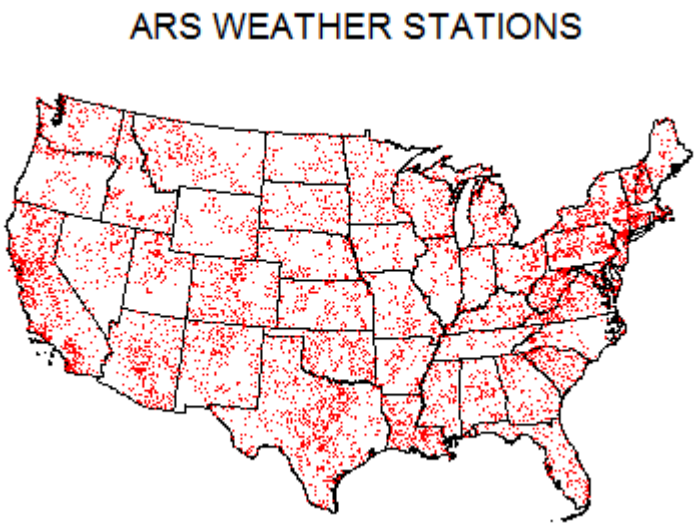

Figure 3.1*: Map of weather stations pulled from USDA ARS climate data*

The ETCCMDI indices (Table 3.1) were calculated for each weather station in the data set. Using the R programming language, the weather stations were broken down on a year to year basis using the climdex.pcic package developed by the ETCCMDI for analyzing their indices. These index values depend on annual analysis of daily data yielding an index value for each year in the data set. Once the index values were determined for each year between 1950 and 2010, a linear regression was run to analyze the trend over the 60-year period. The slope of each indices' regression was pulled out to examine long term trends for each index at each weather station. Furthermore, the slope's significance level in the regression, the P value for the F-test of each regression, and the R^2 value were pulled out to test for significance. In the end, the linear fit was forced on each index at each weather station regardless of wellness of fit to monitor trends.

In addition to the linear fit, the Mann-Kendall test was performed on the index values over the period of 1950 to 2010. The Mann-Kendall test in a nonparametric test that aims to explain the difference between later observed data and earlier observed data (Meals et al., 2011). The Mann-Kendall test statistic S can be calculated by:

$$S = \sum_{i=1}^{n-1} \sum_{j=i+1}^{n} sign(y_j - y_i)$$

Where $y_j - y_i$ is the difference between a later measured value and an earlier value. S indicates the direction and magnitude of a trend with a positive S indicating a trend of larger values later in the time series and a negative value indicating a trend of smaller values later in the time series. The test statistic for the Mann-Kendall Test is calculated by:

$$\tau = \frac{S}{n * n - 1)/2}$$

The null hypothesis states that there is no trend and is rejected if τ and S are very different from zero. This test was completed for the historical data to further examine the trend in the climactic indices over time.

Table 3.1: *ETCCDMI final indices*

Index	Name	Description
FD	Frost Days	Count of days when TN (daily minimum temperature) < 0°C
SU	Summer Days	Count of days when TX (daily maximum temperature) > 25°C.
ID	Icing Days	Count of days when TX < 0°C
TR	Tropical Nights	Count of days when TN > 20°C
GSL	Growing Season Length	Count between first span of at least 6 days with daily mean temperature TG>5°C and first span after July 1st (Jan 1st in SH) of 6 days with TG<5°C.
TXX	Monthly maximum temperature	Monthly maximum value of daily maximum temperature
TNX		Monthly maximum value of daily minimum temperature
TXN		Monthly minimum value of daily maximum temperature
TNN		Monthly minimum value of daily minimum temperature
TN10p		Percentage of days when TN < 10th percentile of the 1961-1990 base period
TX10p		Percentage of days when TX < 10th percentile of the 1961-1990 base period
TN90p		Percentage of days when TN > 90th percentile of the 1961-1990 base period
TX90p		Percentage of days when TX > 90th percentile of the 1961-1990 base period
WSDI	Warm spell duration index	Count of days with at least 6 consecutive days when TX > 90th percentile of the 1961-1990 base period
CSDI	Cold Spell Duration Index	Count of days with at least 6 consecutive days when TN < 10th percentile of the 1961-1990 base period
DTR	Daily Temperature Range	Monthly mean difference between TX and TN
Rx1day		Monthly maximum 1-day precipitation
Rx5day		Monthly maximum consecutive 5-day precipitation
SDII	Simple Precipitation Intensity Index	Sum of precipitation on wet days over the number of wet days in a year.
R10mm		Count of days when precipitation (PRCP) ≥ 10mm
R20mm		Count of days when PRCP ≥ 20mm
Rnnmm		Annual count of days when PRCP ≥ set threshold.
CWD	Wet Spell Index	Maximum number of consecutive days with daily PRCP ≥ 1mm
CDD	Dry Spell Index	Maximum number of consecutive days with daily PRCP < 1mm
R95pTOT		Count of days when daily PRCP > 95th percentile of the 1961-1990 baseline period
R99pTOT		Count of days when daily PRCP > 99th percentile of the 1961-1990 baseline period
PRCPTOT		Total annual rainfall

The indices' slope values were plotted across the United States to analyze spatial trends within the country. They were first kept as point values to preserve the raw results as a general baseline for analysis. A regional approach was then taken to break down the United States and analyze broader trends over an area. As determined by Karl and Koss, The NOAA National Centers for Environmental

Information identifies 344 climate divisions in the country which in turn were used to determine the nine climactic regions NOAA (Figure 3.2) uses for analysis today (as cited in U.S. Climate Divisions). The mean value, maximum value, minimum value, and standard deviation of each climactic region's indices' slope values were calculated and assessed.

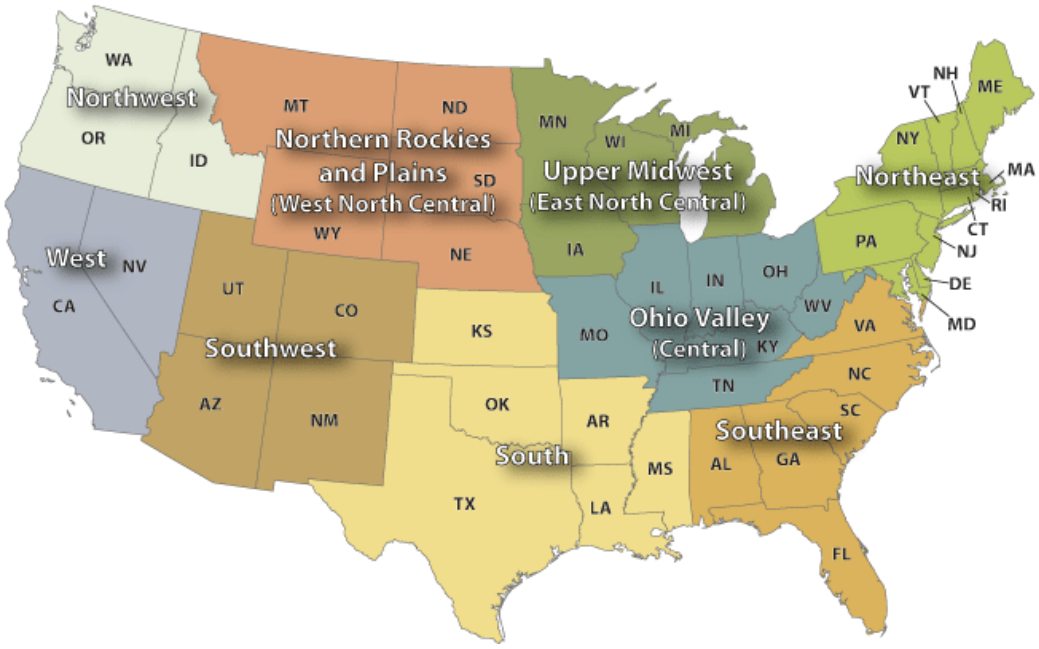

Figure 3.2: *NOAA Climactic Regions (Sanchez-Lugo)*

A county level breakdown the indices was conducted to further breakdown the country and work to create a simple spatial interpolation of climate trends across the United States. As with the NOAA climactic regions, the mean value, maximum value, minimum value, and standard deviation of each indices' slope value for each county was calculated. Maps were then generated for each index at a county level.

3.4 Results and Discussion

3.4.1 Historical Point Values

The ETCCMDI indices selected in this study were plotted at the weather station locations to inspect spatial distribution of positive and negative trend values. With indices linked to temperature shifts,

red indicates an increasing trend towards warming and blue indicates a decreasing trend towards cooling. Indices related to precipitation shifts have a reversed scheme with blue indicating an increasing trend towards more precipitation and blue indicating a decreasing trend toward less precipitation. The size of the point indicates the magnitude of the slope value.

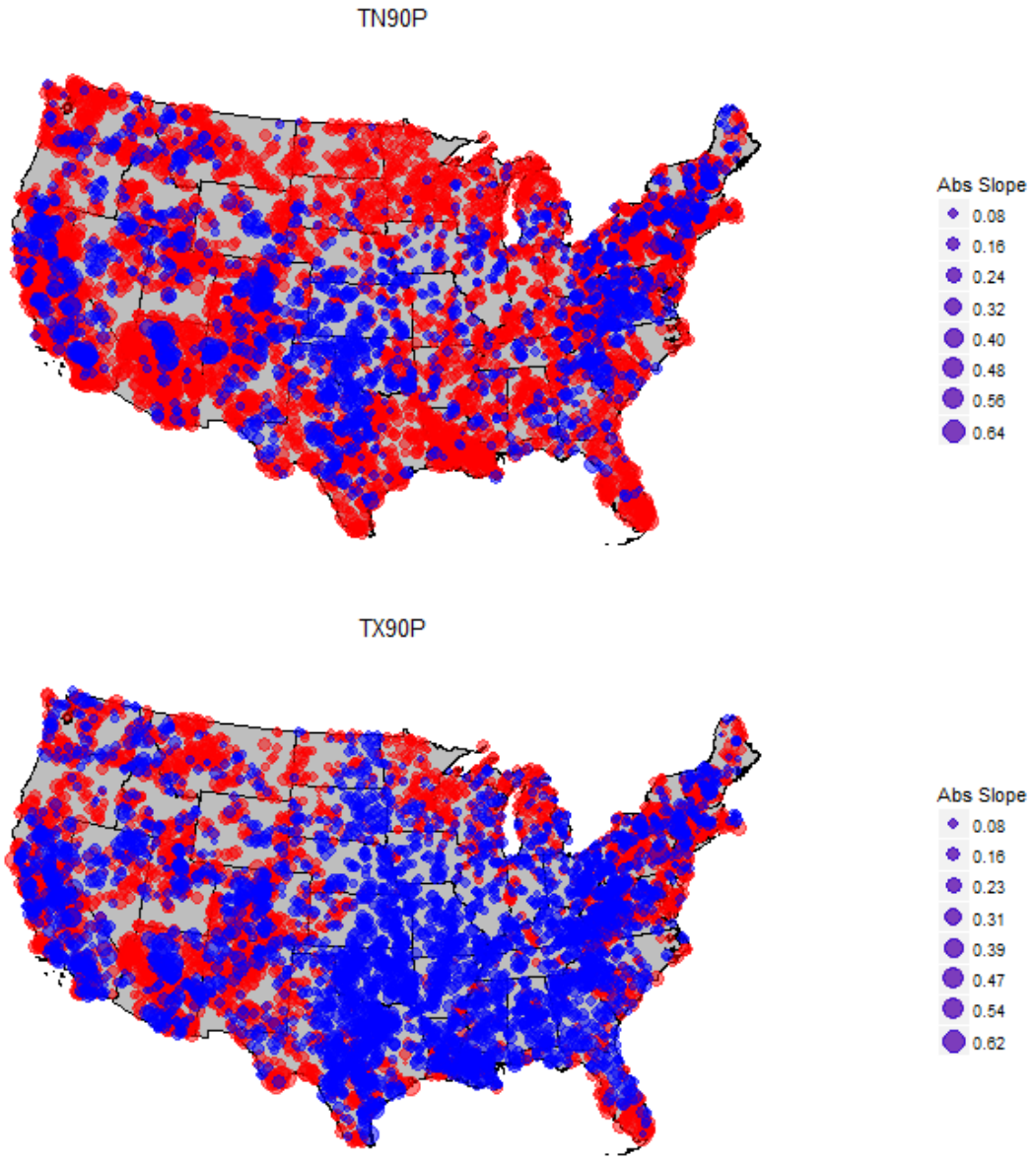

Figure 3.3: *Slope values for indices dealing with counts of days above the 90th percentile. (a) Daily minimum temperature across the United States. (b) Daily Maximum temperature across the United States. Larger points indicate greater change.*

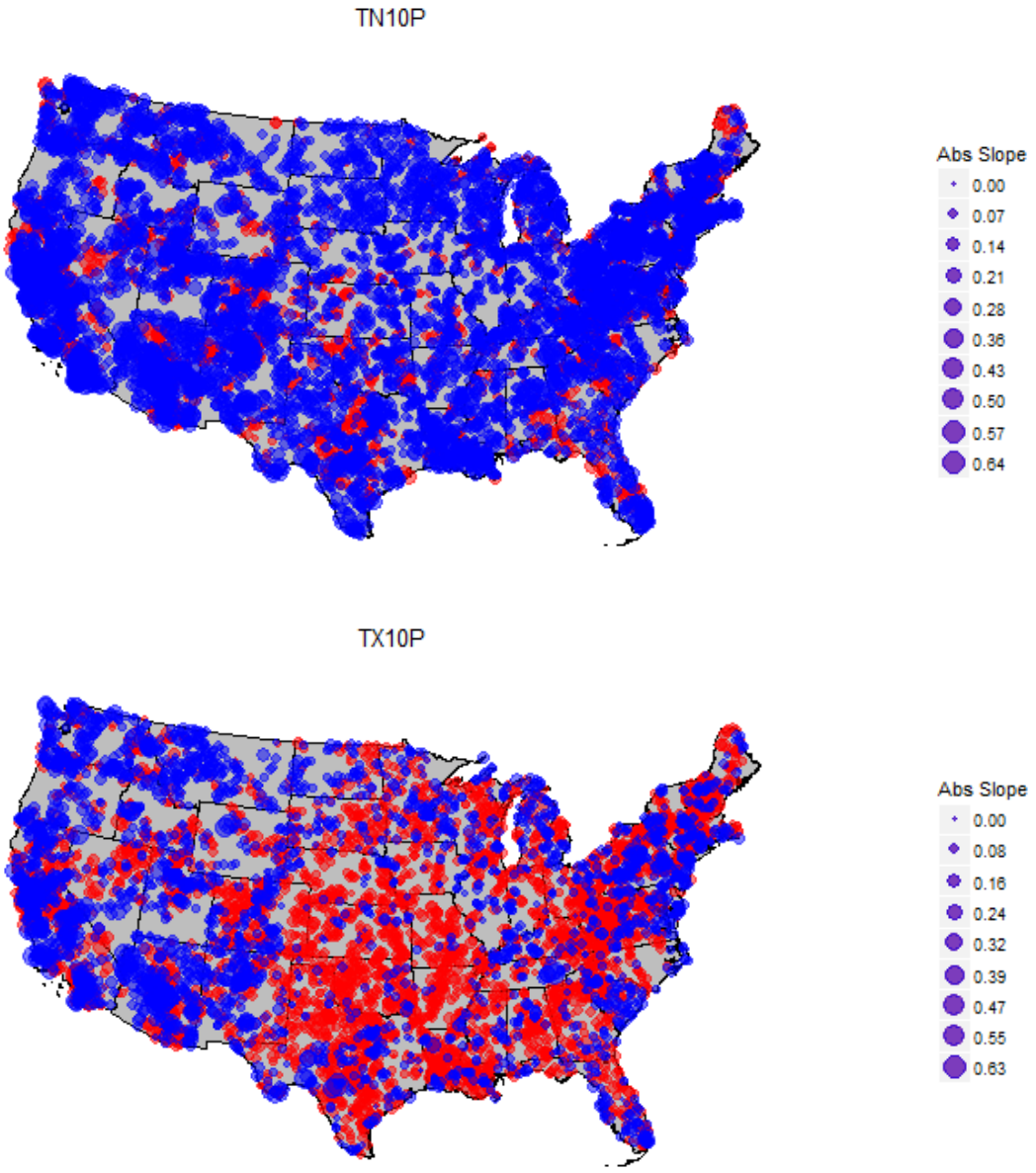

Figure 3.4: *Slope values for indices dealing with counts of days below the 10th percentile. (a) Daily minimum temperature across the United States. (b) Daily Maximum temperature across the United States. Larger points indicate greater change.*

Throughout the country, there has historically been a good deal of spatial variability in climate shifts. Even between two weather stations that are relatively close to one another, differing trends can be seen. Several factors such as topography, urbanization, and population shifts can greatly impact weather station's climate trends at a small scale. Figures 3.3 and 3.4 clearly demonstrate this variability as

numerous cases of a couple stations having an opposite trend compared to the stations surrounding them. This variability makes analyzing broad trends across sections of the country difficult, resulting in this methodology being much more reliable at this point scale for local analysis.

This historical data shows an interesting trend in warming throughout the United States. Average temperature has been reported to be on the rise on average across the country. Figure 3.3a shows that much of this warming may be coming in the form of a rise in daily minimum temperatures. Large groups of weather stations have shown trends towards more days exceeding the 90th percentile of daily minimum temperatures over the past 60 years. This indicates days are getting hot and never cooling off at night, resulting in high temperatures all day. These increases could lead to devastating heat waves where temperatures never reach a comfortable range, giving respite from sweltering heat.

Across the country, there is little change and in some cases, slight decreases in the daily maximum temperatures when compared to the 90th percentile of daily maximum temperatures. While these daily maximums appear to be decreasing, daily minimum temperature are rising across the United States when compared to the 90th percentile of daily minimum temperatures. Across the country, it appears that extreme daily maximums are not drastically growing leading to an increase in unbearably hot days.

The second set of maps found in Figure 3.4 examine the daily maximum and minimum temperature trends in comparison to the 10th percentile from the baseline period. As Figure 3.4a shows, many weather stations across the entire country have experienced a decrease in the number of days in a year which saw minimum temperatures below the 10th percentile. The maximum temperatures however are far more variability with clusters on the coasts experiencing a decrease in days where the maximum daily temperature is below the 10th percentile but an increase in the middle parts of the country.

Table 3.2: *Regression values for the observed temperature indices summarized over the entire data set for the United States*

INDEX	MEAN VALUE	MEAN R^2	MEAN F-TEST P-VALUE
TN90P	0.0489	0.1410	0.1807
TX90P	-0.0033	0.0868	0.2417
TN10P	-0.0677	0.1549	0.1578
TX10P	0.0088	0.0834	0.2454

Linear regressions do not fit well on average for these selected indices when generalizing over the United States. Low average R^2 can be seen over the continental US for all four indices. The significance level of the regression fairs better than the R^2 values, however still fails to reach significant enough levels (Table 3.2).

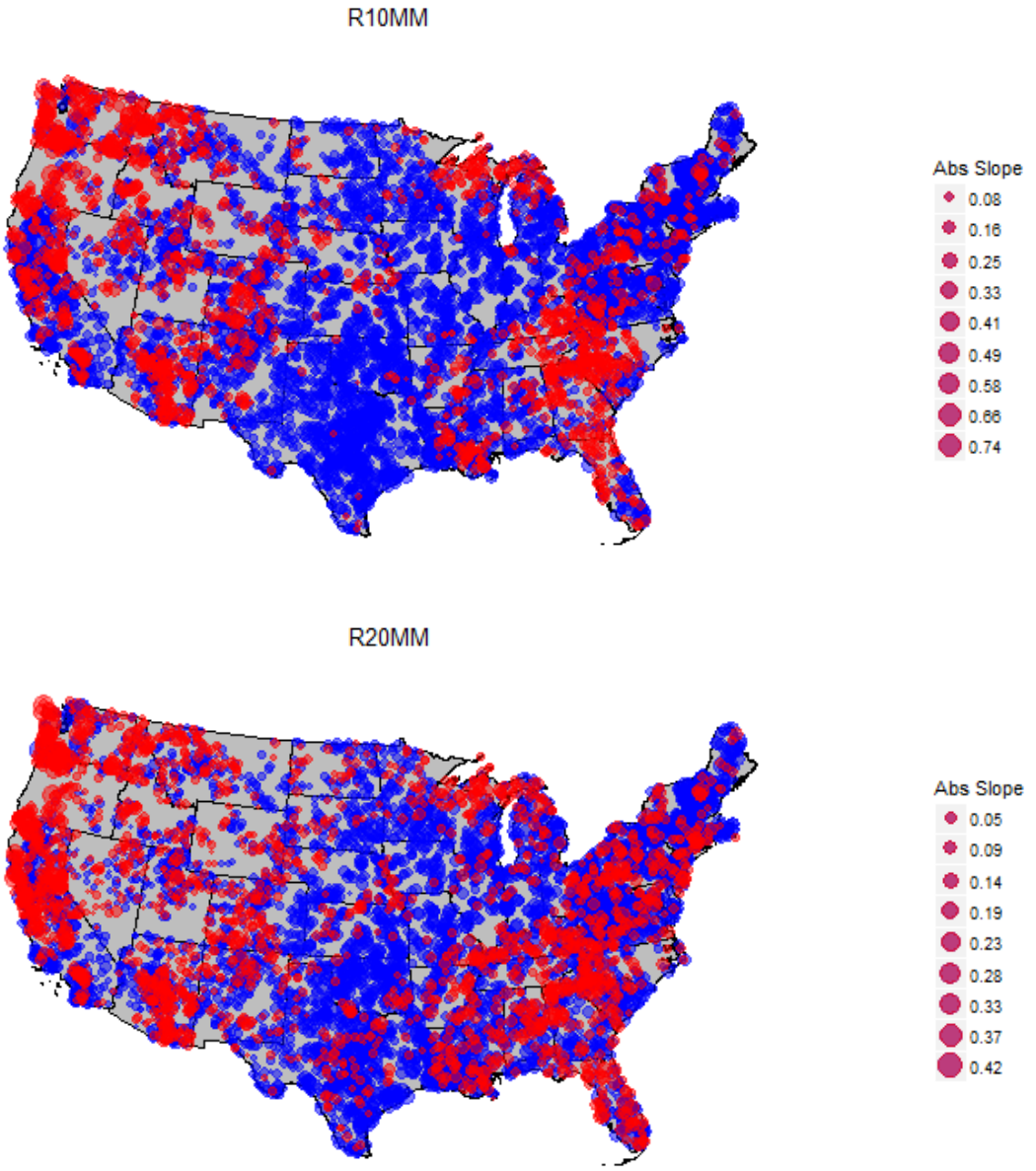

Figure 3.5*: Slope values for indices dealing with counts of days exceeding precipitation amounts. (a) 10mm daily rainfall. (b) 20mm daily rainfall. Larger points indicate greater change with blue indicating an increase slope value (more rainfall).*

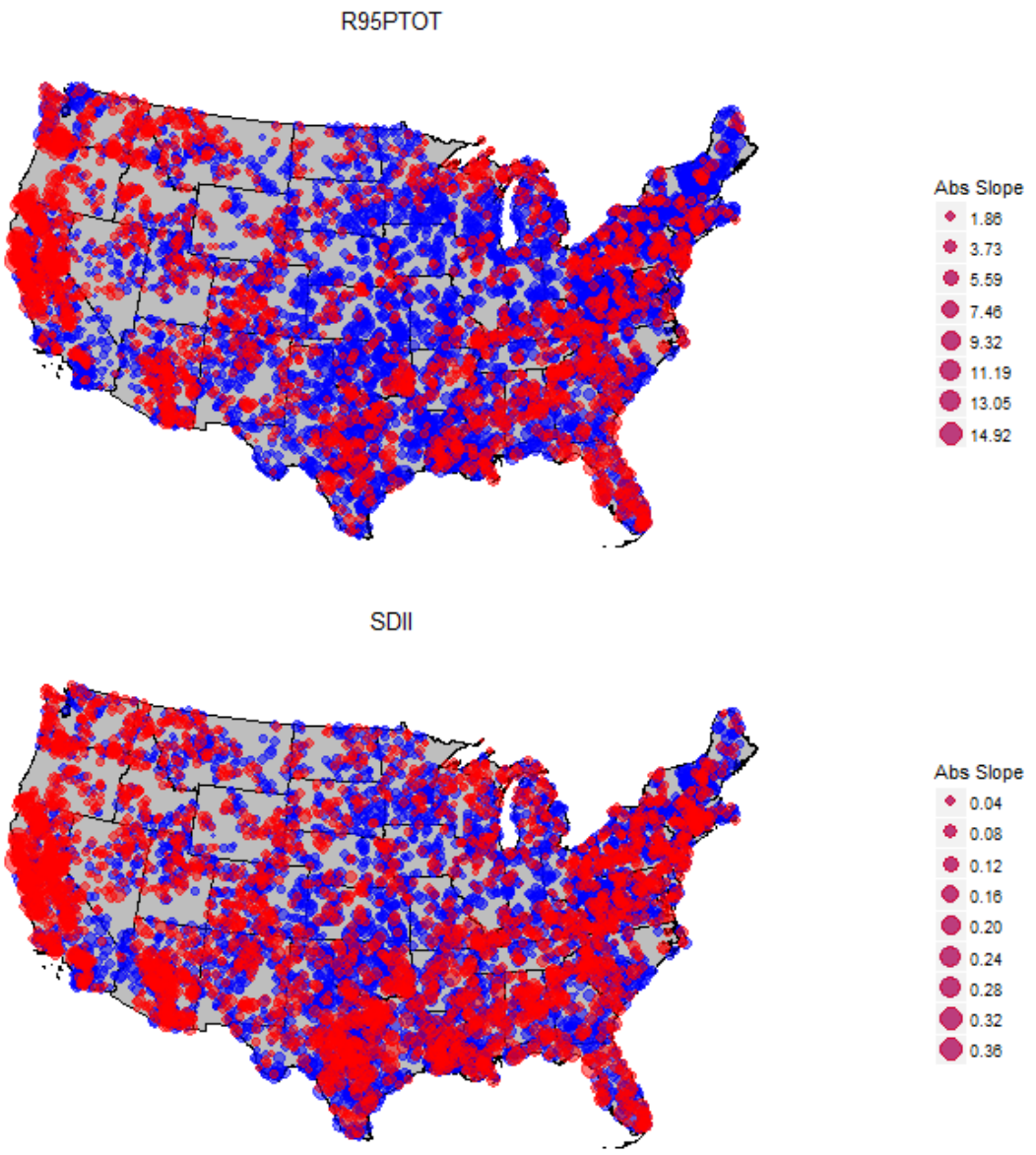

Figure 3.6: *Slope values for indices dealing with other precipitation analysis. (a) Sum of precipitation amounts for days where daily precipitation exceeds the 95th percentile from the baseline period 1961-1990. (b) Sum of annual precipitation on wet days with rainfall > 1mm, over the number of wet days.*

Precipitation trends across the United States tends to be far more variable than temperature trends (Figures 3.5 & 3.6). Weather stations near one another tend to differ greatly in some parts of the country such as the east coast. Like with temperature trends, several factors can influence this variability at a local scale. Furthermore, due to the complex process by which precipitation occurs, warming trends can have differing effects on locations, keeping in line with the idea of wet places get wetter and dry places get

dryer. Increased temperatures can cause increased evaporation, but they can also cause a slowing of the cooling and condensation process vapor undergoes as it rises through the atmosphere. The areas that seem to undergo more variability and big changes are on the coasts where warming of the oceans may contribute to large shifts in precipitation trends as moisture availability in the atmosphere changes in these areas.

Figure 3.5 shows a general trend through the middle third of the country and the northeast toward more days with high amounts of precipitation while other pockets of the country show a dryer trend such as the southwest. The more extreme R20mm has less drastic change than its R10mm counterpart indicating that extreme rainfall above 20mm has not increased as rapidly.

The R95PTOT tells a similar story of several parts of the country being wetter than the 95th percentile from 1961-1990, however it tends to be more variable than the R10mm and R20mm with several parts of the country showing decreases. Furthermore, the SDII shows many weather stations across the country are receiving less intense rainfall over the years as wet days are yielding less rainfall in total.

Table 3.3: *Regression values for the observed precipitation indices summarized over the entire data set for the United States*

INDEX	MEAN VALUE	MEAN R^2	MEAN F-TEST P-VALUE
R10MM	0.0339	0.0486	0.3117
R20MM	0.0194	0.0556	0.3094
R95PTOT	0.5120	0.0602	0.2989
SDII	0.0044	0.1230	0.2045

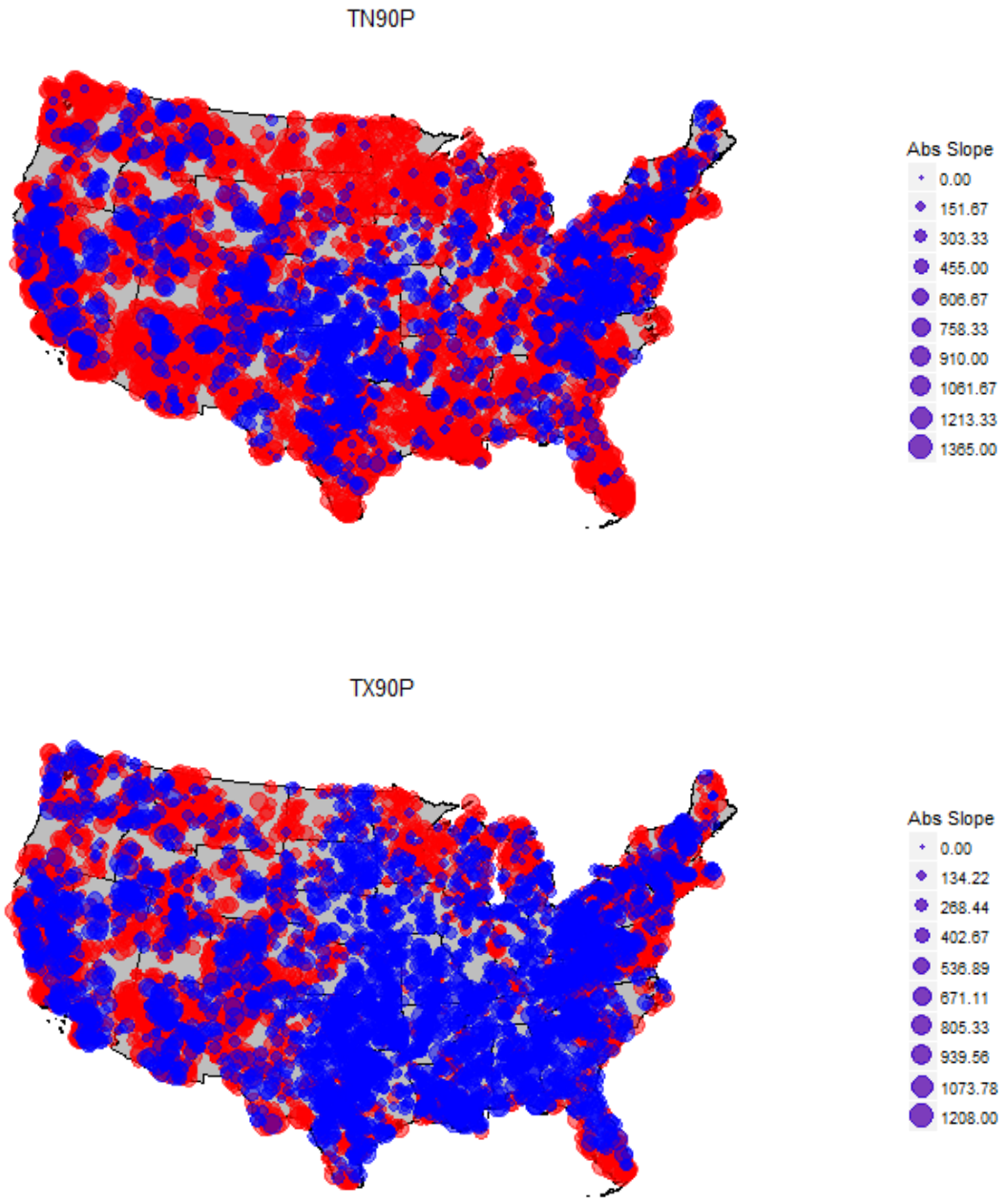

Figure 3.7: *Mann-Kendall S values for indices dealing with counts of days above the 90th percentile. (a) Daily minimum temperature across the United States. (b) Daily Maximum temperature across the United States. Larger points indicate greater change.*

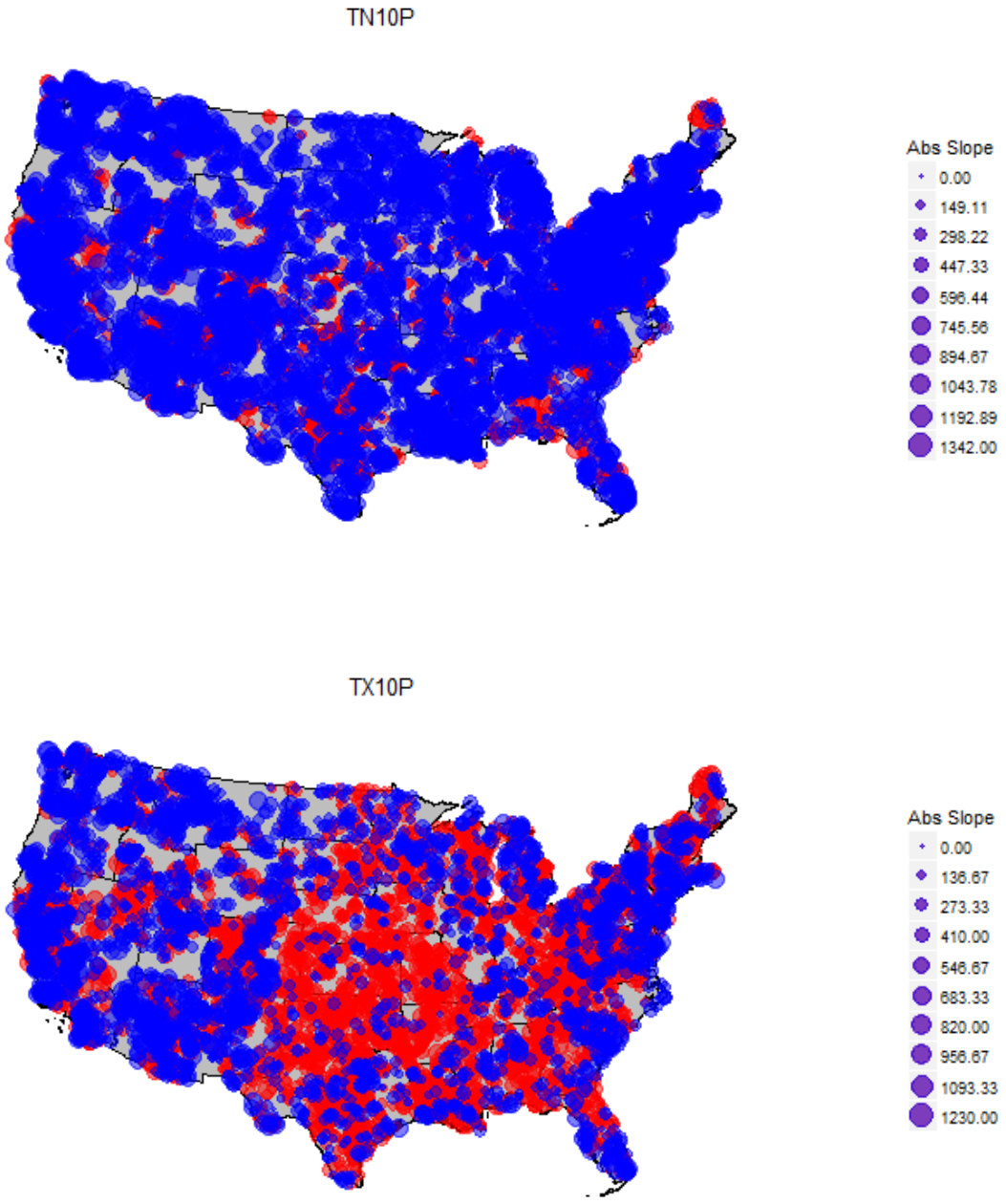

Figure 3.8: *Mann-Kendall S values for indices dealing with counts of days below the 10th percentile. (a) Daily minimum temperature across the United States. (b) Daily Maximum temperature across the United States. Larger points indicate greater change.*

The Mann-Kendall test reveals similar patterns to the linear regression, notably warming of daily minimum temperatures in the south and southwest and pockets of cooling on the east coast, central United

States, and California (Figure 3.7). Again, variability at small scales can be quite drastic in some cases. However, due to the strong trends found in some areas, the Mann-Kendall test does appear to have stronger spatial trends with more concentrated pockets of weather stations differing from those around them. Large parts of the country once again show cooling or little change in regards to the TX90P index (Figure 3.8).

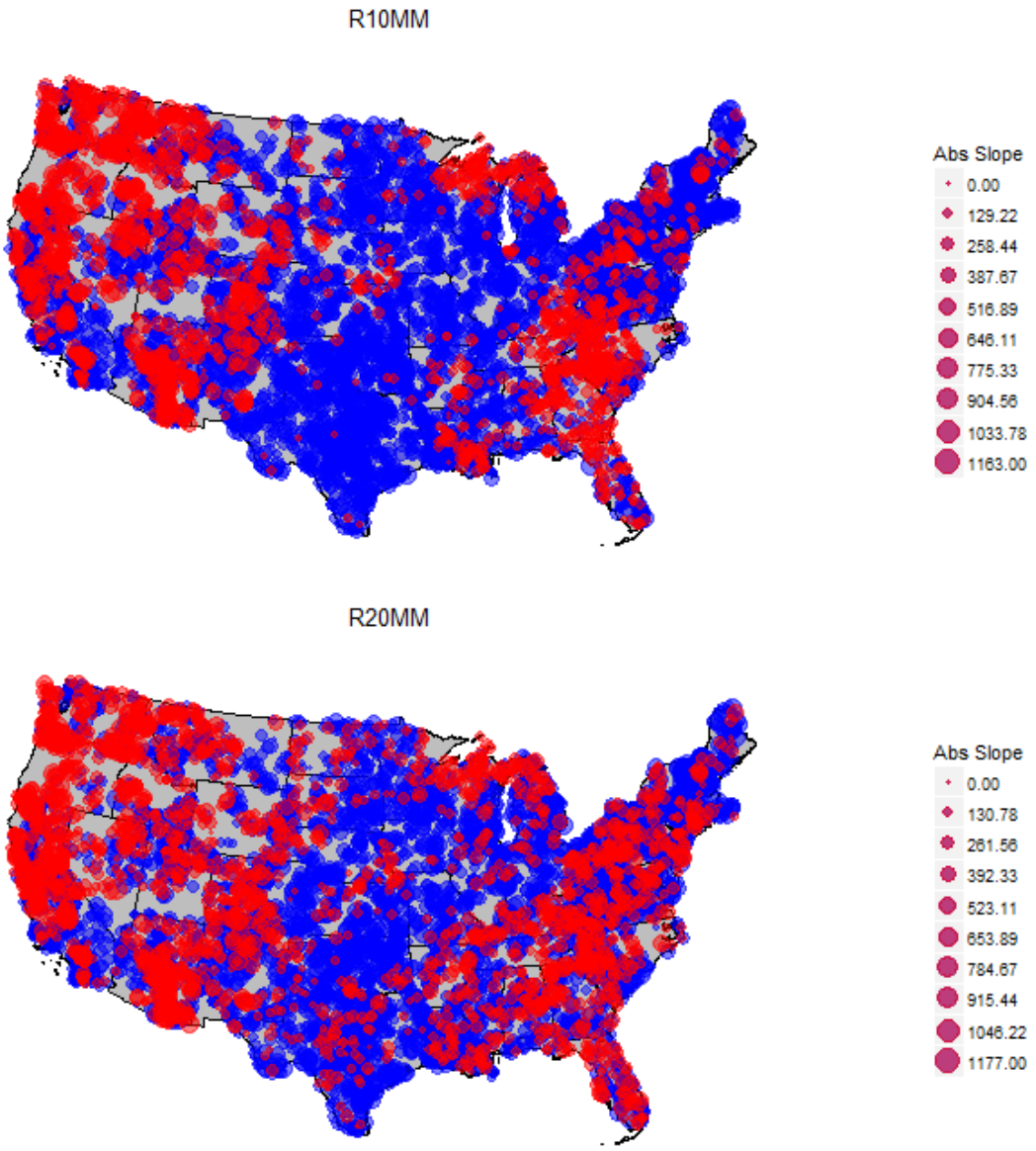

Figure 3.9*: Mann-Kendall S values for indices dealing with counts of days exceeding precipitation amounts. (a) 10mm daily rainfall. (b) 20mm daily rainfall. Larger points indicate greater change with blue indicating an increase slope value (more rainfall).*

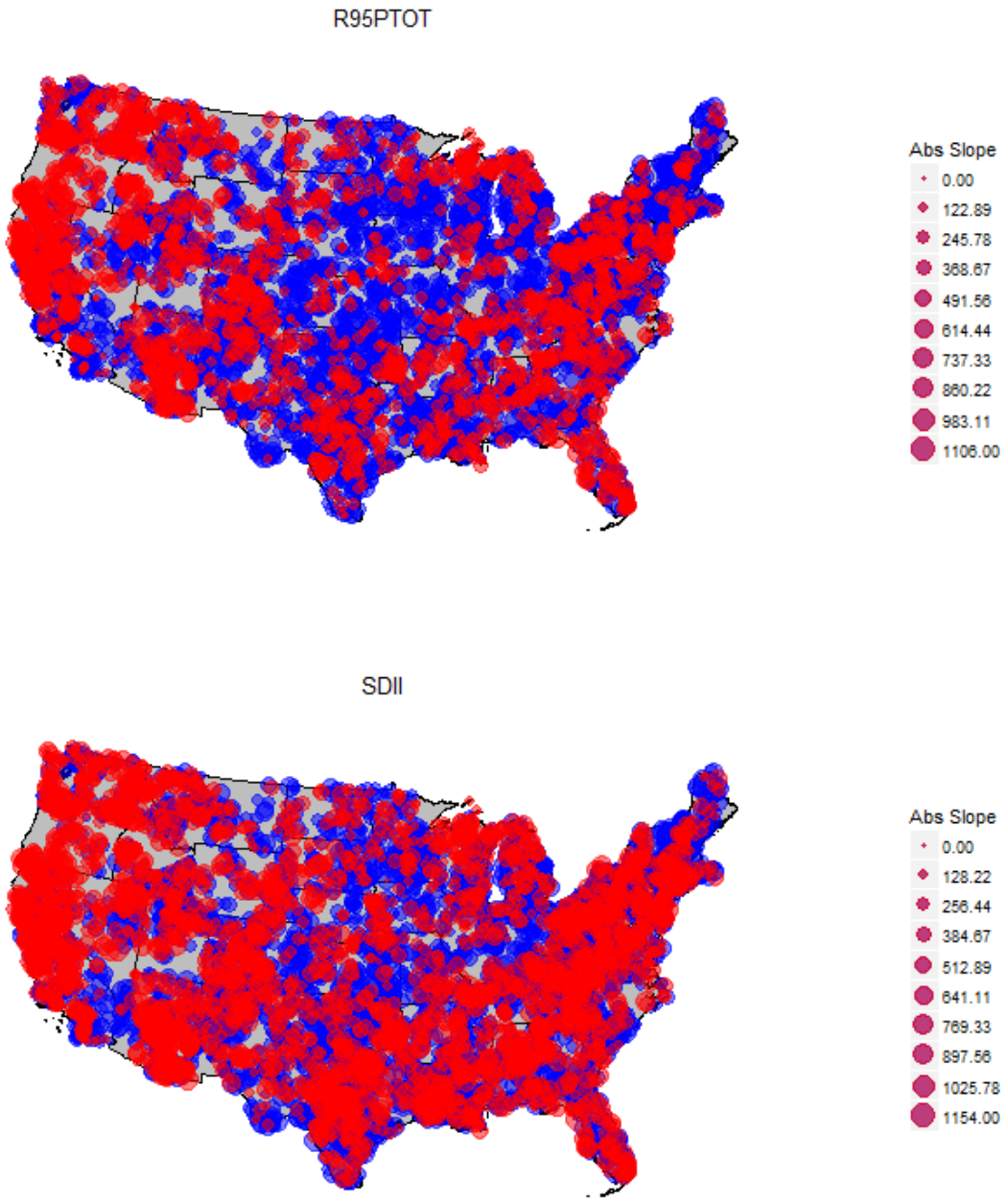

Figure 3.10: *Mann-Kendall S values for indices dealing with other precipitation analysis. (a) Sum of precipitation amounts for days where daily precipitation exceeds the 95th percentile from the baseline period 1961-1990. (b) Sum of annual precipitation on wet days with rainfall > 1mm, over the number of wet days.*

3.4.2 **County Analysis**

Breaking down the point data into a country trend allows for an in-depth analysis over the United States as a pseudo spatial interpolation method. The indices were averaged over the counties in the same way they were over the NOAA climactic regions.

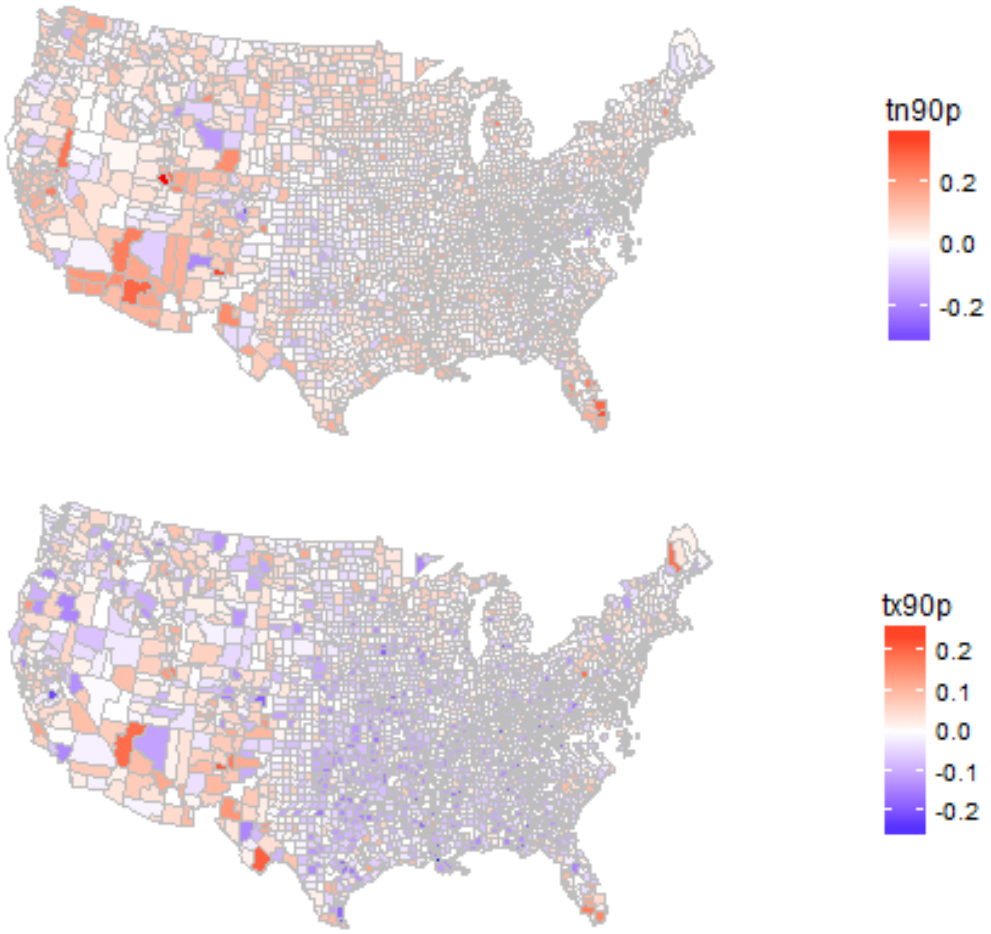

Figure 3.11: *Mean slope values for each county's 90th percentile indices. (a) Daily Minimum temperature. (b) Daily Maximum temperature*

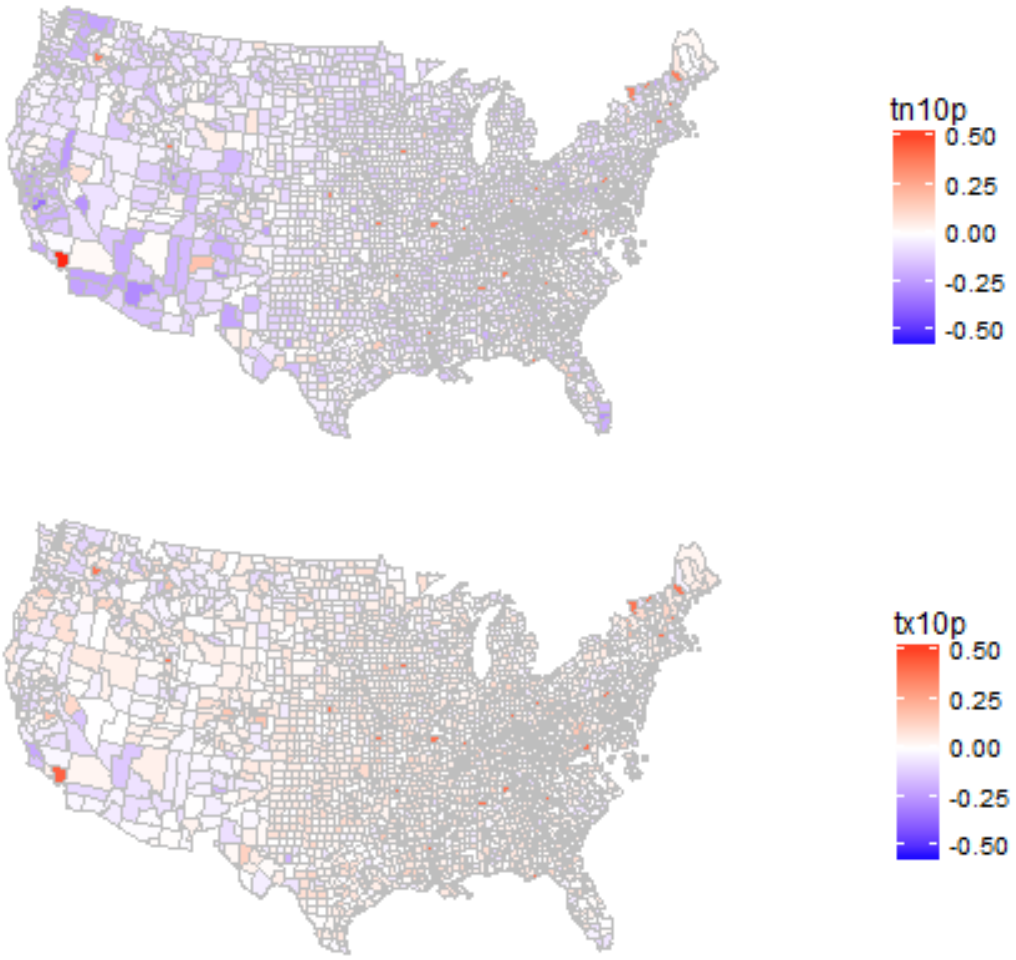

Figure 3.12: *Mean slope value for each county's 10th percentile indices. (a) Daily Minimum temperature (b) Daily Maximum temperature*

The county analysis takes the point data and summarizes it in a small scale without jumping to a broad scale that loses the variability seen in point data. This approach identifies counties that will undergo large shifts in these indices compared to all other counties. This captures spatial trends while summarizing these indices in a way that lends itself to further analysis. Since counties keep strong records of population change, land cover, and other data, these county values can be incorporated into future models that predict what changes in county level to various factors impacts shifts in extreme climate values.

This analysis does at times fail to capture strong trends in this analysis. As the USDA ARS weather data has some gaps in certain counties with weather station coverage and reporting, not all

counties are accounted for. In addition, the range of slope values in indices tends to be low, resulting in a range of values that does not represent changes well for all indices. Further refining of a gradient could fix this in large scale studies. At a local level, this analysis still will reveal county trends with numerous applications.

Counties across the country follow the pattern of higher daily minimum temperatures year to year with little change to a decrease in maximum daily temperatures. This is particularly evident in the western counties of the United States. The daily minimum temperatures in western counties are mostly staying above the 10^{th} percentile of daily minimum temperatures from the baseline period (Figure 3.12a). Daily maximum temperatures are barely changing in regards to the 10^{th} percentile with most counties hovering around a slope of zero (Figure 3.12b).

Due to the nature of the indices and an inconsistent spread of weather stations across every county in the United States, many areas go underrepresented in the analysis. However, this method allows for a closer look at how micro climates and individual differences between counties impact the increase or decrease of these indices.

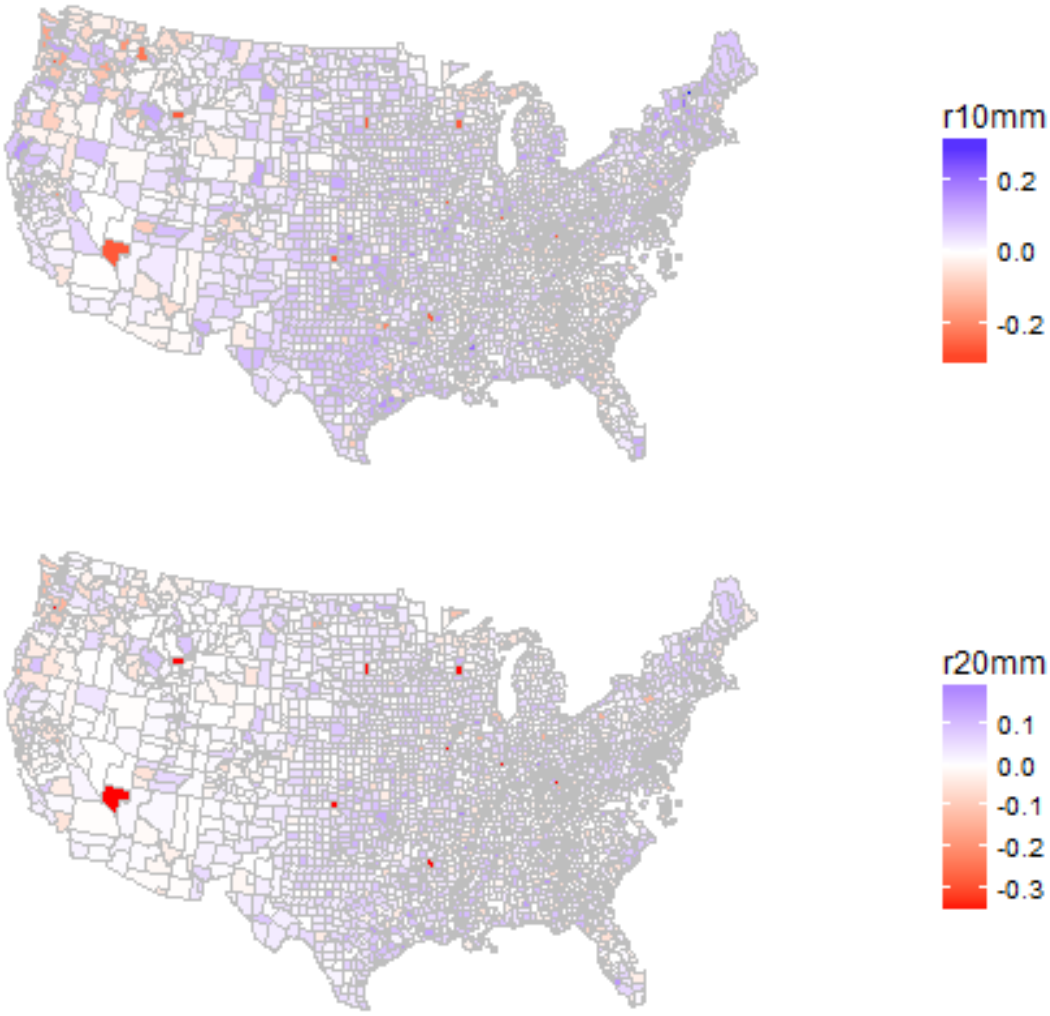

Figure 3.13: *Average slope values for each county's precipitation threshold indices. (a) Exceeding 10 mm. (b) Exceeding 20 mm.*

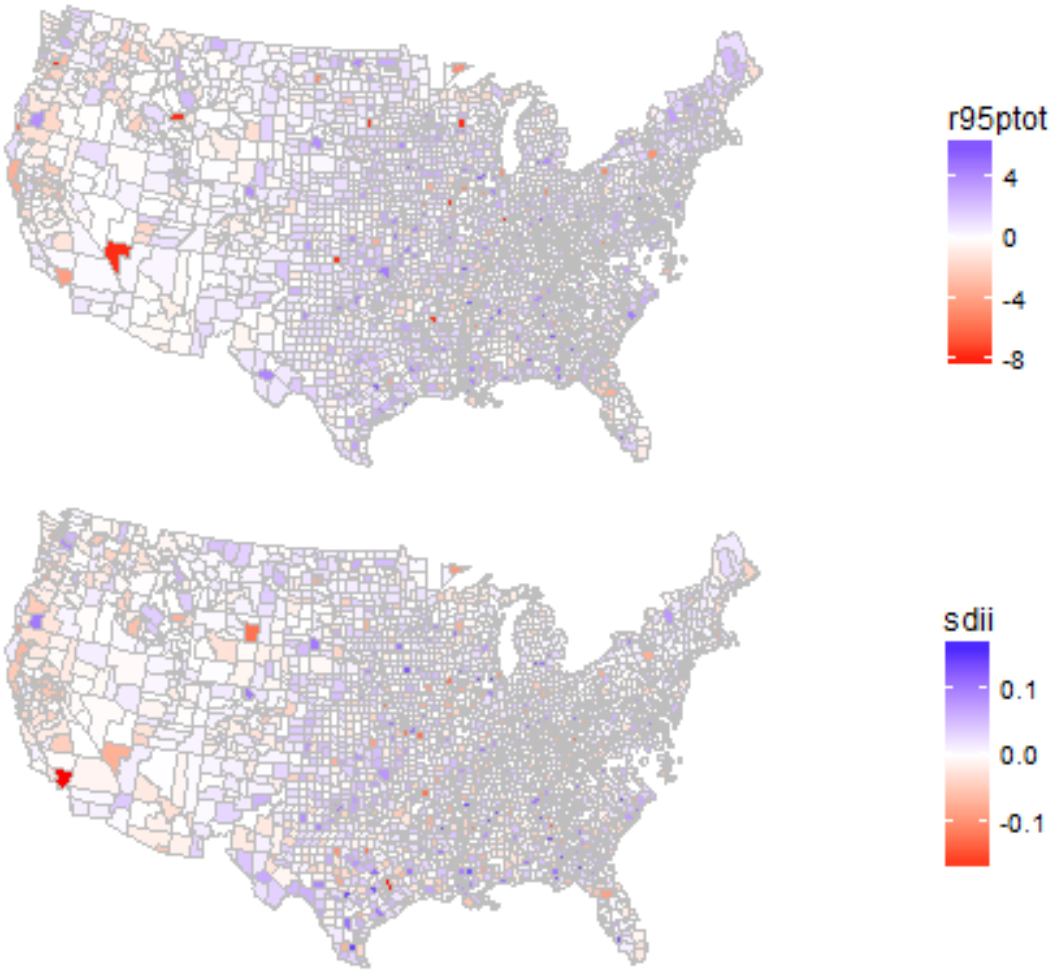

Figure 3.14: *Average slope values for each county's precipitation intensity indices. (a) Total precipitation for events exceeding the 95th percentile. (b) Annual precipitation intensity over all wet days.*

As with the temperature county analysis, the precipitation county analysis reveals interesting trends that can be further used in future analysis that uses county data over time to try to determine what changes have impacts on shifts in extreme climate trends. One notable example is Clark County in southern Nevada. Clark County is home to Las Vegas which has seen a large amount of urbanization and population growth over the past decades. With the R10mm, R20mm, and R95PTOT, Clark County has seen some of the largest shifts towards drying across the country (Figures 3.13a&b and Figure 3.14a).

Analyzing these trends in regards to changes in the area could reveal how things like urbanization influence climate trends in certain areas.

Precipitation analysis at the county level shows similar patterns to what point data demonstrated. Counties in the middle third of the country and the east coast are seeing more rainfall with the west coast and the southwest have not seen more rain or barely any changes at all. Intensity of rainfalls appears to be going up in a similar way with several counties seeing heavier rainfalls in the south and Mississippi Basin area (Figure 3.14).

3.4.3 NOAA Climactic Regions Analysis

Generalizing spatial trends across the country can better be accomplished using the NOAA climactic regions to summarize what is changing in different areas. The previous analysis that was done on a country wide level was repeated for each of the nine regions.

Table 3.4: *Mean slope values for temperature indices for each NOAA climactic region for observed weather data*

REGION	TN90P	TX90P	TN10P	TX10P
NORTHWEST	0.0643 (+/- 0.0926)	0.0297 (+/- 0.0771)	-0.0935 (+/- 0.1118)	-0.0427 (+/- 0.0839)
WEST	0.0762 (+/- 0.1502)	0.0138 (+/- 0.1163)	-0.1105 (+/- 0.1657)	-0.0194 (+/- 0.1122)
SOUTHWEST	0.0960 (+/- 0.1622)	0.0431 (+/- 0.1395)	-0.1036 (+/- 0.1447)	-0.0110 (+/- 0.0961)
SOUTH	0.0303 (+/- 0.0830)	-0.0527 (+/- 0.0829)	-0.0406 (+/- 0.0703)	0.0317 (+/- 0.0570)
WEST NORTH CENTRAL	0.0463 (+/- 0.0729)	0.0105 (+/- 0.0617)	-0.0563 (+/- 0.0623)	-0.0057 (+/- 0.0604)
EAST NORTH CENTRAL	0.0429 (+/- 0.0460)	0.0128 (+/- 0.0462)	-0.0664 (+/- 0.0561)	0.0062 (+/- 0.0488)
CENTRAL	0.0240 (+/- 0.0592)	-0.0463 (+/- 0.0628)	-0.0728 (+/- 0.0724)	0.0357 (+/- 0.0680)
NORTHEAST	0.0299 (+/- 0.0749)	0.0201 (+/- 0.0724)	-0.0471 (+/- 0.1218)	0.0308 (+/- 0.1072)
SOUTHEAST	0.0344 (+/- 0.0942)	-0.0199 (+/- 0.0882)	-0.0407 (+/- 0.0811)	0.0187 (+/- 0.0591)

The climactic region approach yields results consistent with the national trends. All regions have increasing minimum temperatures as seen by TN90P values in Table 3.4. TN10P has consistent decreases in all regions further supporting the trend that minimum temperatures have been on the rise. Maximum temperatures have largely been increasing as TX90P has increased in most regions except Central, Southeast, and South. The changes are all relatively small however. TX10P is also increasing in most regions indicating maximum temperatures are falling below the 10th percentile for maximum temperature.

Table 3.5: *Mean slope values for precipitation indices for each NOAA climactic region for observed weather data*

REGION	R10MM	R20MM	R95PTOT	SDII
NORTHWEST	-0.0462 (+/- 0.1193)	-0.0249 (+/- 0.0720)	-0.3941 (+/- 2.0721)	-0.0070 (+/- 0.0253)
WEST	0.0163 (+/- 0.0670)	-0.0040 (+/- 0.0501)	-0.4649 (+/- 1.9706)	-0.0147 (+/- 0.0453)
SOUTHWEST	0.0198 (+/- 0.0647)	0.0046 (+/- 0.0303)	0.1477 (+/- 0.9546)	-0.0004 (+/- 0.0335)
SOUTH	0.0640 (+/- 0.0491)	0.0420 (+/- 0.0473)	1.0366 (+/- 1.9706)	0.0167 (+/- 0.0669)
WEST NORTH CENTRAL	0.0229 (+/- 0.0542)	0.0111 (+/- 0.0263)	0.2832 (+/- 0.8888)	0.0048 (+/- 0.0242)
EAST NORTH CENTRAL	0.0388 (+/- 0.0576)	0.0231 (+/- 0.0396)	0.7133 (+/- 1.3202)	0.0070 (+/- 0.0241)
CENTRAL	0.0522 (+/- 0.0652)	0.0338 (+/- 0.0548)	0.9545 (+/- 1.7648)	0.0105 (+/- 0.0377)
NORTHEAST	0.0683 (+/- 0.0688)	0.0409 (+/- 0.0571)	1.2186 (+/- 1.8001)	0.0089 (+/- 0.0293)
SOUTHEAST	0.0094 (+/- 0.0643)	0.0127 (+/- 0.0628)	0.4050 (+/- 2.4301)	0.0022 (+/- 0.0547)

Heavy precipitation events across the country have risen with all but the Northwest rising in R10MM and all but the Northwest and the West rising in R20MM. These regions have low variability outside of the Northwest for both indices (Table 3.5). Rainfall intensities have been rising very quickly across several regions. The South and Northeast have experienced high values of R95PTOT indicating their heavy rainfalls have been getting heavier. RC95PTOT slopes have high variability in every single region (Table 3.5). While these heavy rainfalls have gotten more extreme, overall intensity throughout all

wet days have hardly changed in every region with SDII values barely reaching a slope of 0.01 in only the South and Central regions.

3.5 Conclusion

Historical analysis of ETCCDMI indices can reveal strong spatial and temporal trends of extreme weather events across the United States. By leveraging daily temperature and rainfall data, extreme events can be monitored to better explain how climate is changing across the country. These trends in extreme weather better explain how climate has been changing in different parts of the country as opposed to using average values. Furthermore, the effectively summarize large daily data sets in a way that is easy to understand and share with researchers.

The ETCCDMI indices for temperature reveal a striking trend of daily minimum temperatures rising over via the TN90P index. Meanwhile, maximum temperatures have not been changing much and in many cases, they go down slightly. This suggests the bulk of warming is coming in the form of days that never sufficiently cool off at night. Furthermore, daily minimum temperatures and daily maximum temperatures are falling below the 10^{th} percentile far less frequently over the span of 1950-2010. This again supports the general warming trend seen across the country and further shows that days are not cooling off as frequently.

These trends carry over into the regional approach taken. This approach better illustrates the spatial trends seen in the point data as it is easier to monitor which regions are changing and how severe the changes have been. County level analysis further breaks the country down and can allow local scientists and policy makers to better understand how their climate is changing and what extremes they can expect at a very local level.

This method of analyzing ETCCDMI indices over a span of time could potentially be used for monitoring climate changes in a region. With improvements to the fit given to a set of indices over a span of time, this method could potentially reveal strong trends that can be used to predict future shifts.

Furthermore, exploring further spatial trends such as land cover and topography around weather stations, better analysis and understanding can be achieved.

Chapter 4

GCM Historical Trends

4.1 Introduction

General Circulation Models (GCMs) aim to simulate climate changes given a set of interactions between the atmosphere, oceans, land masses, and sea ice. These models try to model the heat transfer between these systems to predict daily data for the coming century and beyond. Like most models, GCMs gain confidence from their ability to analyze and work with observed data (Miller et al., 2014). GCMs utilize observed data to bias correct their models and test for accuracy. Predicting shifts in climate can be very difficult since climate is impacted by several factors such as anthropogenic interference (Nazarenko et al., 2015). Using historical simulations allows researchers to better understand the fundamental issues that may arise when trying to predict something so variable as climate.

Before inspecting the usefulness of applying the ETCCMDI indices to future projected climate data, the indices first should be applied to historical simulations made by GCMs. Much like validating their models, this will test the validity of using these indices on GCM data. This study analyzes the trends in the climate indices over the simulation period of 1950-2005 at a point, regional, and county scale. Spatial and temporal trends were analyzed in the same way the observed historical data was analyzed.

These trends then were compared to the observed data set to see the differences between them via error calculations. Furthermore, the data was analyzed to simply check if they followed a similar broad spatial trend to that of the observed data. To compare directly, the GCM data was extracted at a point level at the same locations as the previously studied weather stations. This comparison can determine which GCMs best work with the climate indices in this study and how accurate they are compared to the weather data.

4.2 Literature Review

4.2.1 Global Climate Models

Global Climate Models (GCMs) attempt to combine mathematical models of the atmosphere, oceans, and sea ice to represent the Earth's climate system and the interactions and influences of these three components on the climate system (Climate Modeling, 2016). These models cover a large spectrum of methods to simulate the climate system and anticipate future changes. Of these models, one of the most widely used are General Circulation Models. In recent years, the terms Global Climate Model and General Circulation Model have been used interchangeably by the scientific community. While these two topics overlap, these terms are not completely synonymous as Global Climate Model is a broad term that encompasses many types of models. General Circulation Models attempt to simulate heat transfer in the atmosphere and oceans through the Navier-Stokes equations to model the climate system. These models are used extensively to study climate change and are useful in analyzing changes within a specified region (Flato et al., 2013).

In 1957, Norman Phillips created the first successful General Circulation Model. His work with Joseph Smagorinsky, head of the General Circulation Research Section (GCRS), lead to the improvement and expansion of General Circulation Models. Eventually, the GCRS was renamed to the Geophysical Fluid Dynamics Laboratory (GFDL) and has become one of the oldest and foremost modeling institutions. The GFDL has developed several General Circulation Models over its tenure, the most recent being the GFDL-CM3, the GFDL's major contribution to the IPCC Fifth Assessment Report. This iteration of their model improved over past models by including aerosol-cloud interactions, chemistry impacts on climate, linking the troposphere to the stratosphere, and generally updating and improving the land model (Griffies et al., 2011).

As climate research continued and developed, several other GCMs were created by research groups. The Community Climate System Model (CCSM) is a circulation model created by the University Corporation for Atmospheric Research (UCAR). The current model, the CCSM4, was developed in 2010

as an improvement on the CCSM3. The major improvements the CCSM4 made over the CCSM3 was the prediction of the climate effects from the El Niño-Southern Oscillation (ENSO) (Gent et al., 2011). The model incorporates several submodels developed by the working group, notably the Community Atmosphere Model and the Climatological Data Ocean Model.

These GCMs focus on predicting future climate trends through their advanced simulations. The GCMs have also been run on historical data to estimate past trends. The GFDL-CM3 and the CCSM4 both have been run to simulate past climate trends from 1950 through 2004 and 2005 respectively. The result is daily maximum temperature, minimum temperature, and precipitation data for the entire globe.

4.3 Methods

Before the ETCCMDI indices can be applied to future projected climate data from the CCSM4 and GFDL-CM3, a comparison must be made between the observed historical data and the historical simulations from these GCMs. The GCM data comes in a downscaled, bias corrected, multiband raster format. Each band represents a different day of the simulation with each multiband raster spanning about 10 years of daily data. Maximum temperature, minimum temperature, and daily precipitation are broken up into individual rasters. The daily value was extracted from each band of each raster and compiled for each weather station analyzed from the USDA database.

The 27 ETCCMDI indices were calculated over the span of GCMs simulation period. To analyze their change over time, a linear regression was fit to each index. The slope value of each regression was obtained for every weather station as an indicator of this change in climate over time. Regression analysis was also done to determine correctness of fit. The fit was forced upon the data to get an idea of general trend, regardless of fit.

Plots were made for each index, showing the changes of indices at the weather stations previously analyzed for observed climate data. These initial point value plots serve as the raw result to demonstrate trends. To summarize the results, the average slope values for each of the NOAA Climactic regions were

calculated to analyze regional trends. Finally, the average value of the indices' slope values was calculated for each county in the United States with weather stations present. This was done in an attempt at a simple interpolation method which could better explain what is happening between points.

This historical run for the GFDL-CM3 and CCSM4 were compared against the values from the historical observed data to test their accuracy. This was done at the point scale as well as at the NOAA Climactic Regions scale. A Root Mean Square Error (RMSE) and Mean Absolute Error (MAE) were calculated over all the weather stations and then within each region.

$$RMSE = \sqrt{\frac{\sum_{t=1}^{n}(\hat{y}_t - y_t)^2}{n}}$$

$$MAE = \frac{1}{n}\sum_{t=1}^{n}|\hat{y}_t - y_t|$$

4.4 Results and Discussion

For this study, eight of the ETCCMDI indices were selected for close analysis: TN90P, TX90P, TN10P, TX20P, R10mm, R20mm, R95PTOT, and SDII. The first four indices pertain to temperature with a color scheme for plotting of blue indicating a decrease (cooling trend) and red indicating an increase (warming trend). The last four pertain to precipitation with a color scheme for plotting of red indicating a decrease (drier conditions) and blue indicating an increase (wetter conditions).

4.4.1 **GFDL-CM3 Point Values**

The point values for the GFDL-CM3 were calculated at each weather station's coordinates. The slope values for the linear regressions represent the change in climate conditions. A larger circle indicates a larger slope and therefore more rapid change.

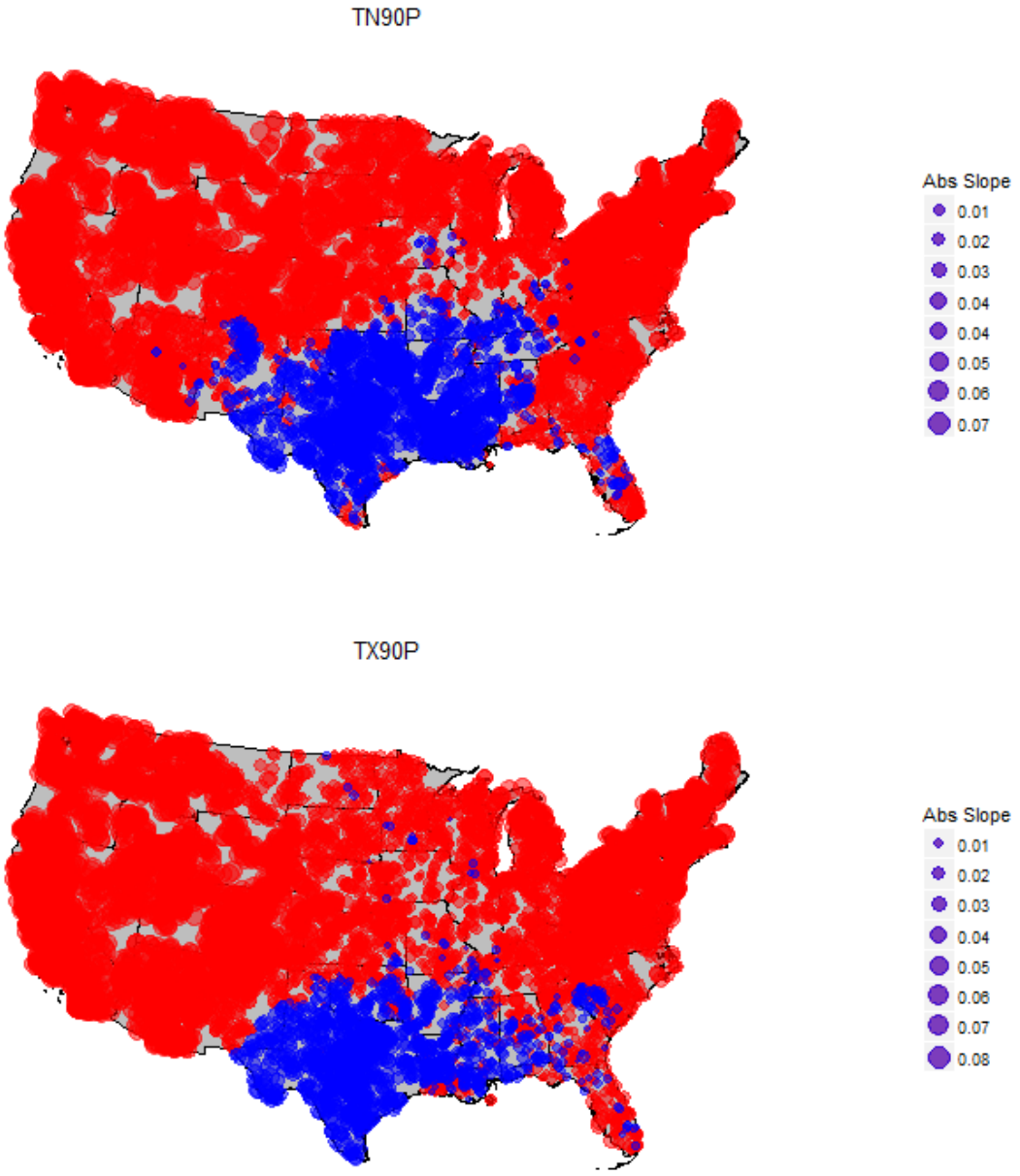

Figure 4.1: *Slope values for indices dealing with counts of days above the 90th percentile using the GFDL-CM3 historical simulation. (a) Daily minimum temperature across the United States. (b) Daily Maximum temperature across the United States. Larger points indicate greater change.*

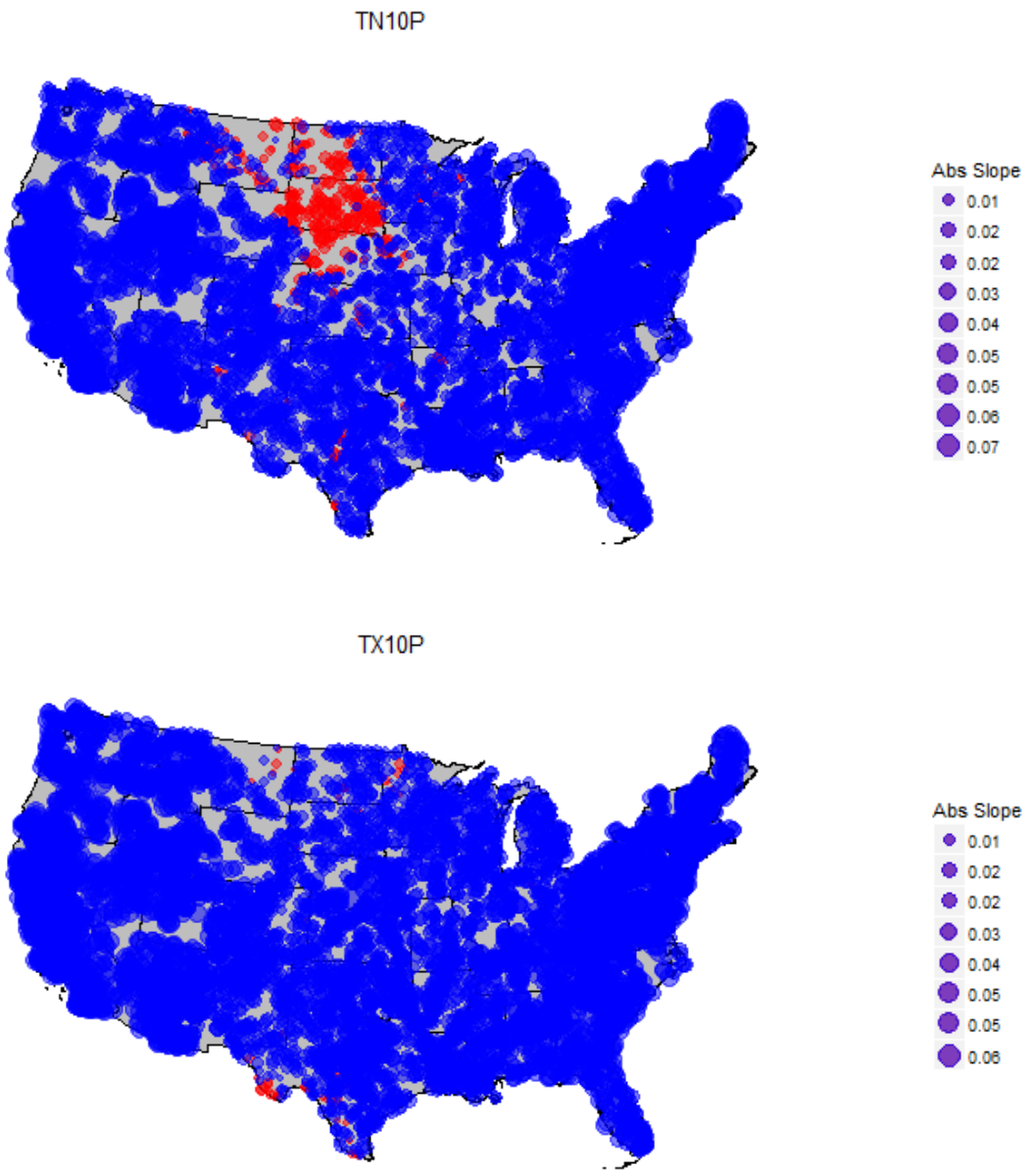

Figure 4.2: *Slope values for indices dealing with counts of days below the 10th percentile from the GFDL-CM3 historical simulation. (a) Daily minimum temperature across the United States. (b) Daily Maximum temperature across the United States. Larger points indicate greater change.*

The first thing to notice with GCM results is how uniform they can be in regards to temperature. GCMs utilize grids over the United States at a resolution of 1/8 of a degree, or about 140 km^2, in size. While these GCMs have becoming finer in their resolution and more accurate, they still tend to be broad in their estimation. Furthermore, they do not capture the subtle differences between different weather stations. They already take into account several factors as it is, but they cannot capture everything that influences climate at local levels.

As seen in Figure 4.1, a general warming trend can be observed across the United States both in regards to maximum daily temperature and minimum daily temperature. Most of the nation has experienced an increase in the percent of days maximum and minimum temperature exceed the 90^{th} percentile from the baseline period. The exception to this being the pocket in the south which has seen a decrease in both indices (Figure 4.1). On the low end of the spectrum, there has been an almost uniform decrease in the number of days going below the 10^{th} percentile both for maximum daily temperature and minimum daily temperature.

These indices show a general warming trend across the country per the GFDL-CM3 historical simulations. This is occurring both with minimum daily temperatures and maximum daily temperatures with some exceptions in small pockets such as the south. These changes are gradual as indicating by the relatively small slope values calculated. The slope values when averaged across the nation all indicate patterns of warming, however with very little confidence in average linear fit (Table 4.1).

Table 4.1: *Regression values for the GFDL-CM3 historical temperature indices summarized over the entire data set for the United States*

INDEX	MEAN VALUE	MEAN R^2	MEAN F-TEST P-VALUE
TN90P	0.0215	0.0220	0.4032
TX90P	0.0287	0.0200	0.4423
TN10P	-0.0201	0.0100	0.5597
TX10P	-0.0267	0.0130	0.4783

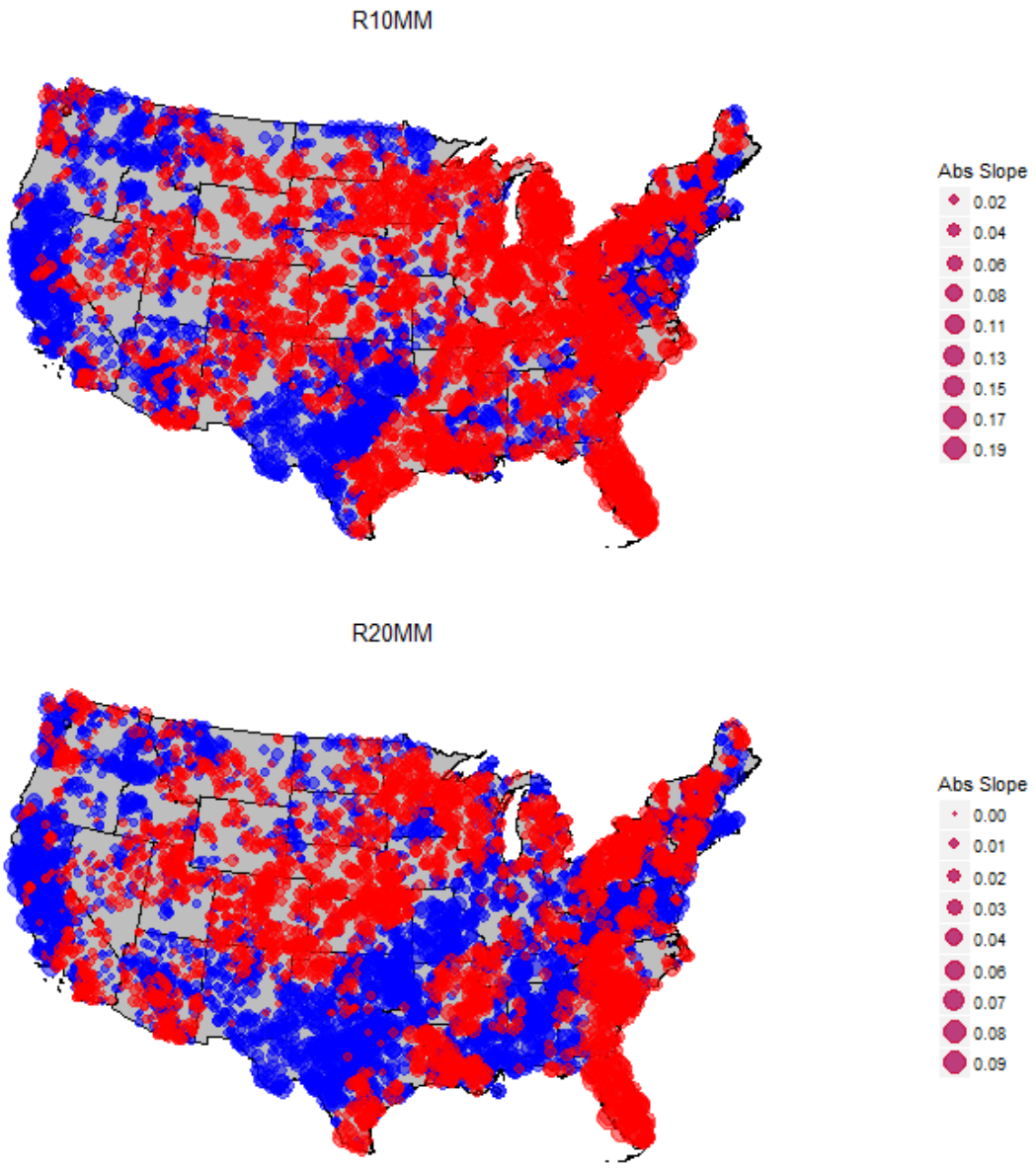

Figure 4.3: *Slope values for indices dealing with counts of days exceeding precipitation amounts using the GFDL-CM3 historical simulation. (a) 10mm daily rainfall. (b) 20mm daily rainfall. Larger points indicate greater change with blue indicating an increase slope value (more rainfall).*

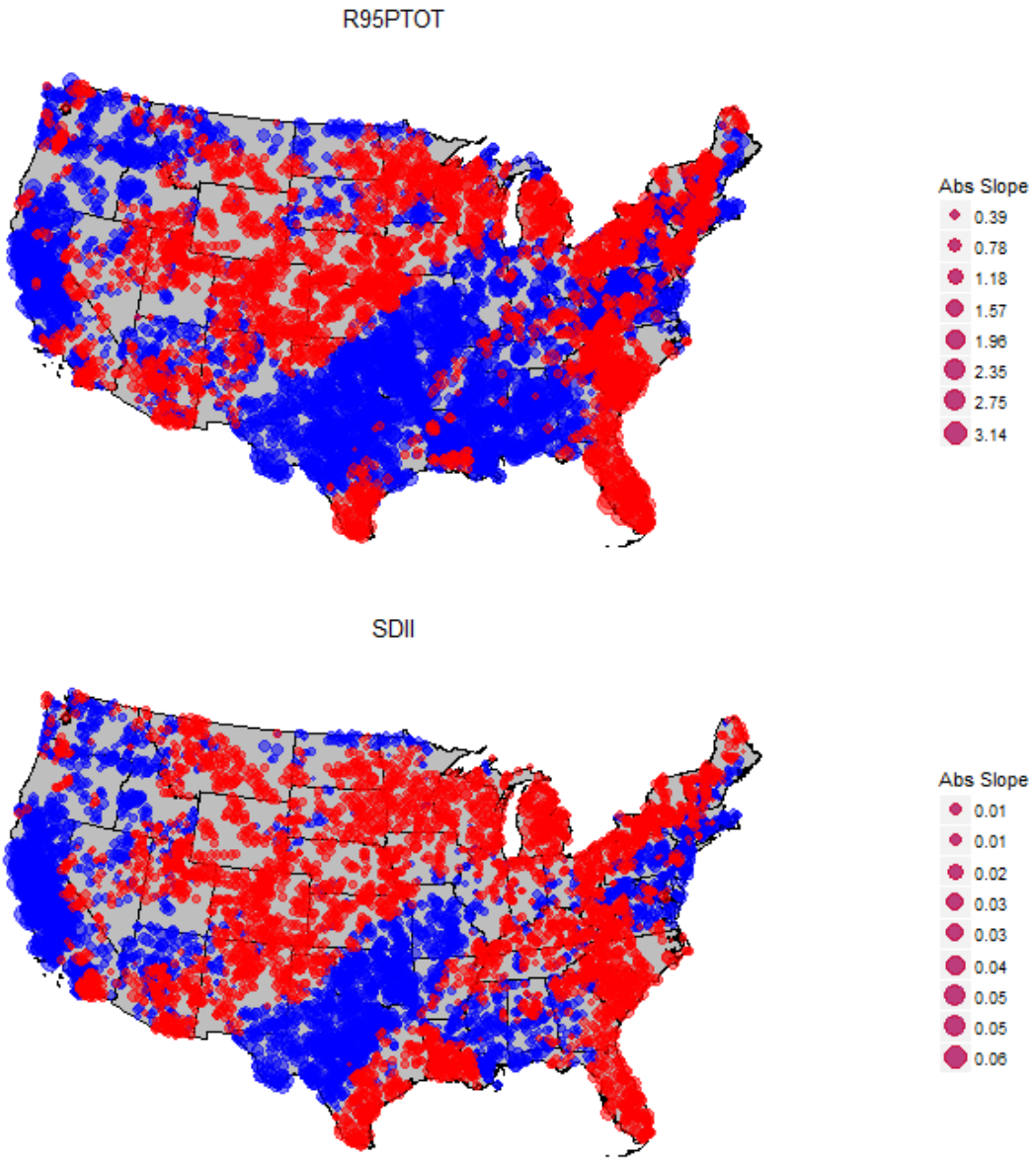

Figure 4.4: *Slope values for indices dealing with other precipitation analysis using the GFDL-CM3 historical simulation. (a) Sum of precipitation amounts for days where daily precipitation exceeds the 95th percentile. (b) Sum of annual precipitation on wet days with rainfall > 1mm, over the number of wet days.*

Precipitation indices are much less uniform over the country as temperature indices are. The GFDL-CM3 shows an increase of days with strong rainfalls on the west coast, parts of the northeast, and a band stretching from Texas up to the Great Lakes (Figure 4.3). The changes in strong daily precipitation is more rapid with R10mm compared to R20mm as very strong rains have mostly lower slope values. With rainfall intensity, the R95PTOT values follow similar spatial trends to that of the R10mm and

R20mm (Figure 4.3a). However, the R95PTOT values appear to be undergoing rapid increases in areas where increases are evident, indicating that heavy precipitation events breaching the 95th percentile have been creating drastically more rainfall over time. The SDII values have experienced very limited change across the country, indicating overall intensity over every precipitation event has not been changing very much (Figure 4.4b).

Nationwide, average change in index value is very small except for R95PTOT (Table 4.2). R10mm on average is decreasing with R20mm increasing. However, again the confidence of fit in these values is very low which is expected.

Table 4.2: *Regression values for GFDL-CM3 historical precipitation indices summarized over the entire data set for the United States*

INDEX	MEAN VALUE	MEAN R^2	MEAN F-TEST P-VALUE
R10MM	-0.0046	0.0113	0.5864
R20MM	0.0022	0.0143	0.5361
R95PTOT	0.1436	0.0153	0.5315
SDII	0.0010	0.0169	0.5200

4.4.2 GFDL-CM3 NOAA Climactic Regions

For each climactic region, the mean slope and standard deviation for each index found using the GFDL-CM3 data was calculated to summarize the indices at a regional scale. These results demonstrate the variability of results when inspecting different parts of the country for their respective trends.

Table 4.3: *Mean slope values for temperature indices for each NOAA climactic region for the GFDL-CM3 historical simulation*

REGION	TN90P	TX90P	TN10P	TX10P
NORTHWEST	0.0487 (+/- 0.0108)	0.0557 (+/- 0.0090)	0.0487 (+/- 0.0113)	-0.0370 (+/- 0.0110)
WEST	0.0408 (+/- 0.0123)	0.0623 (+/- 0.0101)	0.0408 (+/- 0.0087)	-0.0445 (+/- 0.072)
SOUTHWEST	0.0258 (+/- 0.0191)	0.0508 (+/- 0.0182)	0.0258 (+/- 0.0108)	-0.0285 (+/- 0.0109)
SOUTH	-0.0144 (+/- 0.0187)	-0.0090 (+/- 0.0179)	-0.0144 (+/- 0.0077)	-0.0170 (+/- 0.0075)
WEST NORTH CENTRAL	0.0431 (+/- 0.0147)	0.0331 (+/- 0.0154)	0.0431 (+/- 0.0127)	-0.0184 (+/- 0.0094)
EAST NORTH CENTRAL	0.0272 (+/- 0.0111)	0.0203 (+/- 0.0107)	0.0272 (+/- 0.0088)	-0.0174 (+/- 0.0080)
CENTRAL	0.0122 (+/- 0.0138)	0.0226 (+/- 0.0121)	0.0122 (+/- 0.0082)	-0.0227 (+/- 0.0073)
NORTHEAST	0.0370 (+/- 0.0103)	0.0415 (+/- 0.0067)	0.0370 (+/- 0.0130)	-0.0307 (+/- 0.0100)
SOUTHEAST	0.0171 (+/- 0.0138)	0.0134 (+/- 0.0145)	0.0171 (+/- 0.0077)	-0.0311 (+/- 0.0082)

Days with temperatures exceeding the 90th percentile increased across almost all regions in regards to both daily minimum temperature and daily maximum temperature (Table 4.3). As the point data suggested, only the South saw decreases in both TN90P and TX90P in the GFDL historical simulation. TN10P rose across all regions except the South showing that minimum temperatures were going under the 10th percentile more often as time went on in the simulation. On the other hand, TX10P decreased in every region which shows that across the country, daily maximum temperature was going below the 10th percentile far less often, indicating an overall warming pattern.

The standard deviations for each region are quite high when compared to the average slope value for the region. Many regions, such as the Southeast in regards to TN90P and TX90P, have standard deviation values that can result in some weather stations having a completely opposite trend as the average, all within one standard deviation value (Table 4.3).

Table 4.4: *Mean slope values for precipitation indices for each NOAA climactic region for the GFDL-CM3 historical simulation*

REGION	R10MM	R20MM	R95PTOT	SDII
NORTHWEST	0.0111 (+/- 0.0233)	0.0065 (+/- 0.0162)	0.2343 (+/- 0.4101)	0.0017 (+/- 0.0027)
WEST	0.0209 (+/- 0.0241)	0.0128 (+/- 0.0190)	0.3797 (+/- 0.5778)	0.0110 (+/- 0.0119)
SOUTHWEST	-0.0029 (+/- 0.0188)	-0.0017 (+/- 0.0092)	-0.1226 (+/- 0.3028)	-0.0015 (+/- 0.0035)
SOUTH	0.0052 (+/- 0.0357)	0.0068 (+/- 0.0209)	0.6349 (+/- 0.7763)	0.0037 (+/- 0.0075)
WEST NORTH CENTRAL	-0.0047 (+/- 0.0217)	-0.0032 (+/- 0.0112)	-0.1315 (+/- 0.3400)	-0.0024 (+/- 0.0027)
EAST NORTH CENTRAL	-0.0237 (+/- 0.0288)	-0.0065 (+/- 0.0151)	-0.2939 (+/- 0.4334)	-0.0038 (+/- 0.0033)
CENTRAL	-0.0256 (+/- 0.0295)	0.0077 (+/- 0.0191)	0.3318 (+/- 0.5895)	-0.0003 (+/- 0.0038)
NORTHEAST	-0.0031 (+/- 0.0288)	-0.0022 (+/- 0.0159)	-0.1225 (+/- 0.4182)	-0.0001 (+/- 0.0028)
SOUTHEAST	-0.0310 (+/- 0.0470)	-0.0051 (+/- 0.0293)	-0.1049 (+/- 0.8816)	-0.0032 (+/- 0.0049)

Precipitation tends to be far more variable by region in the GFDL historical simulation than temperature. The Northwest, the West, and the South saw increase in the R10mm while these regions plus the Central region saw an increase in R20mm (Table 4.4). All other areas of the country saw decreases on average indicating less heavy rainfall events there. R92PTOT has very large average slope values for all regions, particularly in the Northwest, West, South, and Central regions where the index increased over time in the simulation. However, the SDII slopes had very low shifts indicating the overall intensity for the year barely changed during the simulation.

4.4.3 GFLD-CM3 RMSE and AME Analysis

RMSE and AME was calculated to find the error between the GFDL-CM3 historical simulation's index values and the observed USDA climate data's index values. This was done at both a nationwide and regional level.

Table 4.5: *Nationwide error between the GFDL-CM3 historical simulation and observed data*

INDEX	RMSE	MAE
TN90P	0.1106	0.0800
TX90P	0.0990	0.0723
TN10P	0.1193	0.0861
TX10P	0.1106	0.0800
R10MM	0.0886	0.0676
R20MM	0.0588	0.0426
R95PTOT	1.9741	1.4131
SDII	0.0468	0.0331

Given the relatively small nature of the slopes calculated for these indices, the error values are decently high. The values likely rise due to the nature of GCM predictions being done over a grid. These GCM grid values do not capture all the subtle differences between each of the weather stations leading to a broader prediction that can be off.

Table 4.6: *RMSE and MAE between the GFDL-CM3 historical simulation data and the observed historical data for each NOAA Climactic Region*

		TN90p	TX90P	TN10P	TX10P	R10mm	R20mm	R95pTOT	SDII
Northwest	RMSE	0.0943	0.0806	0.1328	0.0867	0.1335	0.0815	4.218	0.0269
	MAE	0.0728	0.0627	0.1032	0.0628	0.0885	0.0471	1.355	**0.0185**
West	RMSE	0.1549	0.1264	0.1808	0.1151	0.0693	0.0558	4.268	0.0548
	MAE	0.1203	0.0928	0.1438	0.0851	0.0483	0.0366	1.406	0.0391
Southwest	RMSE	0.1776	0.1407	0.1670	0.0969	0.0727	0.0329	1.059	0.0339
	MAE	0.1374	0.1033	0.1311	0.0718	0.0547	0.0233	0.7985	0.0249
South	RMSE	0.0976	0.0961	0.0750	0.0758	0.0814	0.0618	4.159	0.0689
	MAE	0.0796	0.0760	0.0537	0.0594	0.0667	0.0482	1.623	0.0529
West North Central	RMSE	0.0733	0.0630	0.0825	0.0611	0.0667	0.0337	1.081	**0.0255**
	MAE	0.0563	0.0490	0.0676	0.0450	0.0507	0.0253	0.8386	0.0190
East North Central	RMSE	0.0471	0.0445	0.0762	0.0544	0.0910	0.0506	1.679	0.0266
	MAE	0.0365	0.0355	0.0622	0.0448	0.0759	0.0407	1.338	0.0202
Central	RMSE	0.0627	0.0932	0.0915	0.0891	0.1060	0.0600	1.867	0.0390
	MAE	0.0502	0.0755	0.0720	0.0686	0.0890	0.0484	1.471	0.0300
Northeast	RMSE	0.0756	0.0754	0.1262	0.1245	0.1024	0.0726	4.265	0.0308
	MAE	0.0549	0.0521	0.0844	0.0776	0.0832	0.0571	1.812	0.0242
Southeast	RMSE	0.0946	0.0923	0.0809	0.0778	0.0715	0.0877	4.536	0.0551
	MAE	0.0713	0.0711	0.0622	0.0641	0.0566	0.0663	1.940	0.0422

4.4.4 **CCSM4 Point Values**

As with the GFDL-CM3, the CCSM4 data was used to calculate slope values for each weather station. These values were first plotted as point values across the country as a raw data set. The size of the circle indicates how rapid a change occurred, with the same color scheme as before.

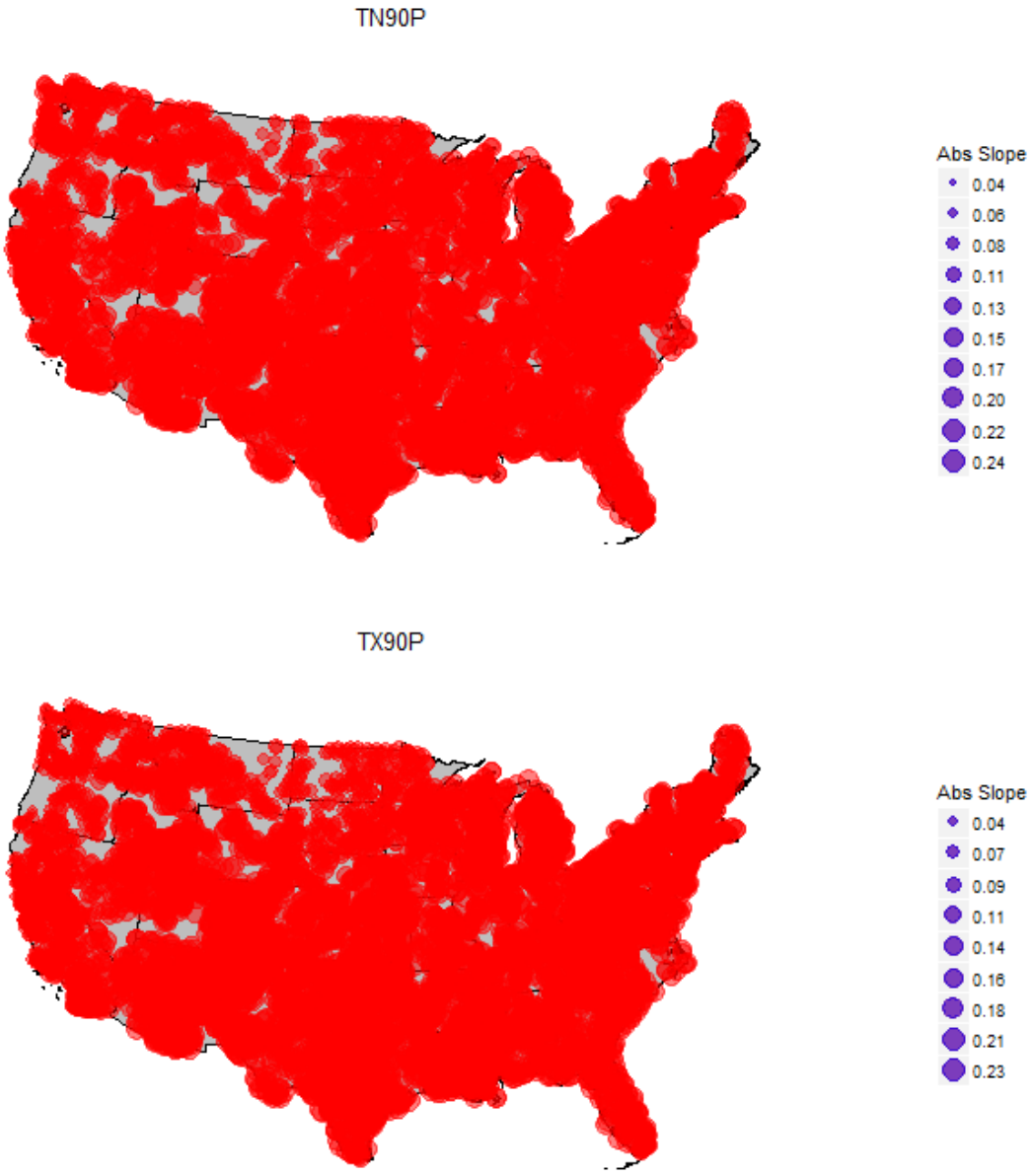

Figure 4.5: *Slope values for indices dealing with counts of days above the 90th percentile using the CCSM4 historical simulation. (a) Daily minimum temperature across the United States. (b) Daily Maximum temperature across the United States. Larger points indicate greater change.*

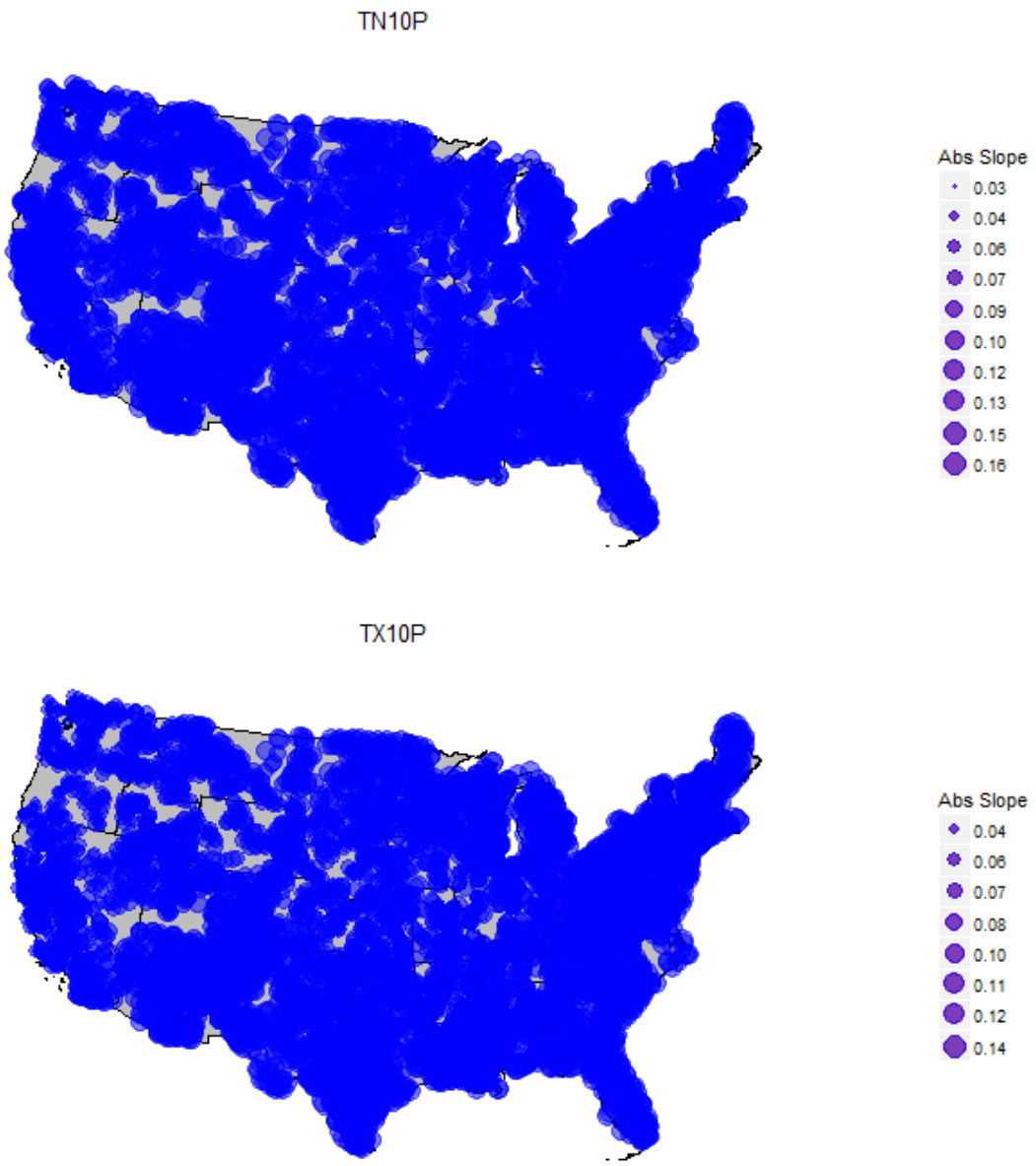

Figure 4.6: *Slope values for indices dealing with counts of days below the 10th percentile from the CCSM4 historical simulation. (a) Daily minimum temperature across the United States. (b) Daily Maximum temperature across the United States. Larger points indicate greater change.*

The CCSM4 historical simulation indicates similar trends to that of the GFDL-CM3 in regards to extreme temperature trends. There is a virtual uniform increase in the number of days exceeding the 90th percentile both form minimum and maximum daily temperature (Figure 4.5). Furthermore, as Figure 4.6 shows, there is a decrease across the entire country of days that fall below the 10th percentile both in maximum and minimum temperature. The CCSM4 historical simulation indicates a nationwide warming

trend in regards to these indices in the point data with very few exceptions.

The nationwide averages tell the same story, indicating an increase across the country in TN90P and TX90P, as well as a decrease in TN10P and TX10P (Table 4.7). While the fit of this regression is very low, this still indicates a general trend of warming in the CCSM4 historical simulation.

Table 4.7: *Regression values for the CCSM4 historical temperature indices summarized over the entire data set for the United States*

INDEX	MEAN VALUE	MEAN R^2	MEAN F-TEST P-VALUE
TN90P	0.1431	0.2571	0.0011
TX90P	0.1489	0.1937	0.0109
TN10P	-0.1044	0.0165	0.0062
TX10P	-0.0922	0.0148	0.0368

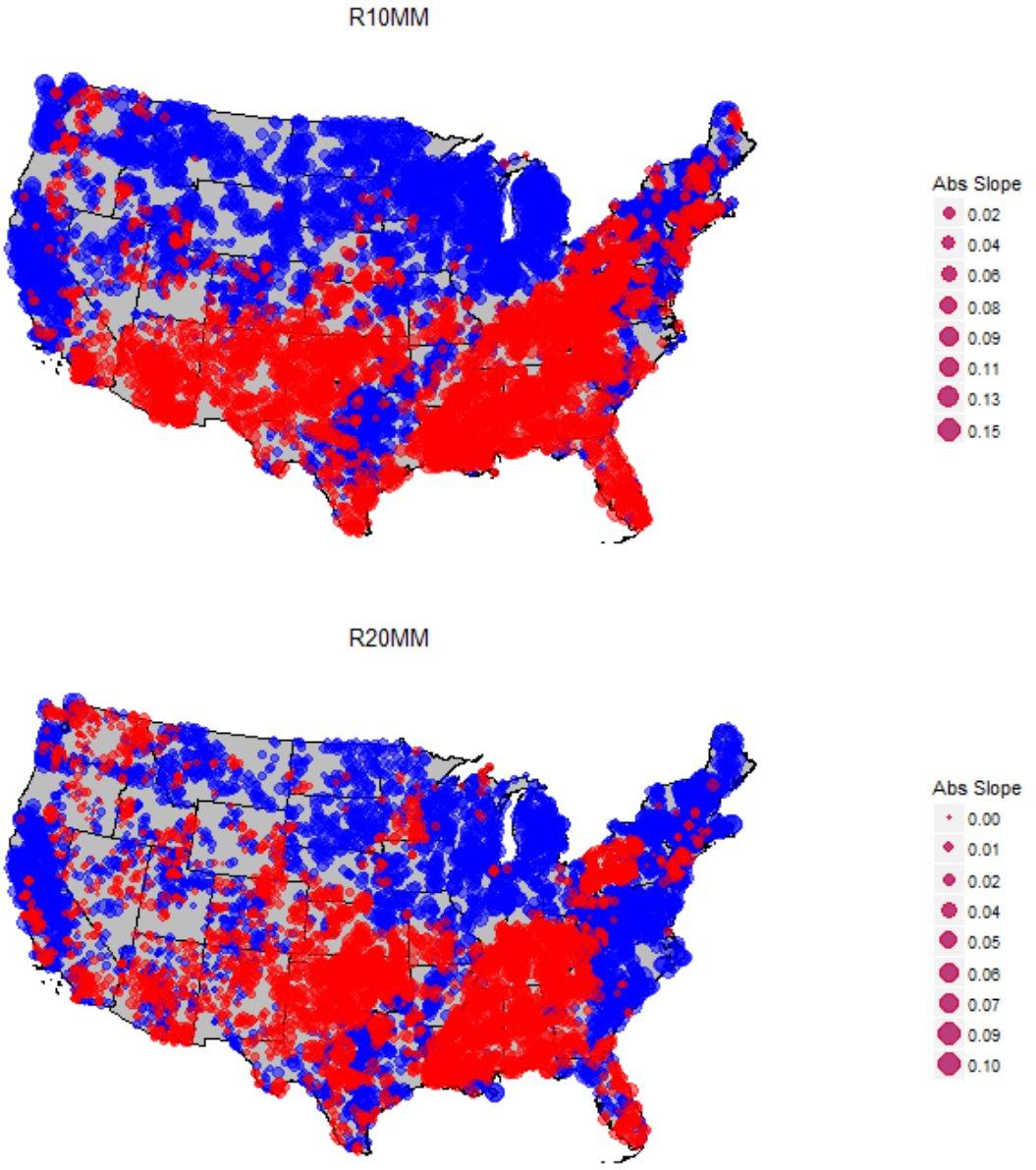

Figure 4.7: *Slope values for indices dealing with counts of days exceeding precipitation amounts using the CCSM4 historical simulation. (a) 10mm daily rainfall. (b) 20mm daily rainfall. Larger points indicate greater change with blue indicating an increase slope value (more rainfall).*

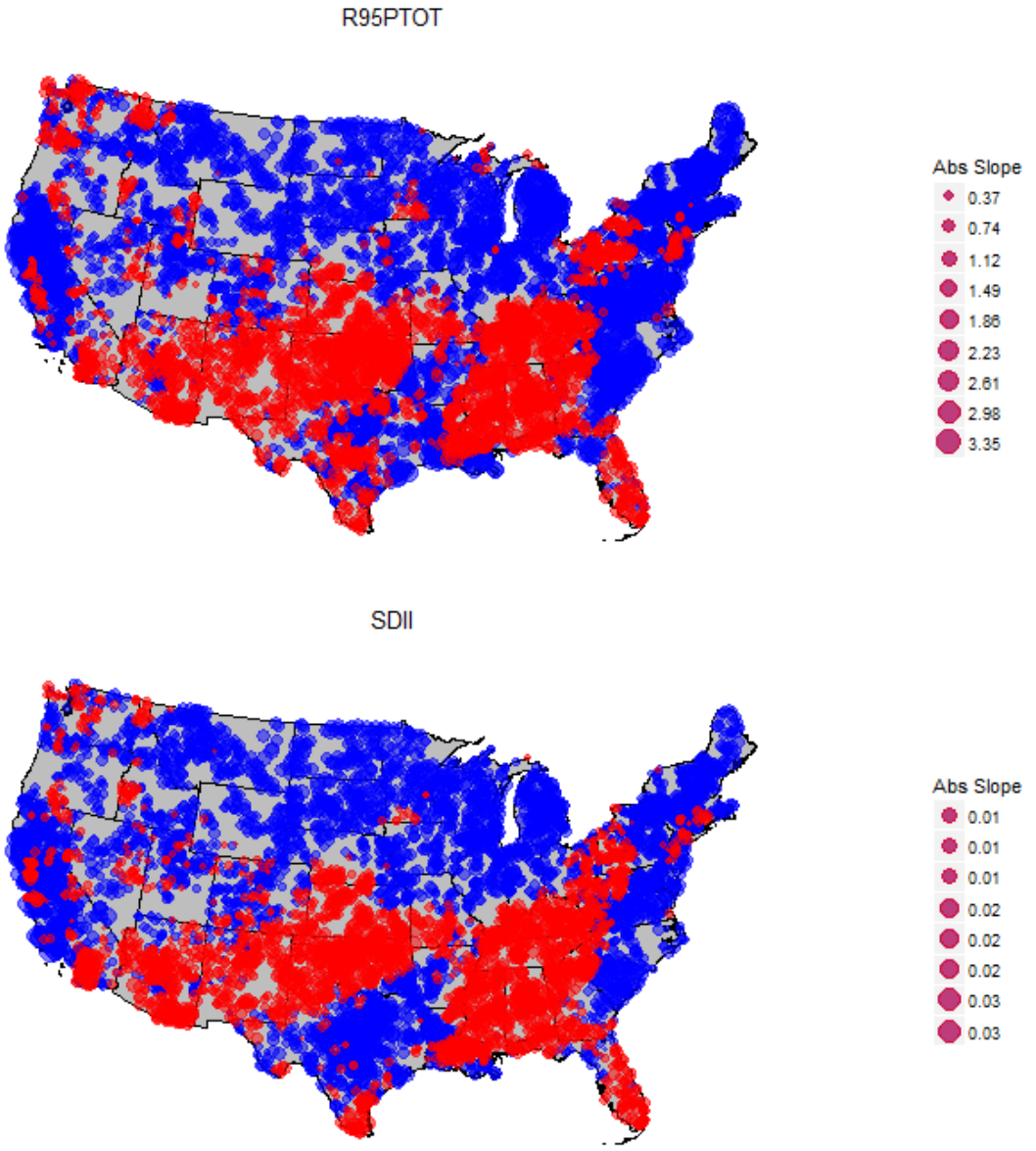

Figure 4.8: *Slope values for indices dealing with other precipitation analysis using the CCSM4 historical simulation. (a) Sum of precipitation amounts for days where daily precipitation exceeds the 95th percentile. (b) Sum of annual precipitation on wet days with rainfall > 1mm, over the number of wet days*

As with the GFDL-CM3, precipitation in the historical simulation is much more variable over the country. Much of the West Coast, Great Lakes, Northeast, and parts of the South showed increases in heavy rainfalls via the R10mm and R20mm indices (Figure 4.7). Large chunks of the South and Southwest have seen a drying trend however per these indices. Rainfall intensity follows a very similar pattern as R95PTOT and SDII have similar spatial trends to R10mm and R20mm (Figure 4.8). R95PTOT

has very large slope values compared to the SDII slope values, indicating intensity on a whole is not changing much, but the intensity of extreme events is changing rapidly.

National averages indicate an increase in heavy precipitation as indicated by average R10mm and R20mm (Table 4.8). Intensity has also increased, although as with other cases, the CCSM4 shows more increase in extreme rainfall intensity via the R95PTOT as opposed to overall intensity via the SDII.

Table 4.8: *Regression values for CCSM4 historical precipitation indices summarized over the entire data set for the United States*

INDEX	MEAN VALUE	MEAN R^2	MEAN F-TEST P-VALUE
R10MM	0.0035	0.0131	0.5472
R20MM	0.0033	0.0155	0.5207
R95PTOT	0.1807	0.0165	0.5103
SDII	0.0014	0.0148	0.5229

4.4.5 CCSM4 NOAA Climactic Regions

As was done with the GFDL-CM3, the CCSM4 index values were averaged over the NOAA Climactic Regions. Results indicate regional trends in the CCSM4 historical simulation and aim to summarize the indices better than national average can.

Table 4.9: *Mean slope values for temperature indices for each NOAA climactic region for the CCSM4 historical simulation*

REGION	TN90P	TX90P	TN10P	TX10P
NORTHWEST	0.1142 (+/- 0.0168)	0.0959 (+/- 0.0331)	-0.0859 (+/- 0.0107)	-0.0619 (+/- 0.0112)
WEST	0.1094 (+/- 0.0247)	0.0994 (+/- 0.0385)	-0.0875 (+/- 0.0120)	-0.0616 (+/- 0.0157)
SOUTHWEST	0.1558 (+/- 0.0295)	0.1898 (+/- 0.0180)	-0.1053 (+/- 0.0140)	-0.0922 (+/- 0.0137)
SOUTH	0.1697 (+/- 0.0182)	0.1824 (+/- 0.0134)	-0.1090 (+/- 0.0213)	-0.0960 (+/- 0.0144)
WEST NORTH CENTRAL	0.1266 (+/- 0.0236)	0.1114 (+/- 0.0321)	-0.0974 (+/- 0.0120)	-0.0813 (+/- 0.0143)
EAST NORTH CENTRAL	0.1339 (+/- 0.0102)	0.1343 (+/- 0.0174)	-0.0948 (+/- 0.0088)	-0.1037 (+/- 0.0129)
CENTRAL	0.1429 (+/- 0.0120)	0.1565 (+/- 0.0123)	-0.1050 (+/- 0.0137)	-0.0937 (+/- 0.0124)
NORTHEAST	0.1374 (+/- 0.0106)	0.1345 (+/- 0.0088)	-0.1051 (+/- 0.0108)	-0.1168 (+/- 0.0092)
SOUTHEAST	0.1560 (+/- 0.0152)	0.1678 (+/- 0.0179)	-0.1350 (+/- 0.0119)	-0.1092 (+/- 0.0100)

Compared to the GFDL-CM3, the CCSM4 historical simulation predicted uniform and much more intense temperature increases. Every region saw a rise in days with maximum and minimum temperatures exceeding the 90th percentile (Table 4.9). The days when these temperatures fell below the 10th percentile also decreased, resulting in a clear warming trend. The deviations in the weather stations is also relatively low indicating most stations in the regions reflect the trends.

Table 4.10: *Mean slope values for precipitation indices for each NOAA climactic region for the CCSM4 historical simulation*

REGION	R10MM	R20MM	R95PTOT	SDII
NORTHWEST	0.0269 (+/- 0.0356)	0.0028 (+/- 0.0137)	0.1041 (+/- 0.3519)	0.0011 (+/- 0.0021)
WEST	0.0181 (+/- 0.0228)	0.0119 (+/- 0.0182)	0.4737 (+/- 0.7411)	0.0040 (+/- 0.069)
SOUTHWEST	-0.0087 (+/- 0.0249)	-0.0005 (+/- 0.0071)	-0.0599 (+/- 0.3251)	-0.0007 (+/- 0.0028)
SOUTH	-0.0165 (+/- 0.0381)	-0.0097 (+/- 0.0212)	-0.1919 (+/- 0.7248)	-0.0003 (+/- 0.0067)
WEST NORTH CENTRAL	0.0284 (+/- 0.0220)	0.0070 (+/- 0.0091)	0.3855 (+/- 0.2725)	0.0044 (+/- 0.0032)
EAST NORTH CENTRAL	0.0556 (+/- 0.0254)	0.0172 (+/- 0.0152)	0.6652 (+/- 0.4797)	0.0059 (+/- 0.0030)
CENTRAL	-0.0064 (+/- 0.0489)	-0.0003 (+/- 0.0278)	-0.0241 (+/- 0.7731)	-0.0008 (+/- 0.0055)
NORTHEAST	0.0108 (+/- 0.0289)	0.0159 (+/- 0.0185)	0.5494 (+/- 0.5082)	0.0028 (+/- 0.0027)
SOUTHEAST	-0.0283 (+/- 0.0371)	0.0005 (+/- 0.0295)	0.2223 (+/- 0.8746)	-0.0007 (+/- 0.0051)

The CCSM4 historical simulation predicted more extreme precipitation than the GFDL-CM3 appears to. On a regional basis, the CCSM4 predicted all but the South, Southwest, Southeast, and Central regions received more high precipitation events per the R10mm and R20mm indices (Table 4.10). The CCSM4 like the GFDL-CM3 has R95PTOT depicting very high intensity shifts in extreme events especially in the West, East North Central, West North Central, and Northeast. Like the GFDL-CM3, the CCSM4 shows very minimal change in the overall intensity across each region.

Standard deviations for the R10mm are noticeably high as one standard deviation could flip the trend in some regions (Table 4.10). The R20mm on the other hand has much lower standard deviation

values. The RCP95TOT has again the highest deviation as regions tend to see great variability between their stations 95th percentile precipitation event intensities.

4.4.6 CCSM4 RMSE and MAE Analysis

Index values obtained from the CCSM4 historical analysis were compared against the index values obtained from the observed weather data from the USDA database. This was done with by calculating RMSE and MAE to see how close the GCM data matched the actual data. This was done on national and regional level.

Table 4.11: *Nationwide error between the CCSM4 historical simulation and observed data*

INDEX	RMSE	MAE
TN90P	0.1462	0.1206
TX90P	0.1887	0.1624
TN10P	0.1181	0.0865
TX10P	0.1356	0.1149
R10MM	0.0867	0.0654
R20MM	0.0595	0.0423
R95PTOT	4.0011	1.4050
SDII	0.0461	0.0322

The error between the CCSM4 historical index slope values and the observed values is relatively high given the slope values are rather small. The CCSM4 seems to line up much better in the cases of observing maximum temperatures and precipitation (Table 4.11). The R95PTOT has high error but it is the index that was largely the most variable and the most extreme of the group.

Table 4.12: *RMSE and MAE between the CCSM4 historical simulation data and observed historical data for each NOAA Climactic Region*

		TN90p	TX90P	TN10P	TX10P	R10mm	R20mm	R95pTOT	SDII
Northwest	RMSE	0.1058	0.1058	0.1134	0.0878	0.1469	0.0804	4.1588	0.0265
	MAE	0.0848	0.0857	0.0862	0.0659	0.0987	0.0448	1.2610	0.0179
West	RMSE	0.1529	0.1508	0.1670	0.1211	0.0683	0.0565	4.4260	0.0504
	MAE	0.1130	0.1138	0.1304	0.0908	0.0486	0.0363	1.4968	0.0343
Southwest	RMSE	0.1784	0.2032	0.1451	0.1253	0.0709	0.0315	1.0134	0.0334
	MAE	0.1366	0.1677	0.1086	0.1016	0.0548	0.0223	0.7489	0.0245
South	RMSE	0.1641	0.2496	0.0965	0.1397	0.0981	0.0743	4.4384	0.0698
	MAE	0.1439	0.2378	0.0787	0.1310	0.0835	0.0594	1.8820	0.0540
West North Central	RMSE	0.1153	0.1250	0.0733	0.0977	0.0592	0.0269	0.9394	0.0246
	MAE	0.0923	0.1069	0.0551	0.0829	0.0405	0.0205	0.7154	0.0183
East North Central	RMSE	0.1037	0.1328	0.0608	0.1201	0.0640	0.0415	1.3802	0.0247
	MAE	0.0935	0.1238	0.0485	0.1106	0.0502	0.0328	1.0554	0.0184
Central	RMSE	0.1331	0.2133	0.0777	0.1470	0.0886	0.0655	4.0803	0.0391
	MAE	0.1208	0.2033	0.0576	0.1334	0.0719	0.0525	1.6338	0.0299
Northeast	RMSE	0.1313	0.1360	0.1364	0.1840	0.0917	0.0613	1.8931	0.0296
	MAE	0.1140	0.1177	0.0866	0.1492	0.0730	0.0467	1.4676	0.0229
Southeast	RMSE	0.154	0.212	0.127	0.142	0.079	0.069	4.497	0.054
	MAE	0.136	0.194	0.107	0.132	0.061	0.053	1.919	0.041

4.5 Conclusion

GCM simulations try to account for as many variables as possible. However, given the complexity of climate systems and how many things can impact their trajectory over time, these models must make broad estimates. This can be seen through the climate index analysis as the data tends to be far less variable than the observed data. Spatial trends tend to be more uniform and far reaching whereas observed data had many more pockets where weather stations were on a different trajectory than those surrounding them.

When testing for the errors between the observed and simulated data, they tend to be high given how gradual the slope coefficients are for this analysis. The GCMs do a decent job of capturing the essence of what is happening spatially with the trends in extreme weather indices, however they tend to miss on how rapid the changes are occurring. Further analysis into properly fitting regressions to the indices over time could yield stronger results as a simple linear fit may not be the best method.

Applying this analysis to future projected GCM data can potentially yield promising results, particularly in trying to identify spatial trends. Given the uncertainty of future trajectories of greenhouse gases, the GCM data sets may over or under estimate the severity of change depending on their set criteria. However, this analysis can be used to determine overall temporal and spatial shifts in climate throughout the United States by using simulated data sets from the GFDL-CM3 and CCSM4 models.

Chapter 5

GCM Future Trends

5.1 Introduction

Global temperatures have steadily been on the rise for the past few decades, due to rises in greenhouse gas concentrations. As more greenhouse gases enter the atmosphere, more infrared heat is trapped by these gases, raising global temperatures. This trend towards rising global temperatures is likely to continue for the coming century as concentrations continue to rise. Furthermore, due to the severity of changes that have already occurred, the effects of rising concentrations are likely to continue if human caused greenhouse gas emissions were to cease immediately (Pachauri et al., 2014). This continued rise regardless of stopping all emissions comes from several feedback loops such as death and damage of large forests that typically act as greenhouse gas sinks. Greenhouse gas emissions have continued to steadily rise, exceeding the levels needed to limit warming between 1.5°C and 2°C (Victor et al., 2014). The issue of climate change therefore is likely to continue with or without human intervention making prediction of climate trends vital to better prepare to deal with them.

To understand the future developments with climate change, prediction models must be created and used to estimate likely scenarios. While these models can be very precise, it is important to remember they are not definitive predictions of what is to come with climate change (Collins et al., 2014). Predicting climate change does not work the same way predicting short term weather patterns does. The sheer number of variables and possibilities of human interaction makes accurate predicting difficult. However, these predictions can illustrate possible trajectories based off certain set criteria and human intervention.

General Circulation Models (GCMs) aim to predict daily weather data based off a set of equations that incorporate thermodynamic processes between the atmosphere, oceans, land masses, and sea ice. By choosing a set of criteria to use in their simulations, GCMs can model several likely scenarios for the future of the climate system. While comprehensive, these GCMs still have areas to be improved as

many processes still are not well incorporated into them such as permafrost and soil moisture processes (Collins et al., 2013). However, these models serve as a template for the coming century and what to expect for the Earth's climate system.

This study leveraged the GFDL-CM3 and CCSM4 GCMs to obtain future predicted daily climate data. Using this daily data set, the ETCCMDI core indices could be calculated for the coming century. A linear fit was forced on the data set to analyze the coming trends in the indices and how they can be expected to change. This process allows for an analysis of extreme weather patterns to come rather than observing average shifts in temperature and precipitation.

5.2 Literature Review

5.2.1 Representative Concentration Pathways

The IPCC has developed four greenhouse gas emission scenarios that serve as a baseline for modeling future climate change (Pachauri et al., 2014). These Representative Concentration Pathways (RCPs) indicate the amount of greenhouse gases that could be emitted under various mitigation scenarios spanning strict mitigation to no mitigation with high emissions. These RCPs not only look at the overall concentration levels of greenhouse gases, but the trajectory of the concentration levels over long periods of time (Moss et al. 2010).

RCP scenarios analyze greenhouse gasses and the amount of energy they will reflect through radiative forcing. Radiative forcing is the amount of radiation absorbed by the earth minus the amount that escapes the atmosphere at returns to space. Positive radiative forcing indicates a warming and a negative forcing indicates cooling. Radiative forcing is represented by Watts of energy per square meter of the surface of the Earth.

The four RCP scenarios are named by the amount radiative forcing they predict at stabilization conditions. The pathways are RCP4.6, RCP4.5, RCP6, and RCP8.5. Their radiative forcing stabilization all occurs by the year 2100 except for RCP8.5 which predicts continued rise of forcing after 2100

(Cubasch et al., 2013). RCP scenarios are used at length in climate modeling to better predict what will occur given different greenhouse gas concentrations.

Integrated Assessment Models (IAMs) were the primary tools used to develop the RCP scenarios. These "raw" scenarios that emerged needed to be turned into usable data sets that considered several historical factors, chemical analysis, and carbon cycle modeling (Collins et al., 2013). The combination of these considerations and the collaboration between several working groups provided a baseline for concentration and emissions prediction to be built off in future climate modeling (Meinshausen, 2011).

Various GCMs will take different forcing agents into consideration in their future projections. These forcing agents consist of greenhouse gases, aerosols, and other factors such as land use. Each major GCM takes these RCP and run simulations for each RCP to get a spectrum of predicted climate data for every possible concentration pathway.

5.2.2 **Future Temperature Trends**

As greenhouse gas emission continue to rise, global temperatures can be expected to continue to rise with them. In the time between 2016 and 2035, surface temperatures are expected to rise by 0.3°C and 0.7°C (Pachauri et al., 2014). The warming trends observed over the past decades can be expected to continue, and in some cases, will accelerate depending on greenhouse gas emissions from human activities. For all RCP values, the average global temperature rises during all parts the 21st century, with higher rises as RCP goes up apart from 2046-2065 when RCP4.5 has a higher increase than RCP6.0 (Collins et al.).

Future warming patterns will vary depending on geographic location on the globe. Historically, modelling has typically shown higher temperatures of land compared to over the oceans worldwide (Manabe et al., 1990). The Arctic sees an alarming rate of heating compared to most of the globe with warming occurring at 4.2 to 4.4 times the average on Earth (Collins et al, 2013). This amplified warming may be due to positive feedback loops linked to ice albedo being lost and the area absorbing more heat

(Bekryaev et al., 2010). These kinds of regional shifts and region specific feedback loops can create diverse warming patterns around the globe.

Temperature extremes are also expected to shift with warming global temperatures and higher concentrations of greenhouse gases. In general, these extremes will take the form of hot extremes across the globe rather than cold extremes (Caesar and Lowe, 2012). The number of record high temperatures can be expected to easily outpace the number of record low days (Collins et al., 2013). Across the globe, heat waves can be expected to rise as temperatures increase. These heatwaves tend to be the result of an increase in seasonal mean temperatures, particularly in the summer (Fischer and Schär, 2010). Shifts in extreme temperatures can cause a great deal of human discomfort, damage to agricultural lands, and an overall increase of energy costs as humans attempt to handle extreme heat.

5.2.3 **Future Precipitation Trends**

Precipitation changes tend to far more variable compared to temperature depending on geographic location. In general, the Coupled Model Intercomparison Project (CMIP5) predicts anywhere from a 0.05 mm per day increase with RCP4.6 conditions, to a 0.15 mm per day increase with RCP8.5 conditions globally (Collins et al., 2013).

Spatial variability depends greatly on several location specific factors. Precipitation shifts rely heavily on energy transfers and specific atmospheric conditions (Schlesinger and Mitchell, 1987). Local moisture availability and air circulation patterns vary from location to location, having large impacts on precipitation amounts and intensity.

As greenhouse gas levels rise, less cooling can occur in the troposphere, resulting in less moisture condensing into precipitation (Andrews et al., 2010). As water evaporates and rises through the atmosphere, it eventually cools at higher altitudes and can eventually condense into rain. With rising temperatures, this process slows and far less moisture condenses. However, an increase in greenhouse gases leads to more warming which can in turn raise the overall moisture levels in the atmosphere which can result in more rain. Furthermore, ocean temperatures will continue to rise into the future which results

in further evaporation increases (Good et al., 2012). These factors lead to precipitation trends that are less uniform over the globe and trends that rely heavily on several conditions in a specific location.

Precipitation extremes can be expected to increase with climbing greenhouse gas levels over the next century. Stronger storms are expected to be more frequent while weaker storms are predicted to decrease (Senevirante et al., 2012). The intensity of rainfall events again depends heavily on location as several areas will see less rainfall and possibly weaker storms as time goes on. It is important to note that there is no relationship between the intensity of storms predicted and the total amount of rainfall predicted for the coming century (Senevirante et al. 2012). While storms may get stronger, it does not mean that average rainfall values will rise as a direct result of this.

5.3 Methods

Future projected daily climate data was extracted from the GFDL-CM3 and CCSM4 at the location of the weather stations selected in this study. Extracting at these points allows for a direct comparison between historical trends observed and the future trends predicted. This was done for the RCP4.6 and RCP6.0 simulations of the GFDL-CM3 as well the CCSM4. These were selected due to their availability within both GCM data sets used for this study.

Using daily maximum temperature, daily minimum temperature, and daily precipitation predicted in the GCMs over the span of 2000-2100, the 27 ETCCDI indices were calculated for each year in the given span of time. A linear regression was run to estimate the change of these indices over time. This change was represented using the slope coefficient determined from the regression. In addition, the linear regression was checked for wellness of fit. However, regardless of wellness, the fit was forced upon the data to analyze a general trend.

The slope values for eight selected indices were analyzed in depth for this study. These indices are TN90P, TX90P, TN10P, TX10P, R10MM, R20MM, R95PTOT, and SDII (Table 5.1). The slope values for each index were plotted across the United States as point values to analyze raw spatial trends.

Next, the slope values at each weather station were averaged within the NOAA Climactic Region they fell into. This averaging allowed the trends to be approached from a regional view point to see exactly how different parts of the nation are shifting. The slope values were then averaged within each county across the country to analyze country trends. This analysis was done as a crude linear interpolation and to determine trends at a small scale.

5.4 Results and Discussion

The eight selected indices are comprised of four indices that monitor temperature trends (TN90P, TX90P, TN10P, TX10P) and four that monitor precipitation trends (R10MM, R20MM, R95PTOT, SDII). The trends for these indices are represented using two different color scales depending on if they represent temperature or precipitation. For temperature trends, red indicates a positive slope or increasing temperature trend while blue indicates a negative slope or decreasing temperature trend. This is reversed for precipitation with blue indicating a positive slope or increasing precipitation trend while red indicates a decreasing slope or decreasing precipitation trend.

5.4.1 **GFDL-CM3 Point Values**

As was done with the GCM historical simulations, point values for regression slopes were plotted over the United States to create a raw spatial data set. This data set represents the predicted trends at the location of each weather statin analyzed in this study. A larger circle indicates a larger absolute slope value and the color represents the direction of the trend.

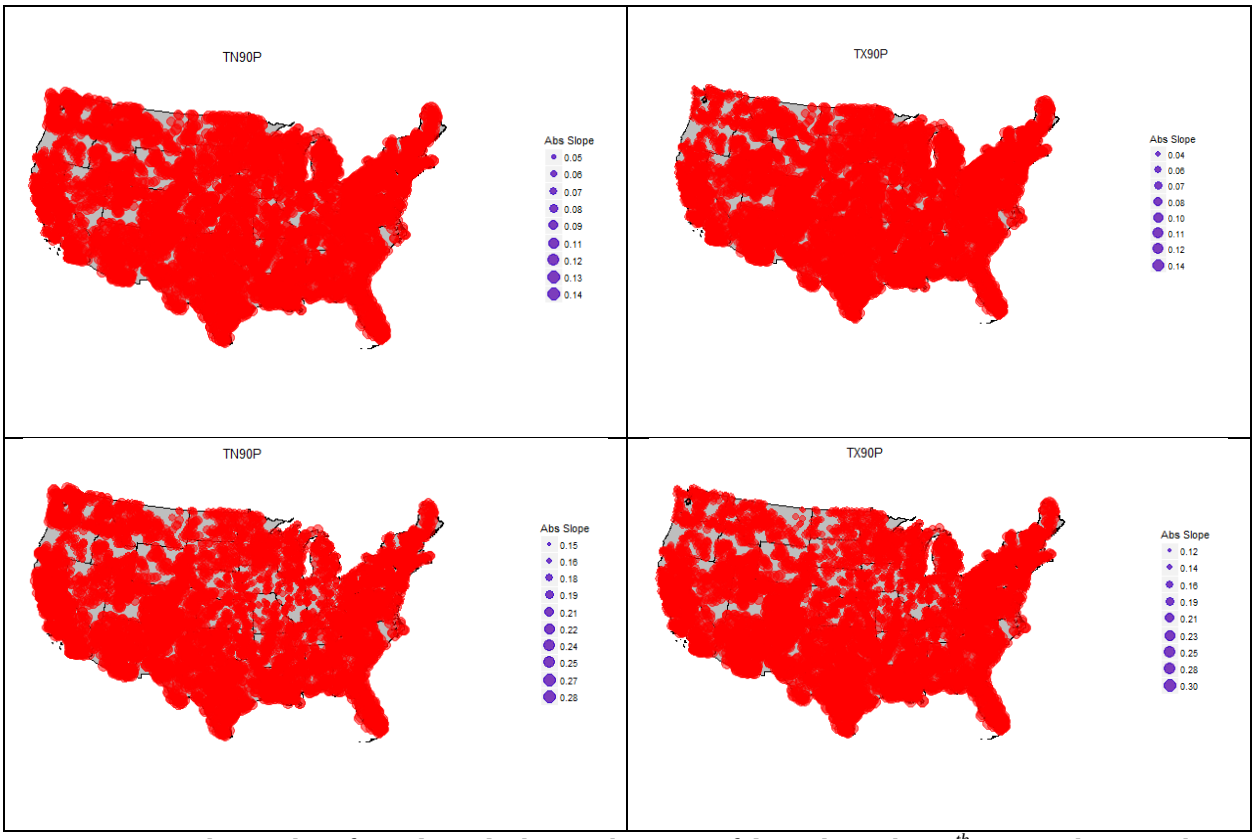

Figure 5.1: *Slope values for indices dealing with counts of days above the 90th percentile using the GFDL-CM3 simulations. (a) Daily minimum temperature across the United States for RCP4.6. (b) Daily minimum temperature across the United States for RCP6.0. (c) Daily Maximum temperature across the United States for RCP4.6. (d) Daily Maximum temperature across the United States for RCP6.0.*

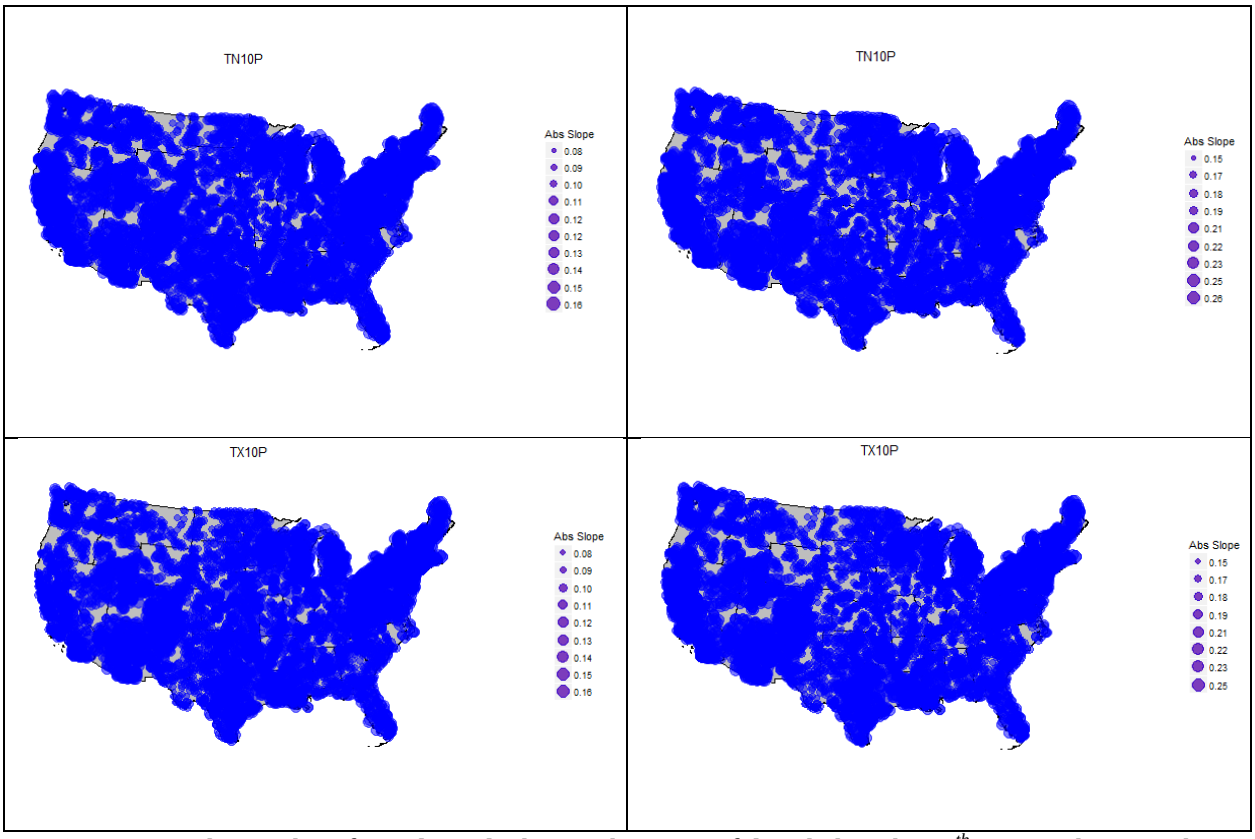

Figure 5.2: *Slope values for indices dealing with counts of days below the 10th percentile using the GFDL-CM3 simulations. (a) Daily minimum temperature across the United States for RCP4.6. (b) Daily minimum temperature across the United States for RCP6.0. (c) Daily Maximum temperature across the United States for RCP4.6. (d) Daily Maximum temperature across the United States for RCP6.0.*

The GFDL-CM3 simulations all show a trend towards increasing temperatures, across both RCPs. Daily minimum and maximum temperatures will exceed the 90th percentile at an increased rate as Figure 5.9 shows. This trend is uniform throughout the entire country with relatively high slope values. On the bottom end of the spectrum, Figure 5.10shows daily minimum temperatures will fall below the 10th percentile at a decreasing rate across the United States.

As Table 5.13 shows, the average trend over the United States holds up with the point data observations. Furthermore, the GFDL-CM3 has a far better linear fit than any other model analyzed thus far.

Table 5.1: *Regression values for the GFDL-CM3 future projected temperature indices summarized over the entire data set for the United States*

Index	RCP	Mean Value	Mean R^2	Mean F-Test P-Value
TN90P	RCP4.6	0.0942	0.3343	4.52E-6
	RCP6.0	0.2021	0.6320	1.32E-16
TX90P	RCP4.6	0.0977	0.2519	0.0003
	RCP6.0	0.2047	0.5386	6.67E-12
TN10P	RCP4.6	-0.1179	0.4093	6.63E-10
	RCP6.0	-0.1946	0.6829	6.66E-20
TX10P	RCP4.6	-0.1123	0.3516	5.53E-8
	RCP6.0	-0.1891	0.6250	7.90E-18

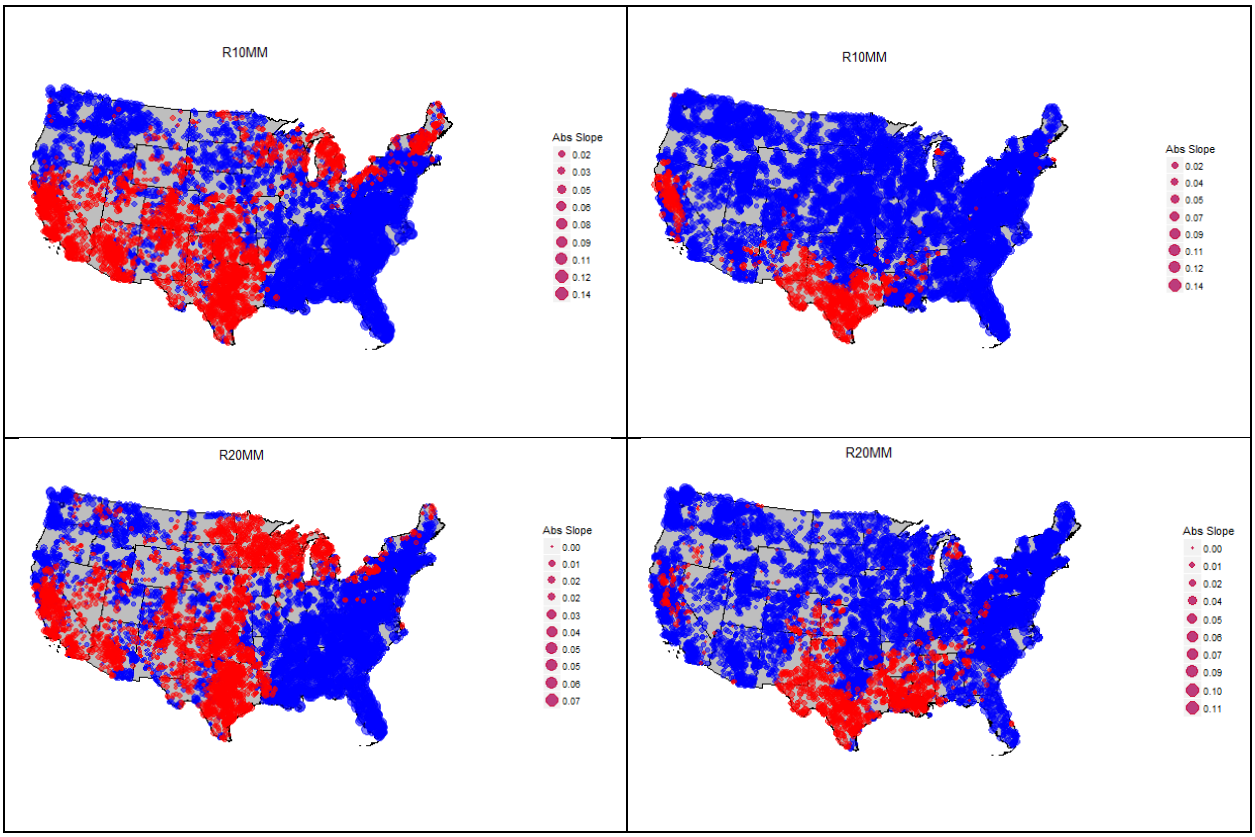

Figure 5.3: *Slope values for indices dealing with days exceeding set precipitation amounts using the GFDL-CM3 simulations. (a) 10mm daily precipitation using RCP4.6. (b) 10mm daily precipitation using RCP6.0. (c) 20mm daily precipitation using RCP4.6. (d) 20mm daily precipitation using RCP6.0.*

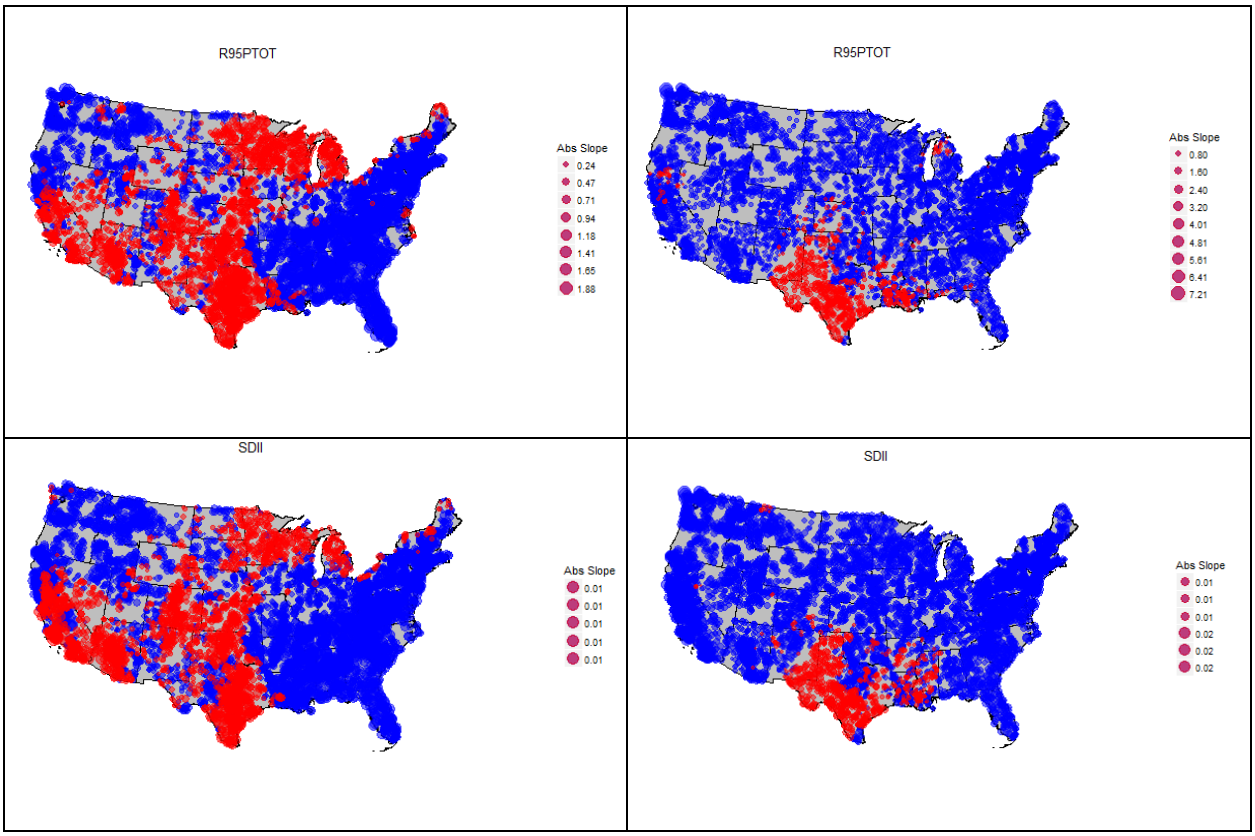

Figure 5.4: *Slope values for indices dealing with days exceeding set precipitation amounts using the GFDL-CM3 simulations. (a) Sum of precipitation amounts for days where daily precipitation exceeds the 95th percentile using RCP4.6. (b) Sum of precipitation amounts for days where daily precipitation exceeds the 95th percentile using RCP6.0. (c) Sum of annual precipitation on wet days with rainfall > 1mm, over the number of wet days using RCP4.6. (d) Sum of annual precipitation on wet days with rainfall > 1mm, over the number of wet days using RCP6.0.*

The GFDL-CM3 future simulations show clear patterns in precipitation shifts across but RCP scenarios. As Figures 4.11a&c show, much of the east coast, Mississippi Basin, and northwest will receive more days exceeding 10 and 20 mm of precipitation each year. When RCP6.0 is used, this trend spreads across the nation, leaving only pockets in the south and California still getting dryer (Figure 5.11b&d). Precipiation intensity follows a nearly identical trend with R95PTOT increasing in these same areas for RCP4.6 and RCP6.0 (Figure 5.12a&b). SDII is increasing in a similar fashion, however its slope values are much lower indicating that overall intensity is changing less rapidly compared to R95PTOT.

Table 5.2: *Regression values for the GFDL-CM3 future projected precipitation indices summarized over the entire data set for the United States*

Index	RCP	Mean Value	Mean R^2	Mean F-Test P-Value
R10mm	RCP4.6	0.2684	0.0158	0.4538
	RCP6.0	0.0288	0.0370	0.2684
R20mm	RCP4.6	0.2930	0.0161	0.4169
	RCP6.0	0.0115	0.0304	0.2930
R95PTOT	RCP4.6	0.2511	0.0160	0.4118
	RCP6.0	0.4358	0.0388	0.2511
SDII	RCP4.6	0.2314	0.01627	0.4336
	RCP6.0	0.0039	0.0425	0.2314

5.4.2 **GFDL-CM3 County Analysis**

To further breakdown the country and analyze trends outside of point data, the index slope values were averaged within the counties across the country. This allows for analysis between points and to get a better sense of what is happening everywhere in the country. For temperature trends, red indicates counties with an increase in slope and blue indicates counties with a decrease in slope. This color pattern is reversed for precipitation indices so that blue indicates areas that are getting wetter. The darker the color, the more rapid the change.

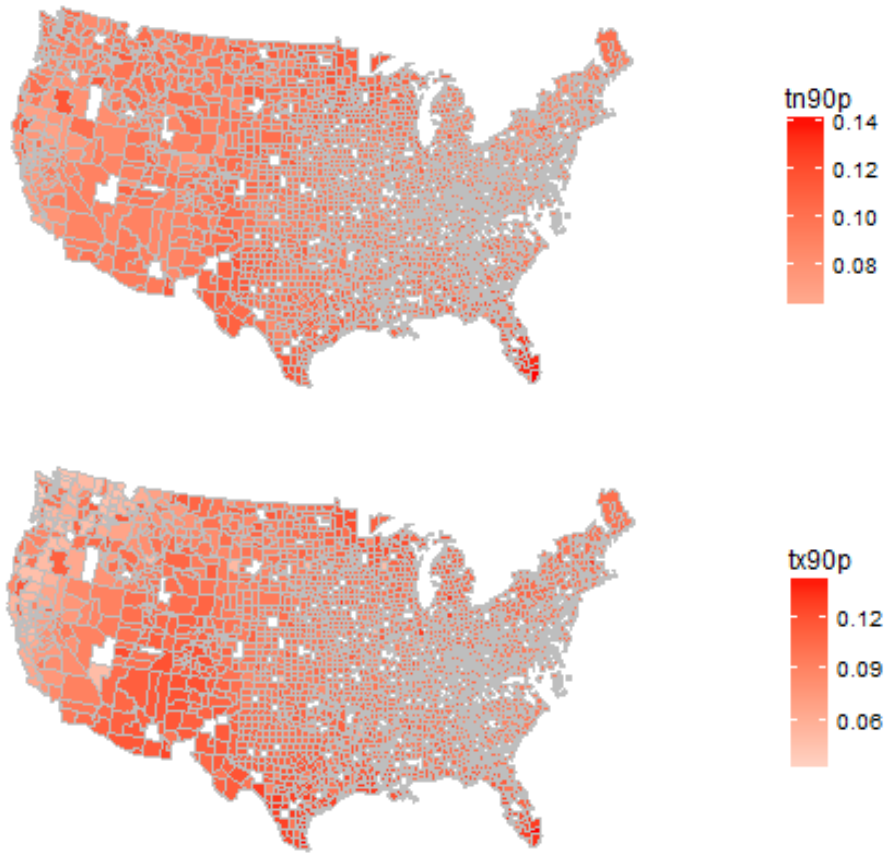

Figure 5.5: *Mean slope values for each county's 90th percentile indices for GFDL-CM3 RCP4.6 data. (a) Daily Minimum temperature. (b) Daily Maximum temperature*

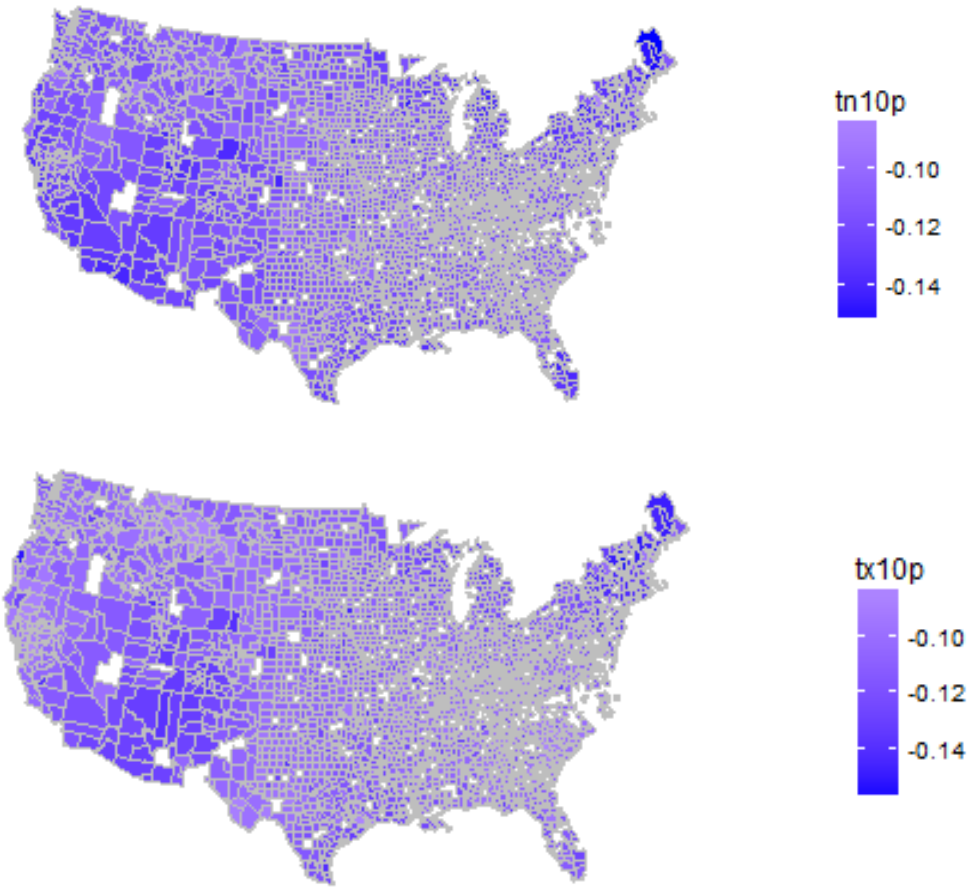

Figure 5.6: *Mean slope value for each county's 10th percentile indices for the GFDL-CM3 RCP4.6 data. (a) Daily Minimum temperature (b) Daily Maximum temperature*

The county analysis for GFDL-CM3 RCP4.6 simulations tells a very similar story as the other analysis performed. All counties will see a general warming trend, both with daily maximum and minimum temperature.

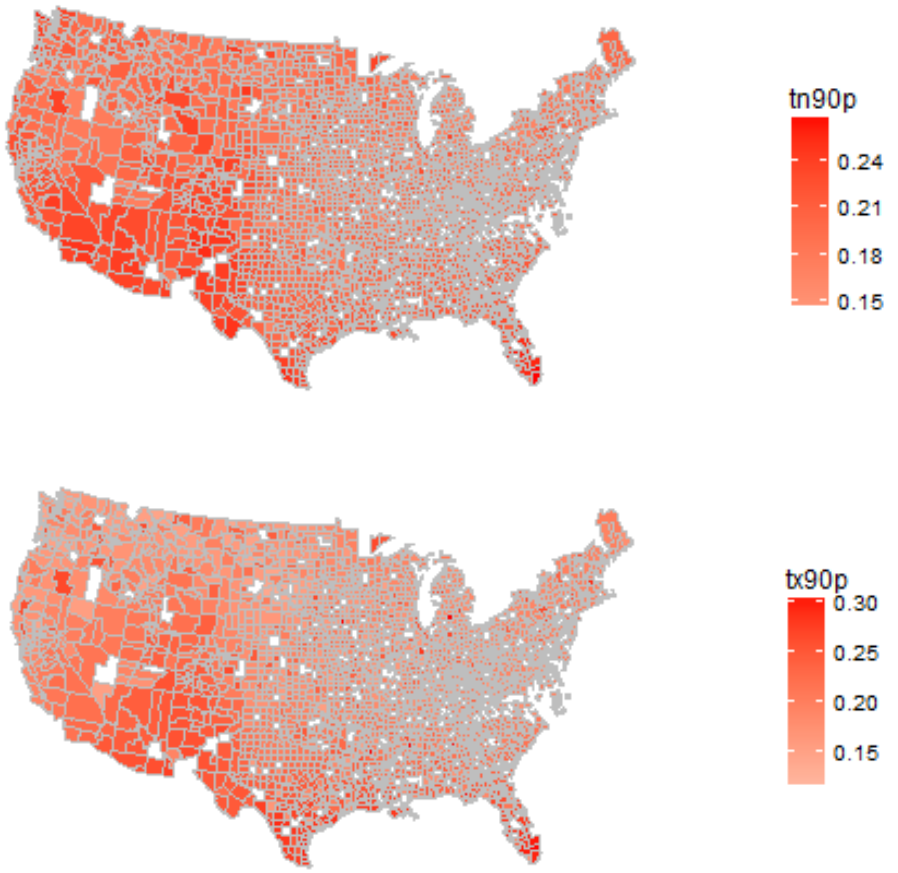

Figure 5.7: *Mean slope values for each county's 90th percentile indices for GFDL-CM3 RCP6.0 data. (a) Daily Minimum temperature. (b) Daily Maximum temperature*

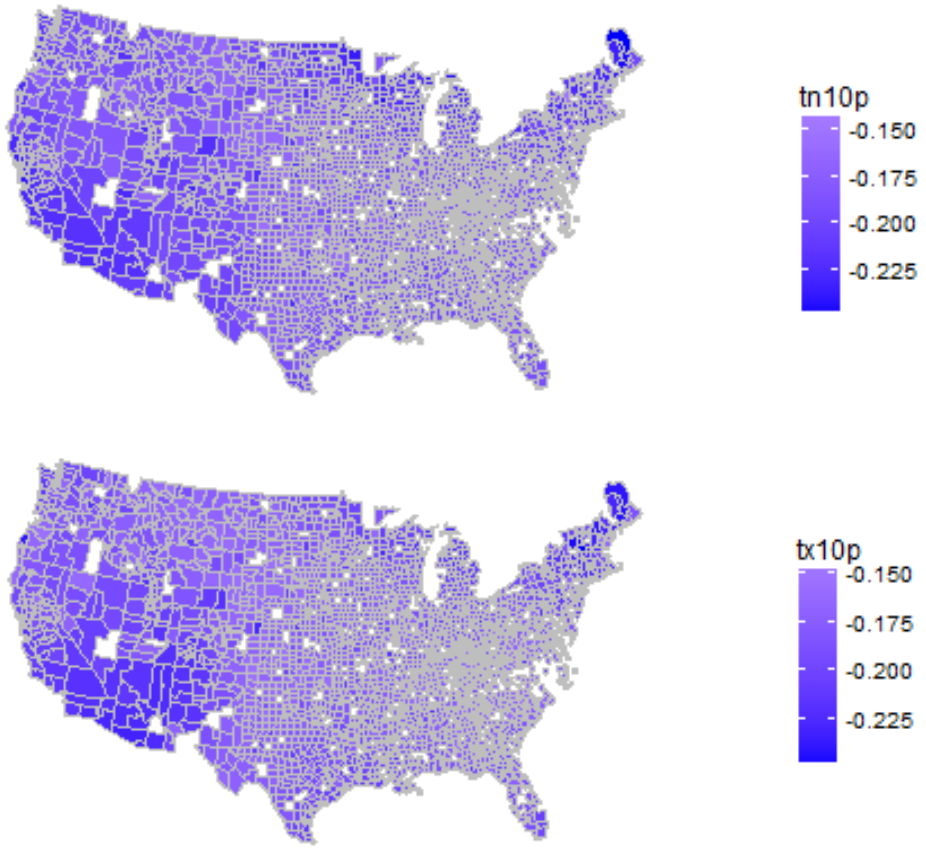

Figure 5.8: *Mean slope value for each county's 10th percentile indices for the GFDL-CM3 RCP6.0 data. (a) Daily Minimum temperature (b) Daily Maximum temperature*

The RCP6.0 simulation follow the same spatial trends as the RCP4.6 simulation on a county level. The largest difference between the two is the large slope values. The RCP6.0 has a more rapid change in the index values, particularly in counties in the south, southwest, and west coast as they experience intense warming patterns.

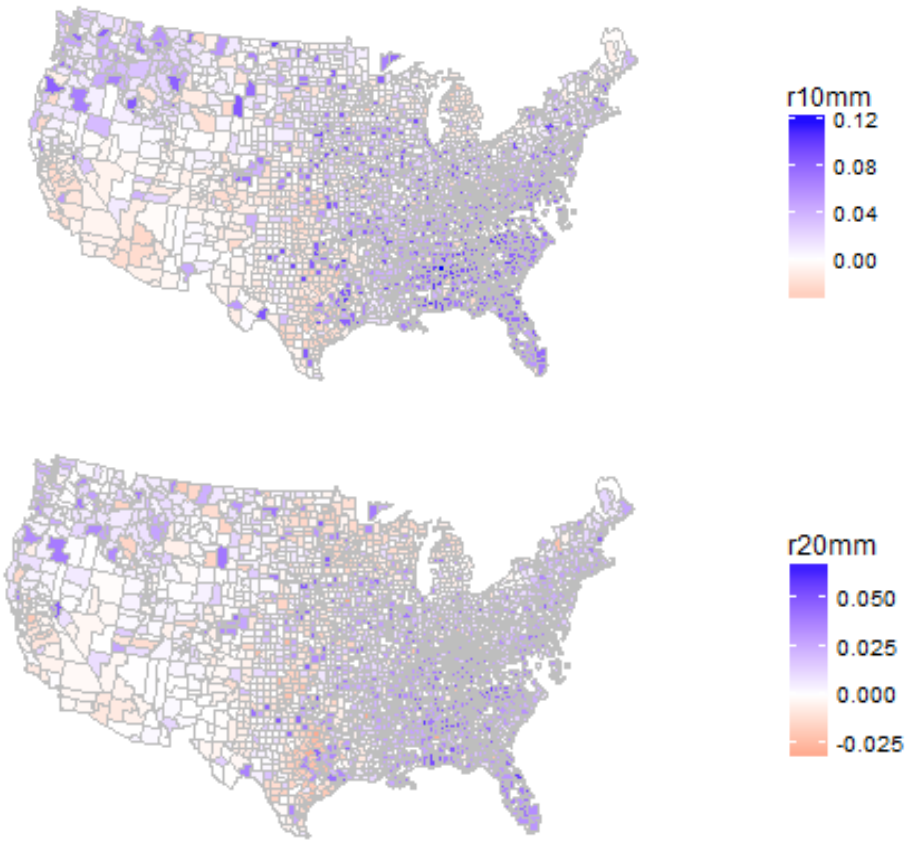

Figure 5.9: *Average slope values for each county's precipitation threshold indices for the GFDL-CM3 RCP4.6 data. (a) Exceeding 10 mm. (b) Exceeding 20 mm.*

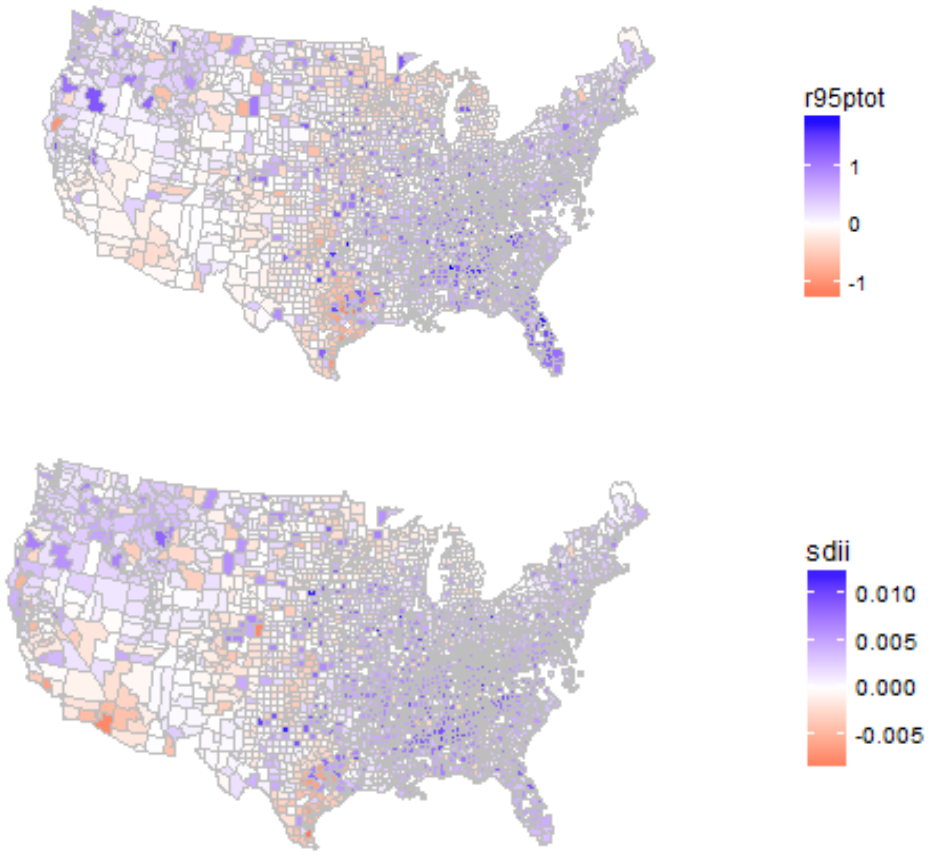

Figure 5.10: *Average slope values for each county's precipitation intensity indices for the GFDL-CM3 RCP4.6 data. (a) Total precipitation for events exceeding the 95th percentile. (b) Annual precipitation intensity over all wet days.*

Precipitation trends for the counties across the countries indicate the eastern half of the country will see increases of the number of days in a year with heavy rainfalls per the GFDL-CM3 RCP4.6 simulation (Figure 5.18). The Pacific Northwest will see increases as well while the middle half of the country sees little change and some decreases. Intensity follows a similar pattern with the east coast seeing a rise in intensity as indicated by R95PTOT (Figure 5.18a).

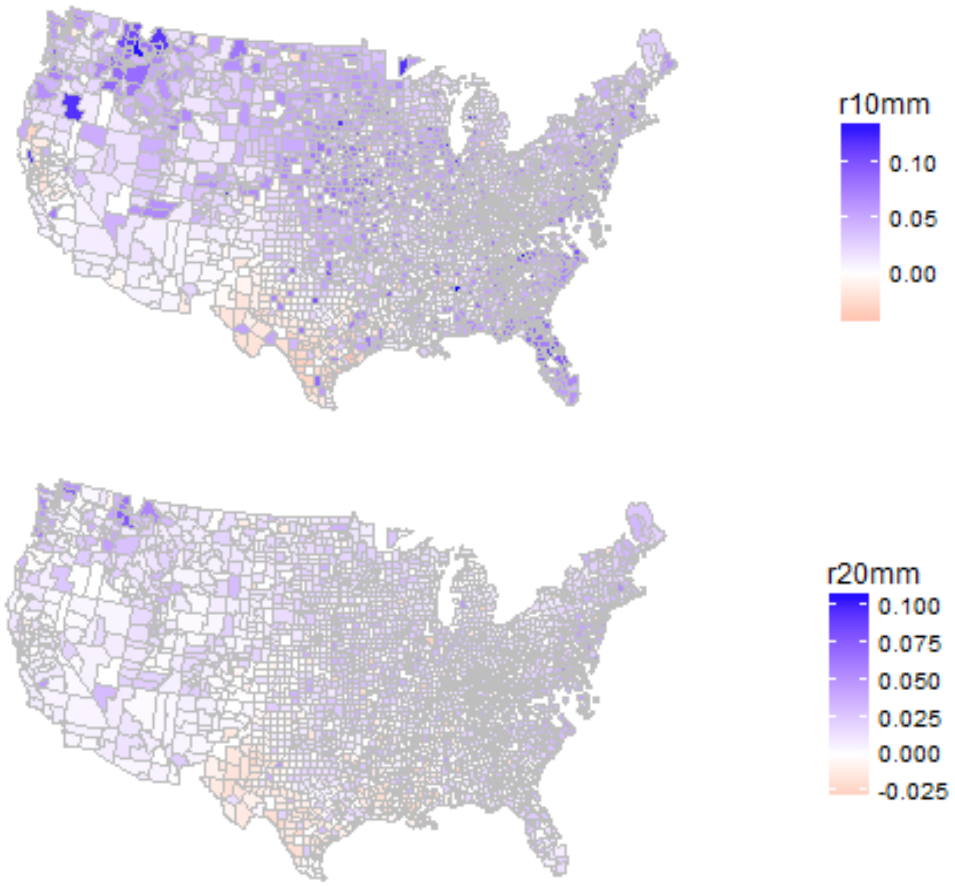

Figure 5.11: *Average slope values for each county's precipitation threshold indices for the GFDL-CM3 RCP6.0 data. (a) Exceeding 10 mm. (b) Exceeding 20 mm.*

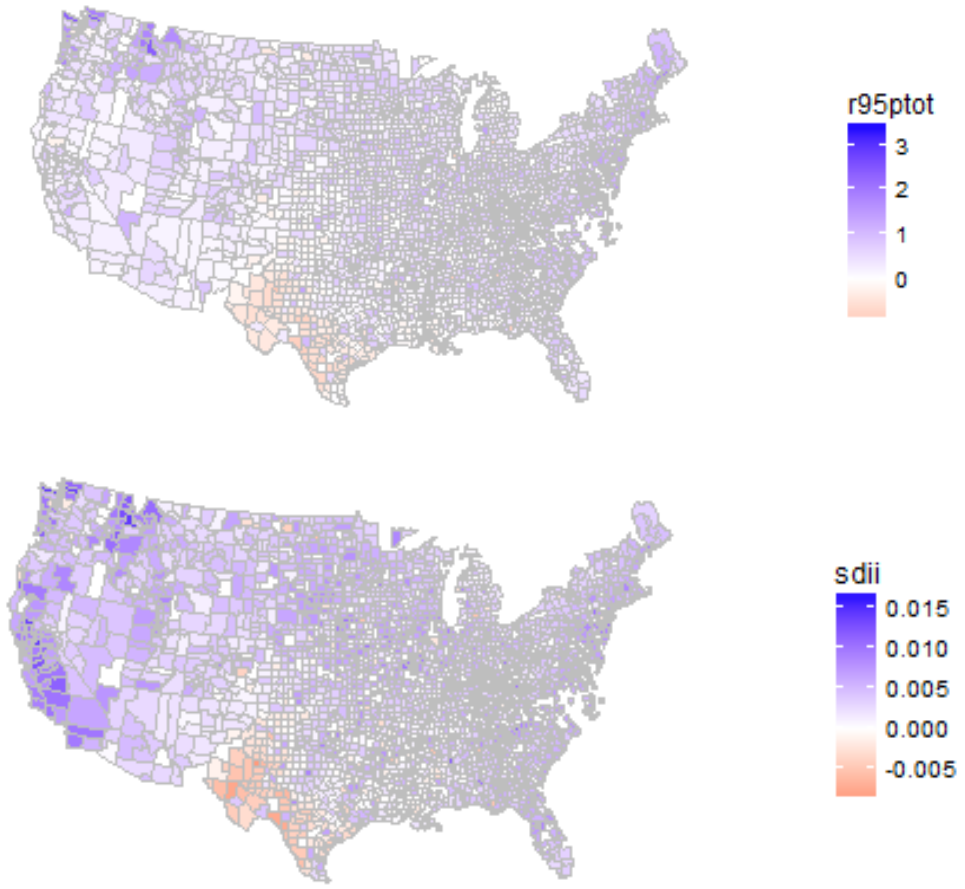

Figure 5.12: *Average slope values for each county's precipitation intensity indices for the GFDL-CM3 RCP6.0 data. (a) Total precipitation for events exceeding the 95th percentile. (b) Annual precipitation intensity over all wet days.*

The RCP6.0 simulations indicate a much broader increase of precipitation across the country. As Figure 5.19a shows, many counties will see increases with the north and northwest seeing the most intense change. As far as intensity, most of the country sees increases except a few counties in Texas (Figure 5.20&b). Counties in the northwest will see the greatest change over the next 100 years if RCP6.0 conditions are met.

5.4.3 **GFDL-CM3 NOAA Climactic Regions**

Analyzing mean trends across the United States for future projected data leads to broad assumptions and inaccurate depictions of what is truly changing with climate. To better analyze shifts in the climate systems across the country, the indices were analyzed across the NOAA Climactic Regions.

Table 5.3: *Mean slope values for temperature indices for each NOAA climactic region for future projected GFDL-CM3 RCP4.6 Data.*

REGION	TN90P	TX90P	TN10P	TX10P
NORTHWEST	0.0896	0.0589	-0.1149	-0.1019
WEST	0.0803	0.0732	-0.1250	-0.1041
SOUTHWEST	0.0952	0.1099	-0.1212	-0.1216
SOUTH	0.0997	0.1108	-0.1116	-0.1111
WEST NORTH CENTRAL	0.0979	0.0896	-0.1048	-0.0990
EAST NORTH CENTRAL	0.1040	0.1090	-0.1214	-0.1198
CENTRAL	0.0886	0.0977	-0.1115	-0.1058
NORTHEAST	0.0878	0.1013	-0.1342	-0.1360
SOUTHEAST	0.1023	0.1013	-0.1167	-0.1033

The GFDL-CM3 RCP4.6 simulation shows an increase in both TX90P and TN90P across all regions with the Southeast and East North Central regions showing the greatest change (Table 5.15). Furthermore, TN10P and TX10P are decreasing across all regions, further supporting the observed warming trend seen in the point value data.

Table 5.4: *Mean slope values for temperature indices for each NOAA climactic region for future projected GFDL-CM3 RCP6.0 data*

REGION	TN90P	TX90P	TN10P	TX10P
NORTHWEST	0.2032	0.1672	-0.1940	-0.1893
WEST	0.2153	0.1980	-0.2107	-0.2021
SOUTHWEST	0.2281	0.2356	-0.1999	-0.2032
SOUTH	0.2034	0.2328	-0.1796	-0.1811
WEST NORTH CENTRAL	0.1903	0.1656	-0.1792	-0.1672
EAST NORTH CENTRAL	0.1832	0.1828	-0.2104	-0.1933
CENTRAL	0.1778	0.1810	-0.1845	-0.1720
NORTHEAST	0.1855	0.1951	-0.2146	-0.2140
SOUTHEAST	0.2141	0.2223	-0.1890	-0.1767

The GFDL-CM3 RCP6.0 simulation shows the same increases; however, the trends indicate more rapid change than the RCP4.6.

Table 5.5: *Mean slope values for precipitation indices for each NOAA climactic region for future projected GFDL-CM3 RCP4.6 data*

REGION	R10MM	R20MM	R95PTOT	SDII
NORTHWEST	0.0190	0.0068	0.2909	0.0022
WEST	-0.0057	-0.0013	0.0221	0.0003
SOUTHWEST	-0.0061	-0.0008	-0.0480	-0.0007
SOUTH	0.0031	0.0001	-0.0804	0.0004
WEST NORTH CENTRAL	0.0104	0.0016	0.0823	0.0010
EAST NORTH CENTRAL	0.0000	-0.0068	-0.2511	-0.0005
CENTRAL	0.0294	0.0162	0.4502	0.0037
NORTHEAST	0.0140	0.0148	0.4338	0.0023
SOUTHEAST	0.0779	0.0331	0.8756	0.0058

On a whole, precipitation trends are far less severe than temperature trends in the GFDL-CM3 simulations. Average slope values for the indices are lower for the most part, indicating slow shifting trends rather than the rapid shifts in temperature. The most notable changes come with precipitation intensity, particularly intensity of strong events. R95PTOT has the largest trends, with large increases on the east coast and smaller trends and decreases in the south. Overall, intensity of rainfall events will not change much as SDII shows in Table 5.17.

Table 5.6: *Mean slope values for precipitation indices for each NOAA climactic region for future projected GFDL-CM3 RCP6.0 data.*

REGION	R10MM	R20MM	R95PTOT	SDII
NORTHWEST	0.0443	0.0219	0.8803	0.0070
WEST	0.0056	0.0059	0.2766	0.0075
SOUTHWEST	0.0138	0.0064	0.2972	0.0027
SOUTH	0.0098	-0.0009	-0.0182	0.0001
WEST NORTH CENTRAL	0.0462	0.0122	0.5181	0.0049
EAST NORTH CENTRAL	0.0393	0.0141	0.4624	0.0043
CENTRAL	0.0403	0.0180	0.6172	0.0041
NORTHEAST	0.0389	0.0244	0.8531	0.0049
SOUTHEAST	0.0576	0.0189	0.6705	0.0049

With the RCP6.0 simulation, trends shift to every region experiencing an increase in R10mm and all but the South seeing an increase in R20mm (Table 5.18). Again, R95PTOT shows the most severe changes as intensity of strong precipitation events will grow. SDII shows little to now real shifts again.

5.4.4 **CCSM4 Point Values**

The index future projected temporal trends were plotted over the nation at the location of the weather station where the GCM data was extracted. This was done with each RCP simulation used in the study. Larger circles indicate a greater absolute slope and the color of the circle indicates which direction the trend is headed.

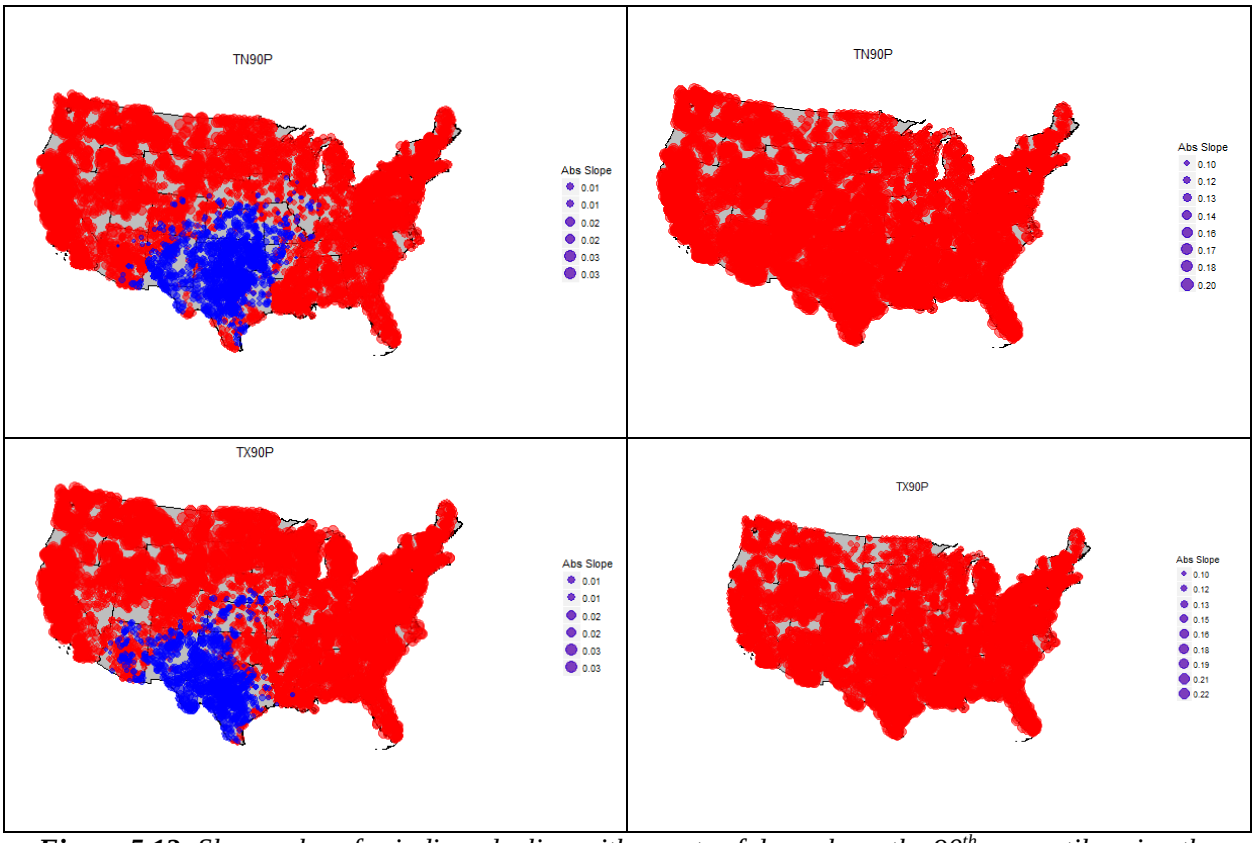

Figure 5.13: *Slope values for indices dealing with counts of days above the 90th percentile using the CCSM4 simulations. (a) Daily minimum temperature across the United States for RCP4.6. (b) Daily minimum temperature across the United States for RCP6.0. (c) Daily Maximum temperature across the United States for RCP4.6. (d) Daily Maximum temperature across the United States for RCP6.0.*

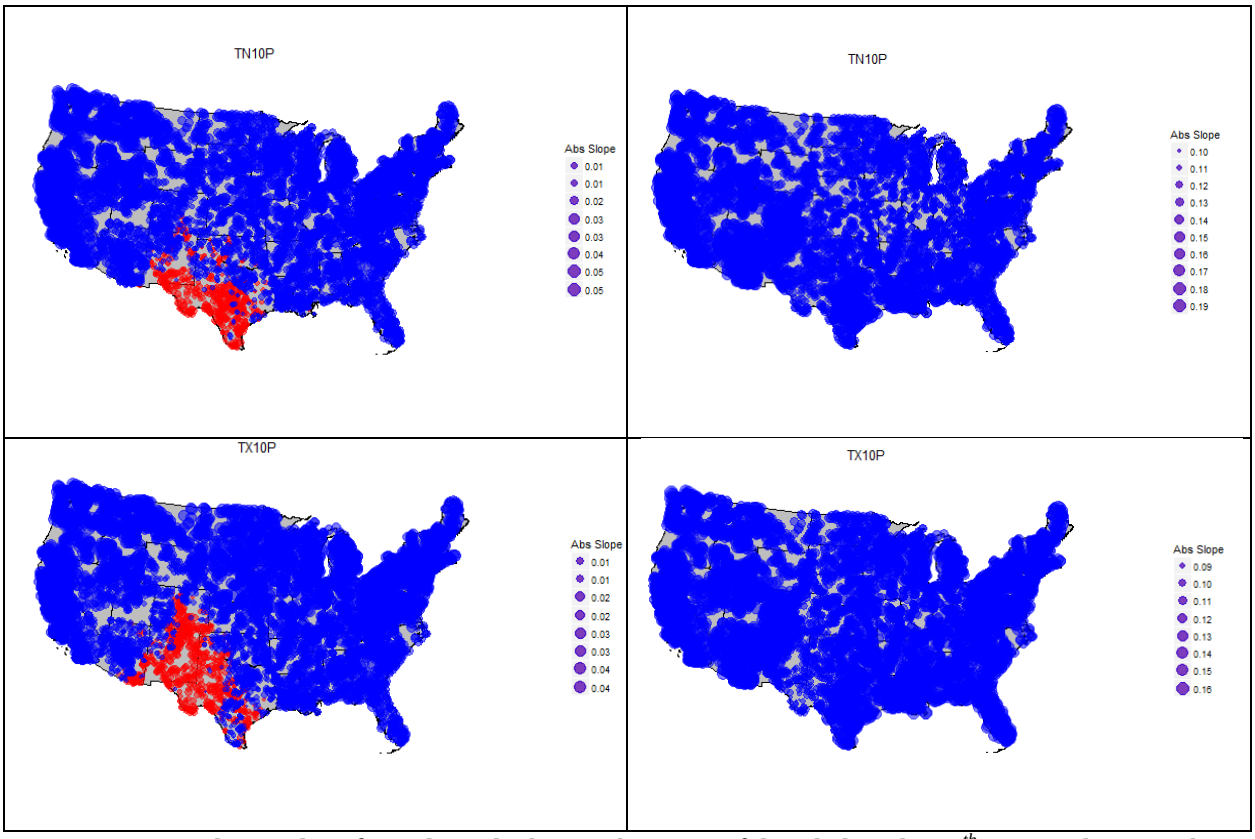

Figure 5.14: *Slope values for indices dealing with counts of days below the 10th percentile using the CCSM4 simulations. (a) Daily minimum temperature across the United States for RCP4.6. (b) Daily minimum temperature across the United States for RCP6.0. (c) Daily Maximum temperature across the United States for RCP4.6. (d) Daily Maximum temperature across the United States for RCP6.0.*

The CCSM4 future simulations indicate a clear warming trend across the nation with daily maximum temperatures as well as daily minimum temperatures rising. The CCSM4 RCP4.6 simulation indicates a clear rise in the number of days exceeding the 90th percentile over time both for daily maximum and minimum temperature, the only exception being a pocket in the south centered on Texas (Figure 5.21a&c). This pocket of decreasing slope values disappears in the RCP6.0 simulation as this simulation uses much higher greenhouse gas levels (Figure 24.21b&d). In Figure 5.22, we see maximum daily temperatures and daily minimum temperatures are falling below the 10th percentile at a decreasing rate, further indicating a warming trend. The exception is again the pocket in the south for the RCP4.6 simulation. The pocket disappears once again in the RCP6.0 simulation.

Table 5.7: *Regression values for the CCSM4 future projected temperature indices summarized over the entire data set for the United States*

Index	RCP	Mean Value	Mean R^2	Mean F-Test P-Value
TN90P	RCP4.6	0.0101	0.0129	0.4210
	RCP6.0	0.1560	0.566	4.09E-14
TX90P	RCP4.6	0.0150	0.0163	0.3744
	RCP6.0	0.1569	0.5035	4.47E-12
TN10P	RCP4.6	-0.0168	0.0300	0.2730
	RCP6.0	-0.1346	0.5468	4.35E-13
TX10P	RCP4.6	-0.0175	0.0280	0.2992
	RCP6.0	-0.1229	0.4568	4.57E-9

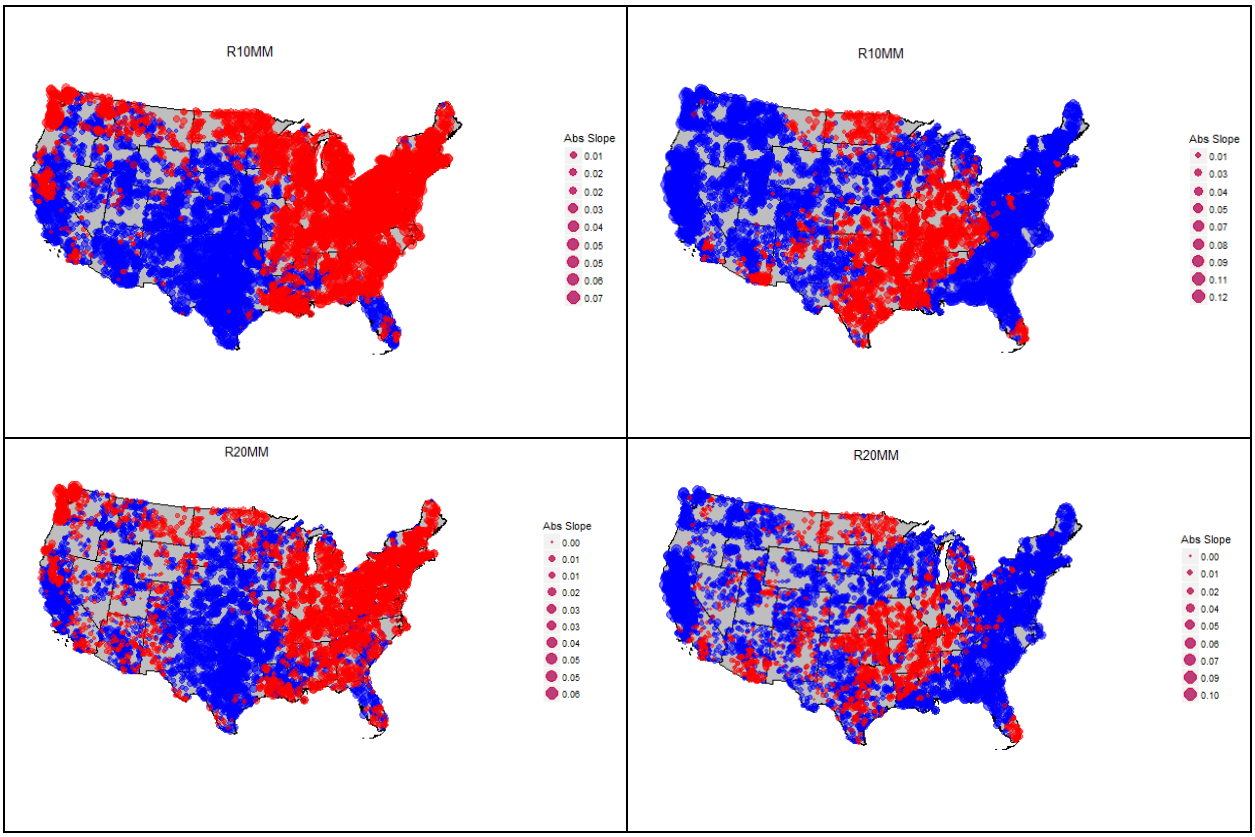

Figure 5.15: *Slope values for indices dealing with days exceeding set precipitation amounts using the CCSM4 simulations. (a) 10mm daily precipitation using RCP4.6. (b) 10mm daily precipitation using RCP6.0. (c) 20mm daily precipitation using RCP4.6. (d) 20mm daily precipitation using RCP6.0.*

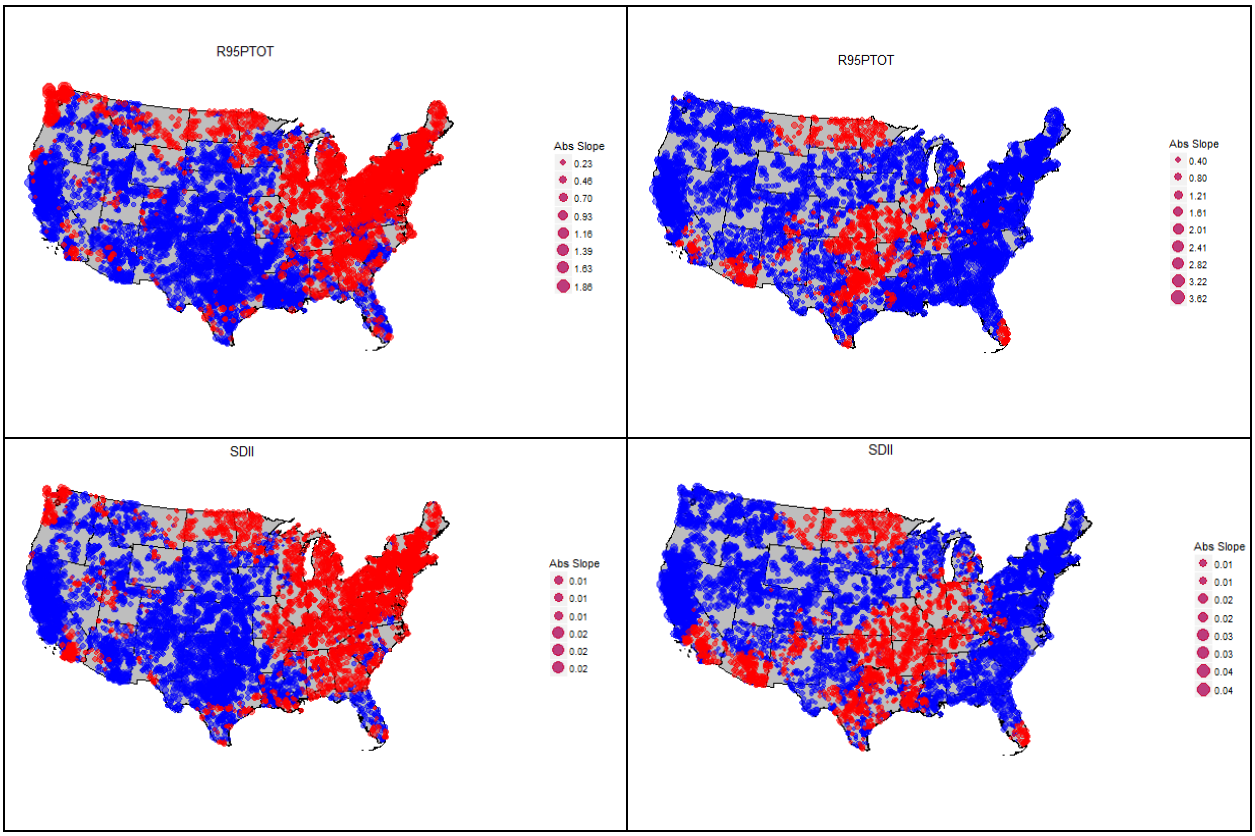

Figure 5.16: *Slope values for indices dealing with days exceeding set precipitation amounts using the CCSM4 simulations. (a) Sum of precipitation amounts for days where daily precipitation exceeds the 95th percentile using RCP4.6. (b) Sum of precipitation amounts for days where daily precipitation exceeds the 95th percentile using RCP6.0. (c) Sum of annual precipitation on wet days with rainfall > 1mm, over the number of wet days using RCP4.6. (d) Sum of annual precipitation on wet days with rainfall > 1mm, over the number of wet days using RCP6.0.*

Precipitation trends very significantly depending on the RCP used in the simulation. A general pattern emerges where the direction of the trends switches depending on the RCP. This can especially be seen on the east coast with each index as a drying trend in the RCP4.6 simulation switches to an increase in precipitation in the RCP6.0. Additionally, the west coast tends towards more precipitation in the RCP6.0 compared to the RCP4.6 (Figure 5.23). A small section in the middle part of the country near Oklahoma is the main area that seems to get dryer in the RCP6.0 simulation. Overall, while year counts of days exceeding 10mm and 20mm are going up, the biggest change comes in the intensity of high precipitation days (Figure 5.23b). R95PTOT increases greatly with large slope values, especially in the

RCP6.0 simulation (Figure 5.24a&b). However, SDII indicates overall intensities throughout the year do not change much as the slope values are close to zero (Figure 5.24c&d).

Table 5.8: *Regression values for the CCSM4 future projected precipitation indices summarized over the entire data set for the United States*

Index	RCP	Mean Value	Mean R^2	Mean F-Test P-Value
R10mm	RCP4.6	-0.0036	0.0138	0.4252
	RCP6.0	0.0160	0.0217	0.3838
R20mm	RCP4.6	-0.0003	0.0124	0.4636
	RCP6.0	0.0087	0.0183	0.4137
R95PTOT	RCP4.6	0.0460	0.0140	0.4328
	RCP6.0	0.3188	0.0220	0.3664
SDII	RCP4.6	0.0010	0.0138	0.4210
	RCP6.0	0.0023	0.0209	0.3962

5.4.5 **CCSM4 County Analysis**

The slope values for the climactic indices were averaged within each county the weather stations fell in as was done in previous analysis. This county summarization allows for a clearer picture of what is happening at a local level and an attempt to explain what is happening between weather stations. This process was done for both RCP4.6 and RCP6.0 in the CCSM4 simulation.

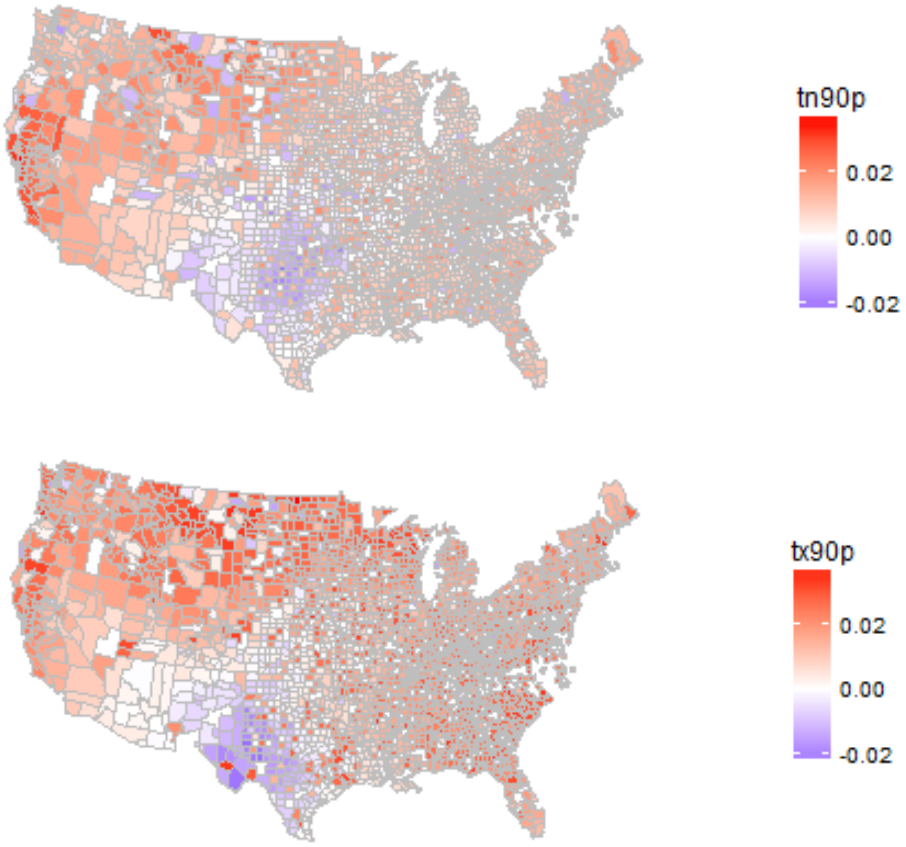

Figure 5.17: *Mean slope values for each county's 90th percentile indices for CCSM4 RCP4.6 data. (a) Daily Minimum temperature. (b) Daily Maximum temperature*

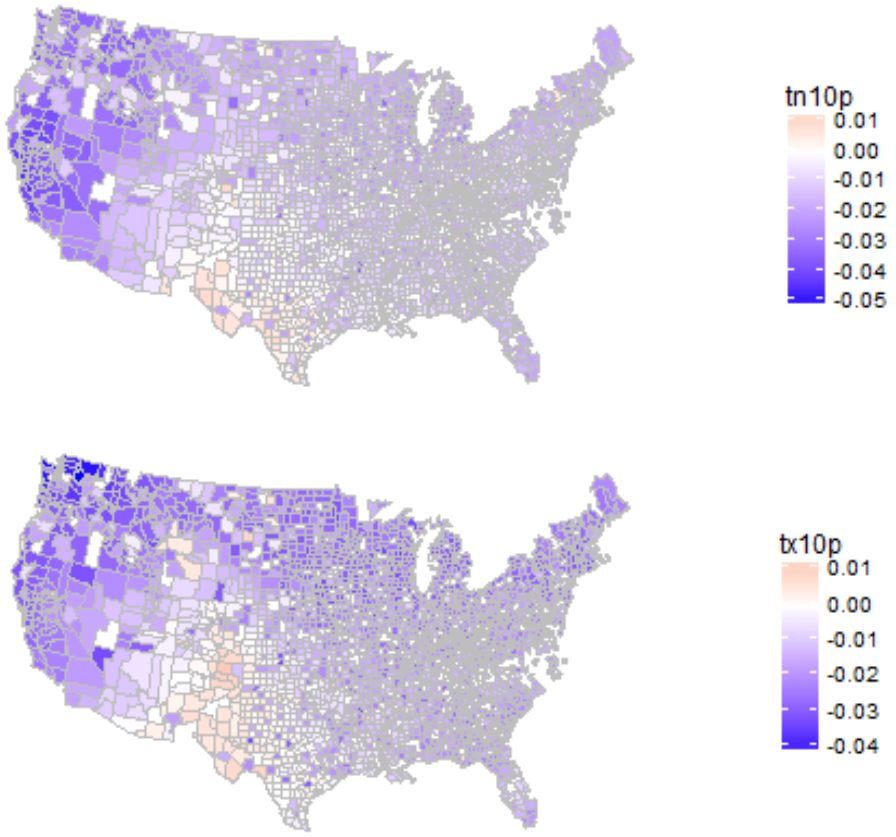

Figure 5.18: *Mean slope value for each county's 10th percentile indices for the CCSM4 RCP4.6 data. (a) Daily Minimum temperature (b) Daily Maximum temperature*

The CCSM4 RCP4.6 predicts many counties will experience warming trends as temperatures exceed the 90th percentile more frequently across the country, particularly on the west coast where warming trends appear to be more rapid (Figure 5.25a&b). On the lower end of the scale, the east coast again sees a decrease in the amount of days below the 10th percentile in daily minimum temperature. This trend continues and is more wide spread for daily maximum temperature falling below the 10th percentile (Figure 5.26a&b).

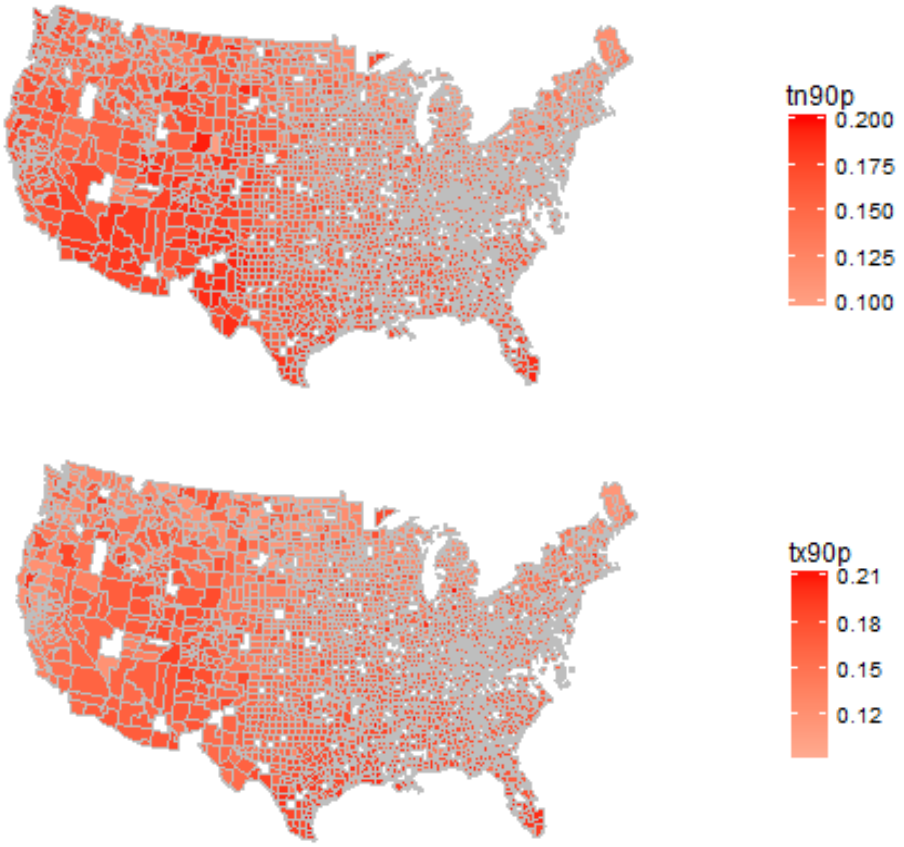

Figure 5.19: *Mean slope values for each county's 90th percentile indices for CCSM4 RCP6.0 data. (a) Daily Minimum temperature. (b) Daily Maximum temperature*

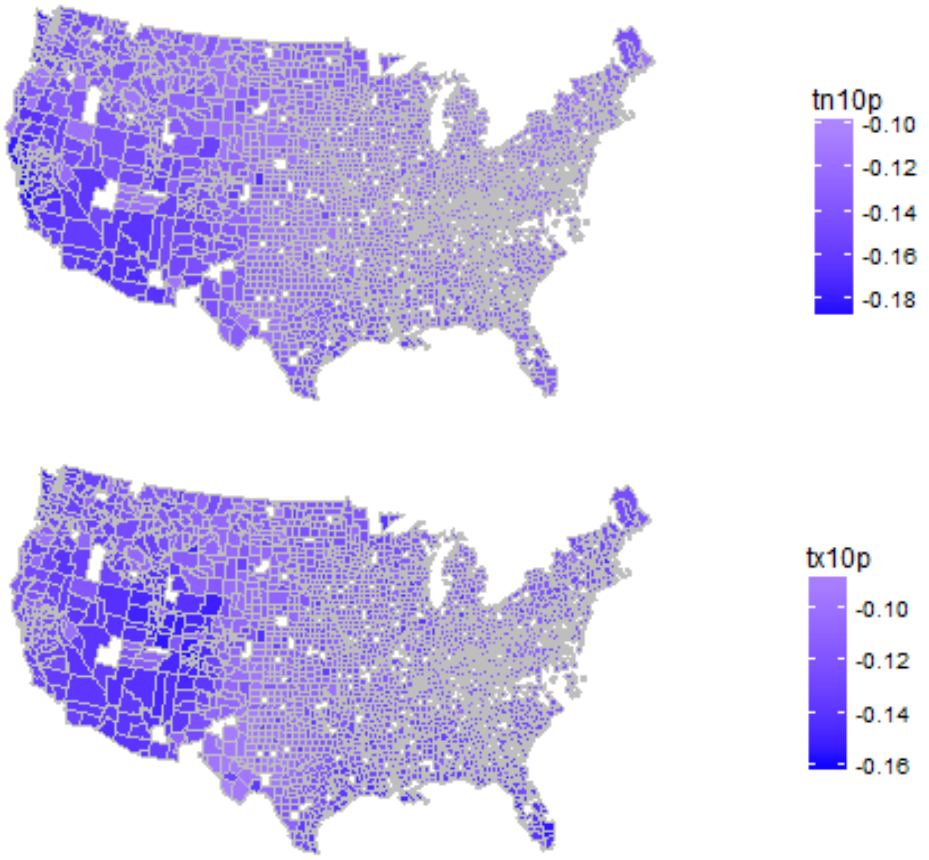

Figure 5.20: *Mean slope value for each county's 10th percentile indices for the CCSM4 RCP6.0 data. (a) Daily Minimum temperature (b) Daily Maximum temperature*

As with the RCP4.6, the CCSM4 RCP6.0 simulation predicts a general warming trend with increases in TN90P and TX90P in virtually all counties across the United States (Figure 5.27a&b). Furthermore, counties see more drastic average slope, particularly in the southwest parts of the country. TX10P and TN10P see drastic decreases, further supporting the warming trend counties are seeing nationwide. Again, these shifts are most severe in the southwest part of the nation (Figure 5.28a&b).

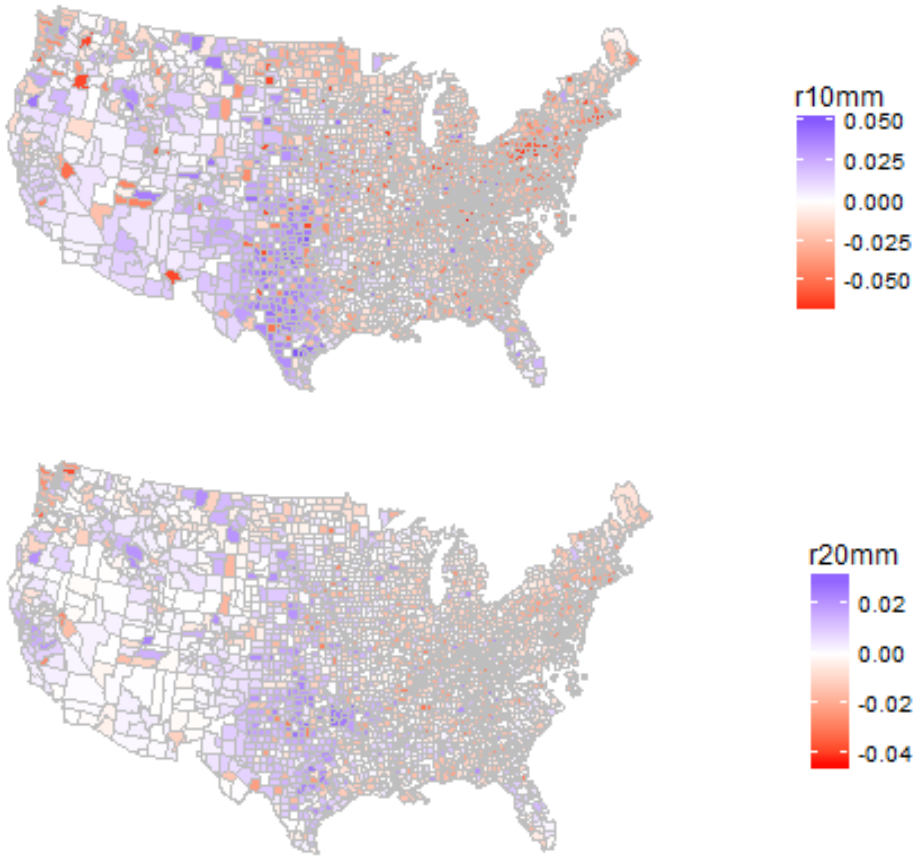

Figure 5.21: *Average slope values for each county's precipitation threshold indices for the CCSM4 RCP4.6 data. (a) Exceeding 10 mm. (b) Exceeding 20 mm.*

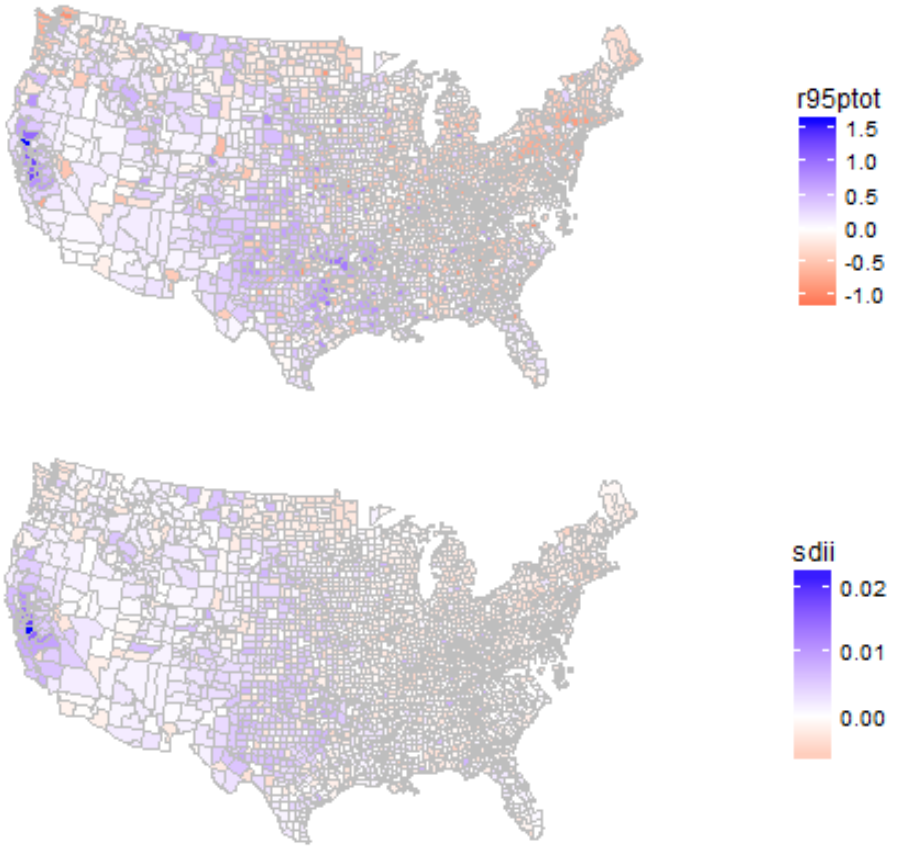

Figure 5.22: *Average slope values for each county's precipitation intensity indices for the CCSM4 RCP4.6 data. (a) Total precipitation for events exceeding the 95th percentile. (b) Annual precipitation intensity over all wet days.*

Precipitation trends in the CCSM4 RCP4.6 simulation indicate trends of slightly dryer conditions on the east coast with the middle part of the country seeing more rainfall as indicated by shifts in R10mm and R20mm (Figure 5.29a&b). Rainfall intensity sees similar spatial trends of dryer conditions on the east coast with the middle third and west coast seeing more intense rainfalls. Pockets in California will see much higher rainfall intensity coming (Figure 5.30a&b).

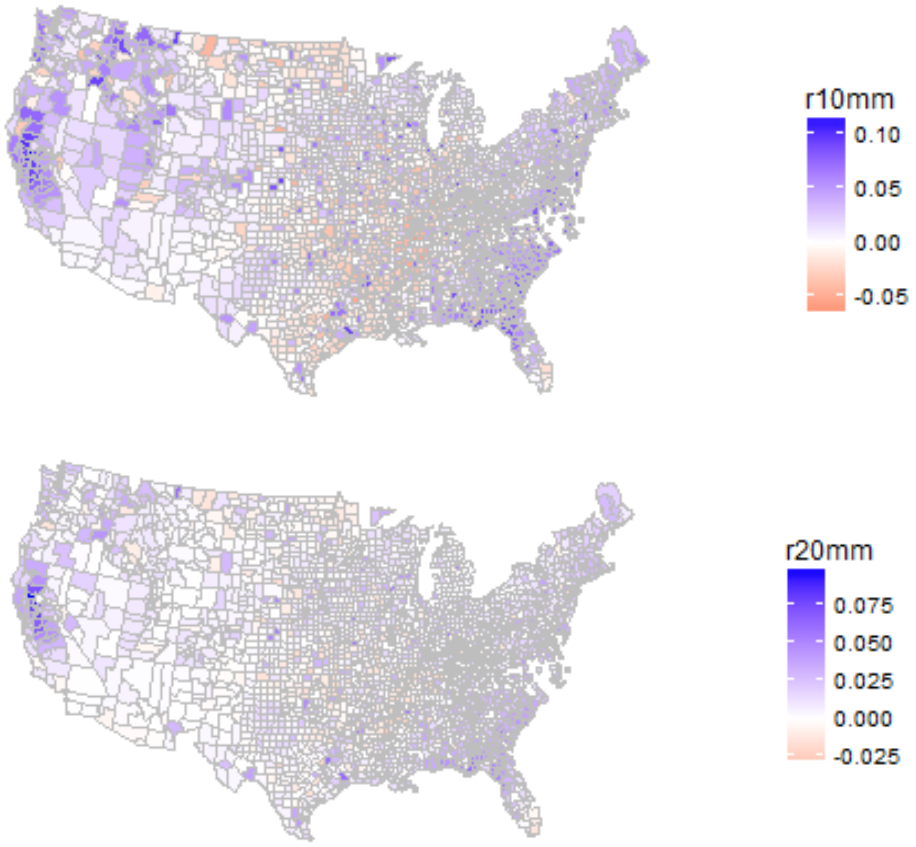

Figure 5.23: *Average slope values for each county's precipitation threshold indices for the CCSM4 RCP6.0 data. (a) Exceeding 10 mm. (b) Exceeding 20 mm.*

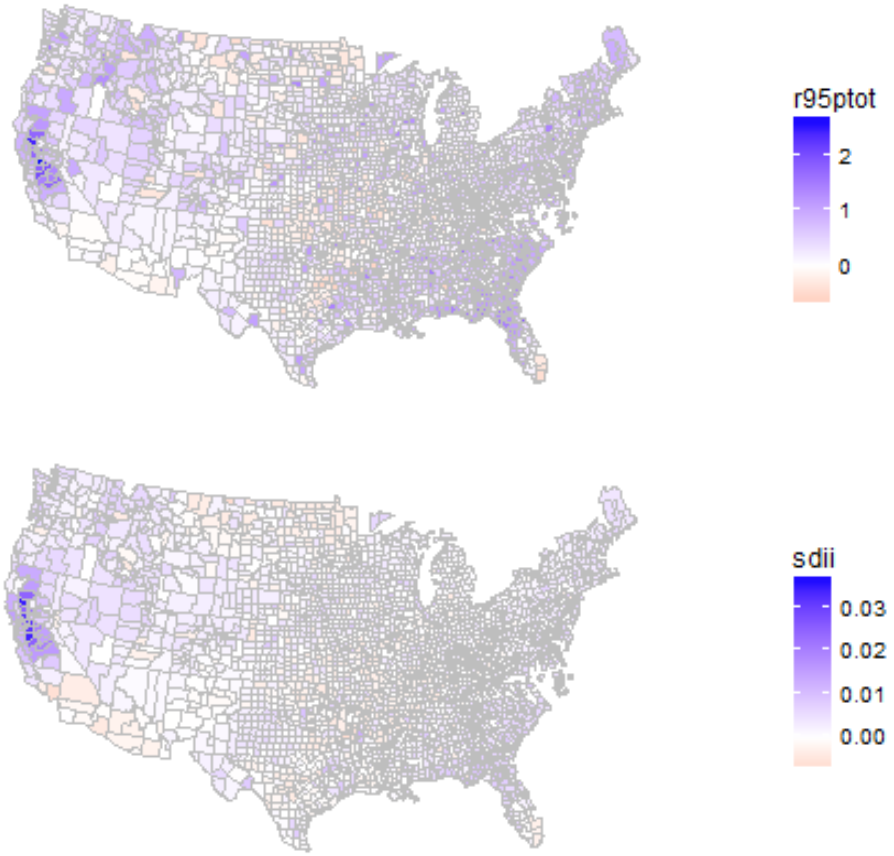

Figure 5.24: *Average slope values for each county's precipitation intensity indices for the CCSM4 RCP6.0 data. (a) Total precipitation for events exceeding the 95th percentile. (b) Annual precipitation intensity over all wet days.*

CCSM4 RCP6.0 sees a large shift in spatial trends compared to the RCP4.6. Most counties on the east coast shift to increases in R10mm and R20mm with many of the counties on the west coast seeing increases as well (Figure 5.31a&b). The middle part of the country sees many more counties appear with decreases in these indices. Rainfall intensity follows suit with R95PTOT switching to increases on the east coast and pockets of very intense rainfall in counties in the west (Figure 5.32a). SDII under the RCP6.0 conditions sees very minimal change across the nation as mostly high rainfall events will go up in intensity.

5.4.6 **CCSM4 NOAA Climactic Region**

To avoid broad, national average generalizations that tend not to properly explain climate trends, the CCSM4 future projected data was averaged over the NOAA Climactic Regions like the GFDL-CM3. This was done over both RCPs and for all indices observed.

Table 5.9: *Mean slope values for temperature indices for each NOAA climactic region for future projected CCSM4 RCP4.6 data*

REGION	TN90P	TX90P	TN10P	TX10P
NORTHWEST	0.0160	0.0231	-0.0332	-0.0329
WEST	0.0224	0.0181	-0.0356	-0.0243
SOUTHWEST	0.0065	0.0050	-0.0101	-0.0034
SOUTH	-0.0018	0.0010	-0.0032	-0.0047
WEST NORTH CENTRAL	0.0168	0.0243	-0.0199	-0.0241
EAST NORTH CENTRAL	0.0098	0.0231	-0.0201	-0.0281
CENTRAL	0.0084	0.0186	-0.0163	-0.0212
NORTHEAST	0.0136	0.0187	-0.0189	-0.0272
SOUTHEAST	0.0130	0.0259	-0.0146	-0.0169

As the point data suggested, almost every region will see increases in TN90P indicating a warming trend based around minimum daily temperatures rising (Table 5.21). The exception in this trend is the South where the pocket of decreasing weather stations could be seen in the point data (Figure 5.21a). TX90P will increase across all regions in the RCP4.6 scenario, further indicating warming patterns. TN10P and TX10P decrease uniformly across the country as temperatures fail to go below the 10^{th} percentile in the coming century.

Table 5.10: *Mean slope values for temperature indices for each NOAA climactic region for future projected CCSM4 RCP6.0 data*

REGION	TN90P	TX90P	TN10P	TX10P
NORTHWEST	0.1560	0.1397	-0.1475	-0.1329
WEST	0.1662	0.1464	-0.1646	-0.1321
SOUTHWEST	0.1782	0.1672	-0.1485	-0.1320
SOUTH	0.1695	0.1762	-0.1305	-0.1162
WEST NORTH CENTRAL	0.1478	0.1324	-0.1228	-0.1143
EAST NORTH CENTRAL	0.1253	0.1334	-0.1235	-0.1181
CENTRAL	0.1452	0.1617	-0.1173	-0.1127
NORTHEAST	0.1220	0.1423	-0.1220	-0.1229
SOUTHEAST	0.1659	0.1768	-0.1325	-0.1287

The RCP6.0 simulation indicates uniform increases across all regions for TN90P and TX90P as well as uniform decreases in TN10P and TX10P (Table 5.22). These changes occur at a more rapid pace than the RCP4.6 simulations for the CCSM4. These rapid changes towards warming can be expected due to the higher concentration of greenhouse gases in the RCP6.0 simulations.

Table 5.11: *Mean slope values for precipitation indices for each NOAA climactic region for future projected CCSM4 RCP4.6 data*

REGION	R10MM	R20MM	R95PTOT	SDII
NORTHWEST	-0.0020	-0.0028	-0.0064	0.0005
WEST	0.0067	0.0042	0.2689	0.0053
SOUTHWEST	0.0125	0.0025	0.1887	0.0019
SOUTH	0.0167	0.0097	0.3757	0.0032
WEST NORTH CENTRAL	0.0030	0.0027	0.0944	0.0013
EAST NORTH CENTRAL	-0.0155	-0.0014	-0.0705	-0.0007
CENTRAL	-0.0285	-0.0089	-0.2351	-0.0020
NORTHEAST	-0.0328	-0.0140	-0.4678	-0.0029
SOUTHEAST	-0.0175	-0.0047	-0.1033	-0.0008

The CCSM4 RCP4.6 simulation yields small changes to the R10mm and R20mm indices (Table 5.23). These small regional averages will mean strong rainfall days will not necessarily become significantly more frequent over time. Table 5.23 however illustrates a strong change in R95PTOT that has been common with this analysis. Most regions will be seeing rapid shifts in the intensity of their strong rainfall days. Notably, the South will see strong increases in R95PTOT while the Northeast will see strong decreases per the CCSM4 RCP4.6 simulation.

Table 5.12: *Mean slope values for precipitation indices for each NOAA climactic region for future projected CCSM4 RCP6.0 data*

REGION	R10MM	R20MM	R95PTOT	SDII
NORTHWEST	0.0381	0.0106	0.4296	0.0045
WEST	0.0403	0.0205	0.5989	0.0089
SOUTHWEST	0.0124	0.0025	0.1595	0.0011
SOUTH	-0.0082	0.0004	0.1048	-0.0002
WEST NORTH CENTRAL	0.0111	0.0040	0.1907	0.0014
EAST NORTH CENTRAL	0.0072	0.0045	0.1683	0.0007
CENTRAL	-0.0056	0.0030	0.1768	-0.0004
NORTHEAST	0.0288	0.0166	0.5274	0.0030
SOUTHEAST	0.0457	0.0228	0.7034	0.0040

The RCP6.0 simulation yields more rapid change in trends than the RCP4.6 simulation. Furthermore, the RCP6.0 simulation shows more regions with increases in R10mm and all regions increasing in R20mm (Table 5.24). The only decreases in R10mm come in the South and the Central regions, and the change is very minimal. The RCP6.0 simulation shows large increases in R95PTOT for all regions unlike the RCP4.6 simulation. On a whole however, SDII remains unchanged in all regions, indicating once again that future intensities will grow mostly for strong rainfall events.

5.5 Conclusion

While analyzing changes in average temperature and precipitation is important to understanding climate change, analyzing and fully understanding shifts in extreme weather patterns helps understand how exactly climate will impact different parts of the country. By applying the ETCCMDI indices to future projected GCM data, climate trends become more apparent and easier to understand. Furthermore, by analyzing these at point, regional, and county scales, spatial trends emerge and describe what parts of the country will change in different ways.

The GCM data in general shows patterns of warming across the entire nation with some exceptions in the RCP4.6 scenario. However, the TN90P and TX90P indices do allow an analysis of how

severe this warming will be. Precipitation tends to be far more variable with certain areas that are dry getting dryer and wetter areas getting wetter. Disagreements do exist between the GFDL-CM3 and CCSM4 in regards to precipitation. Furthermore, different RCP scenarios within each GCM also have disagreements, notably some areas such as the east coast getting dryer in CCSM4 RCP4.6 but getting wetter in RCP6.0.

Regional analysis helps flesh out the spatial patterns and limits the scope to get average values that are more representative than a nationwide average. Most importantly, the regional analysis helps identify which areas will undergo extreme and rapid shifts. The county analysis further limits the scope to better represent what is occurring between the point data. This helps identify which counties could see extreme changes that policy makers and scientist will need to plan to deal with in the coming century.

Chapter 6

Summary and Future Work

Analyzing extreme weather trends can reveal patterns in climate change that would otherwise go unnoticed and leave regions underprepared to deal with climate shifts that will impact them. By using the ETCCMDI indices, spatial and temporal patterns can be analyzed and mapped efficiently and effectively. This study demonstrated the indices' ability to analyze trends in both historical observed data as well as future projected climate model data. While a simple linear model may not be the most effective way of analyzing the trends, this method does depict a general trend of what will occur at a regional level when applied to individual weather station locations.

This analysis provides a basis for analyzing extreme weather trends, however the unreliability of the linear model could be improved upon by designing location specific models to analyze temporal shifts in indices. By applying a machine learning algorithm, a proper model could be fit to specific regions, or even to each weather station to determine a well-fitting model.

In addition to improving the model, more analysis could be done on GCM data to determine which GCMs predict extreme weather patterns the best. As it is, there does not seem to be a good analysis of which GCMs work best compared to one another. This study touched on comparing GCM historical simulations to observed data. This analysis could be continued over numerous GCMs while looking closely at each index within each GCM to see which models work best with individual indices.

Finally, this study specifically looked at trends at individual points around the country. The causes of these trends are not well documented however. As the historical data shows, there can be a great deal of variability between stations, even ones that are relatively close to one another. By looking at factors such as shifts in land cover, topography, and environmental policies implemented in an area, an understanding of why these shifts occur and what conditions cause certain changings will emerge.

References

Andrews, T., Forster, P. M., Boucher, O., Bellouin, N., & Jones, A. (2010). Precipitation, radiative forcing and global temperature change. Geophysical Research Letters, 37(14).

Bekryaev, R. V., Polyakov, I. V., & Alexeev, V. A. (2010). Role of polar amplification in long-term surface air temperature variations and modern Arctic warming. Journal of Climate, 23(14), 3888-3906.

Caesar, J., & Lowe, J. A. (2012). Comparing the impacts of mitigation versus non-intervention scenarios on future temperature and precipitation extremes in the HadGEM2 climate model. Journal of Geophysical Research: Atmospheres, 117(D15).

Ciais, P., Sabine, C. (Ed.). (2014). Carbon and Other Biogeochemical Cycles. In *Climate Change 2013: The Physical Science Basis. Contribution of Working Group I to the Fifth Assessment Report of the Intergovernmental Panel on Climate Change*. Cambridge University Press.

Climate Modeling. (2016, November 28). Retrieved March 16, 2017, from https://www.gfdl.noaa.gov/climate-modeling/

Collins, M. (Ed.). (2014). Long-term Climate Change: Projections, Commitments and Irreversibility. In *Climate Change 2013: The Physical Science Basis. Contribution of Working Group I to the Fifth Assessment Report of the Intergovernmental Panel on Climate Change.* Cambridge University Press.

Cubasch, U. (Ed.). (2014). Introduction. In *Climate Change 2013: The Physical Science Basis. Contribution of Working Group I to the Fifth Assessment Report of the Intergovernmental Panel on Climate Change.* Cambridge University Press.

Easterling, D. R., Alexander, L. V., Mokssit, A., & Detemmerman, V. (2003). CCI/CLIVAR workshop to develop priority climate indices. Bulletin of the American Meteorological Society, 84(10), 1403-1407.

F. (n.d.). U.S. Climate Divisions. Retrieved March 14, 2017, from https://www.ncdc.noaa.gov/monitoring-references/maps/us-climate-divisions.php

Fischer, E. M., & Schär, C. (2010). Consistent geographical patterns of changes in high-impact European heatwaves. Nature Geoscience, 3(6), 398-403.

Flato, G. (Ed.). (2014). Evaluation of Climate Models. In *Climate Change 2013: The Physical Science Basis. Contribution of Working Group I to the Fifth Assessment Report of the Intergovernmental Panel on Climate Change*. Cambridge University Press.

Frich, P., Alexander, L. V., Della-Marta, P. M., Gleason, B., Haylock, M., Tank, A. K., & Peterson, T. (2002). Observed coherent changes in climatic extremes during the second half of the twentieth century. Climate research, 19(3), 193-214.

Gent, P. R., Danabasoglu, G., Donner, L. J., Holland, M. M., Hunke, E. C., Jayne, S. R., ... & Worley, P. H. (2011). The community climate system model version 4. Journal of Climate, 24(19), 4973-4991.

GFDL. (2007). Will the wet get wetter and the dry drier? *GFDL Climate Modeling Research Highlights.*

Good, P., Ingram, W., Lambert, F. H., Lowe, J. A., Gregory, J. M., Webb, M. J., ... & Wu, P. (2012). A step-response approach for predicting and understanding non-linear precipitation changes. Climate dynamics, 39(12), 2789-2803.

Griffies, S. M., Winton, M., Donner, L. J., Horowitz, L. W., Downes, S. M., Farneti, R., ... & Palter, J. B. (2011). The GFDL CM3 coupled climate model: characteristics of the ocean and sea ice simulations. Journal of Climate, 24(13), 3520-3544.

Jones, R., Patwardhan, A. (Ed.). (2014). Foundations for decisionmaking. In *Climate Change 2014: Impacts, Adaptations, and Vulnerability. Contribution of Working Group II to the Fifth Assessment Report of the Intergovernmental Panel on Climate Change*. Cambridge University Press.

Karl, T. R., & Koss, W. J. CN Williams Jr., and PJ Young, 1986: A model to estimate the time of observation bias associated with monthly mean maximum, minimum, and mean temperatures for the United States. J. Climate Appl. Meteor, 25, 145-160.

Kunkel, Kenneth E., Karen Andsager, and David R. Easterling. "Long-term trends in extreme precipitation events over the conterminous United States and Canada." Journal of climate 14.8 (1999): 2515-2527.

Manabe, Syukuro, Kirk Bryan, and Michael J. Spelman. "Transient response of a global ocean-atmosphere model to a doubling of atmospheric carbon dioxide." *Journal of Physical Oceanography* 20.5 (1990): 722-749.

Meinshausen, M., Smith, S. J., Calvin, K., Daniel, J. S., Kainuma, M. L. T., Lamarque, J. F., ... & Thomson, A. G. J. M. V. (2011). The RCP greenhouse gas concentrations and their extensions from 1765 to 2300. Climatic change, 109(1-2), 213.

Miller, R. L., Schmidt, G. A., Nazarenko, L. S., Tausnev, N., Bauer, S. E., DelGenio, A. D., ... & Aleinov, I. (2014). CMIP5 historical simulations (1850–2012) with GISS ModelE4. *Journal of Advances in Modeling Earth Systems*, *6*(2), 441-477.

Moss, R. H., Edmonds, J. A., Hibbard, K. A., Manning, M. R., Rose, S. K., Van Vuuren, D. P., ... & Meehl, G. A. (2010). The next generation of scenarios for climate change research and assessment. Nature, 463(7282), 747-756.

Nazarenko, L., Schmidt, G. A., Miller, R. L., Tausnev, N., Kelley, M., Ruedy, R., ... & Bleck, R. (2015). Future climate change under RCP emission scenarios with GISS ModelE4. *Journal of Advances in Modeling Earth Systems*, *7*(1), 244-267.

Pachauri, R. K., Meyer, L., Plattner, G. K., & Stocker, T. (2015). IPCC, 2014: Climate Change 2014: Synthesis Report. Contribution of Working Groups I, II and III to the Fifth Assessment Report of the Intergovernmental Panel on Climate Change. IPCC.

Raynaud, D., Jouzel, J., Barnola, J. M., Chappellaz, J., Delmas, R. J., & Lorius, C. (1993). The ice record of greenhouse gases. SCIENCE-NEW YORK THEN WASHINGTON-, 259, 926-926.

Solomon, S. (Ed.). (2007). Summary for Policymakers. In *Climate change 2007-the physical science basis: Working group I contribution to the fourth assessment report of the IPCC (Vol. 4)*. Cambridge University Press.

Stocker, T. (Ed.). (2014). Summary for Policy Makers. In *Climate change 2013: the physical science basis: Working Group I contribution to the Fifth assessment report of the Intergovernmental Panel on Climate Change*. Cambridge University Press.

Sanchez-Lugo, E. (n.d.). NOAA Climactic Regions [Digital image]. Retrieved March 14, 2017, from https://www.ncdc.noaa.gov/monitoring-references/maps/us-climate-regions.php

Schlesinger, M. E., & Mitchell, J. F. (1987). Climate model simulations of the equilibrium climatic response to increased carbon dioxide. Reviews of Geophysics, 25(4), 760-798.

Seneviratne, S. I., Nicholls, N., Easterling, D., Goodess, C. M., Kanae, S., Kossin, J., ... & Reichstein, M. (2012). Changes in climate extremes and their impacts on the natural physical environment. Managing the risks of extreme events and disasters to advance climate change adaptation, 109-230.

Trenberth, K. E. (2011). Changes in precipitation with climate change. *Climate Research*, *47*(1-2), 123-138.

Victor D., Zhou, D. (Ed.) (2014). Introductory Chapter. In *Climate Change 2014: Mitigation of Climate Change. Contribution of Working Group III to the Fifth Assessment Report of the Intergovernmental Panel on Climate Change*. Cambridge University Press.

Walsh, J., D. Wuebbles, K. Hayhoe, J. Kossin, K. Kunkel, G. Stephens, P. Thorne, R. Vose, M. Wehner, J. Willis, D. Anderson, S. Doney, R. Feely, P. Hennon, V. Kharin, T. Knutson, F. Landerer, T. Lenton, J. Kennedy, and R. Somerville, 2014: Ch. 2: Our Changing Climate. Climate Change Impacts in the United States: The Third National Climate Assessment, J. M. Melillo, Terese (T.C.) Richmond, and G. W. Yohe, Eds., U.S. Global Change Research Program, 19-67. doi:10.7930/J0KW5CXT.